Designing Intelligent Nano/Microbots: Synthetic Active Matter

1. Introduction to Synthetic Active Matter
2. Powering Active Particle and Fluid Motion
3. Collective Behavior of Autonomous Nano/Microbots

AYUSMAN SEN

Department of Chemistry, Penn State University
E-mail: asen@psu.edu

Grand challenge in science:
Mastering energy and information at the nano/microscale

Create technologies that rival those of living things:

Requires designing *intelligent systems*

Use free energy of chemical fuels to fabricate organized systems driven *far from equilibrium*

Intelligence requires:

- **Information**
- **Ability to process (act on) information – information processor**

Information: Gradient – Chemical, Light

Information processor: Self-powered object

Result of Information + Information Processing:
Collective/Emergent behavior
e.g., Spatial and/or Temporal Assemblies

***Both* information and information processor require continuous input of energy**

Required design elements:

- **Autonomous movement through catalytic energy harvesting**
- **Control of directionality through chemical/light gradients**
- **Inter-bot communication via chemical signals**

Designing Intelligent Nano/Microbots: Synthetic Active Matter

1. *Introduction to Synthetic Active Matter*
2. *Powering Active Particle and Fluid Motion*
3. **Collective Behavior of Autonomous Nano/Microbots**

AYUSMAN SEN

Department of Chemistry, Penn State University
E-mail: asen@psu.edu

APPLICATIONS OF AUTONOMOUS NANO/MICROBOTS

- Motors for nanomachines and biological cells
- Roving sensors
- Active delivery vehicles (versus passive diffusion)
- Patterns and arrays by directed deposition of materials
- Pumps and valves for nanofluidic and bio-chip devices
- Channel-less fluid flow

CATALYSIS IS THE ENGINE OF NANOTECHNOLOGY

Gradient-based Motion

External Fields

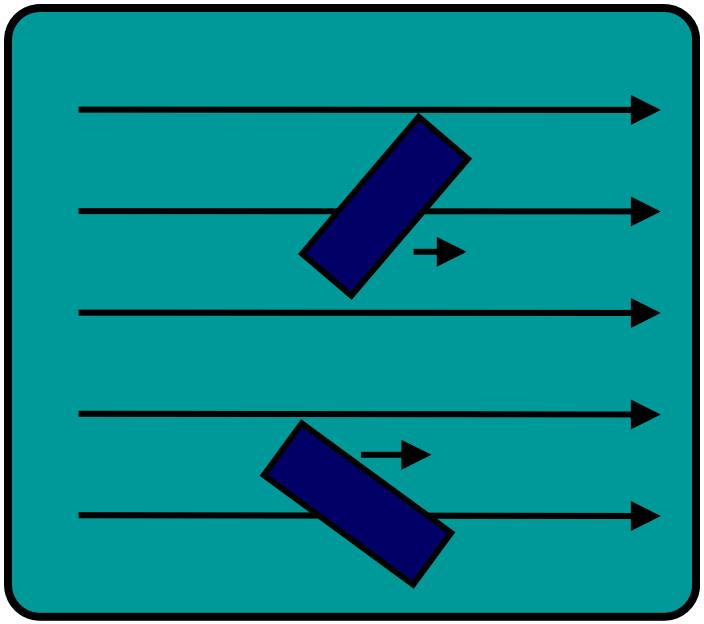

- Many types of fields:
  (*magnetic, chemical, thermal, electric*)
- Energy applied from external source
- Ensemble behavior of all particles

Anderson, *Ann. Rev. Fluid. Mech.*, **1989**

Self-generated Fields

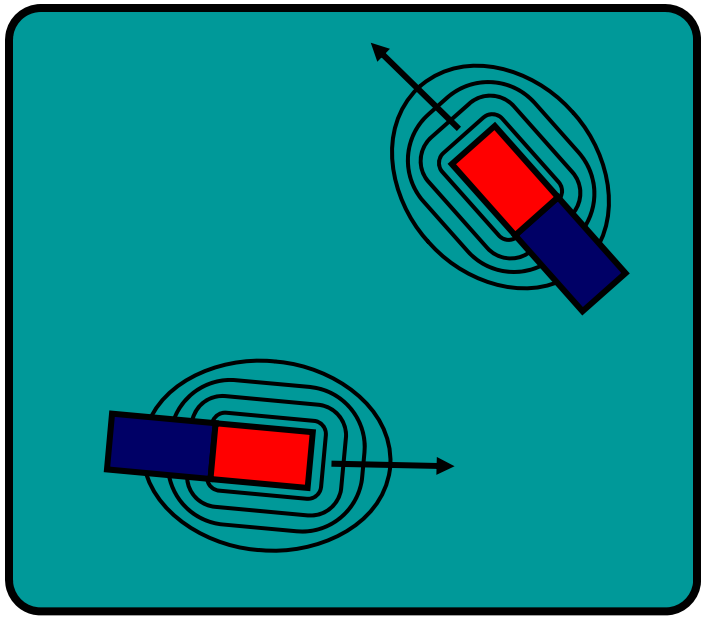

- Catalytically generated fields:
  (*chemical, thermal, electric*)
- Energy harvested locally
- Particles move independently
- Catalysis and asymmetry

Mallouk, Sen, *Chem.—Eur. J.*, **2005**

Powering Motion by Chemical Reactions

Consider the archetypal catalytic reaction: the hydrogenation of ethene to ethane.

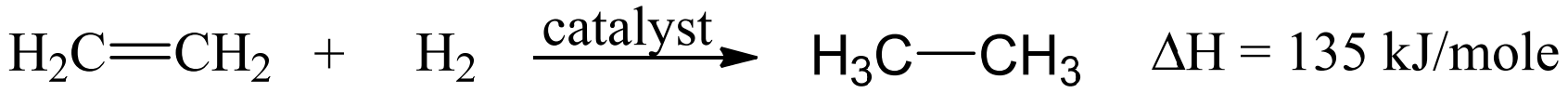

The enthalpy change corresponds to 2.2×10^{-19} Joules per turnover

To move a spherical catalyst particle of radius 10 nm a distance of 100 nm in 1 second (i.e., a speed of 100 nm/sec)

Energy required = force *x* distance

Force = $6\pi\mu RV$ (Stokes Law)
where R is the radius of the sphere, V is the speed and μ is the dynamic viscosity

In a viscous medium like water (dynamic viscosity ~10^{-3} Pa.sec), the energy required for the given movement is 1.9×10^{-24} Joules

This is 5 orders of magnitude smaller than the energy obtained in just 1 turnover in an archetypal catalytic alkene hydrogenation! Turnover *rate* is also important.
Catalytic reactions are effective mechanisms for powering the autonomous movement of nano and micron-sized objects and *even single molecules*.

Life at Low $\mathcal{R}$eynolds Number

$$\mathcal{R} = \frac{\text{Inertial Force}}{\text{Viscous Force}}$$

Forces at $\mathcal{R} << 1$

- Viscosity (drag)
- Surface (interfacial tension)
- Diffusion (Brownian)
- Electrostatic (double-layer)
- *F = ma is irrelevant*

Scallop theorem: Propulsion by *purely* time-reversible reciprocal motion not possible

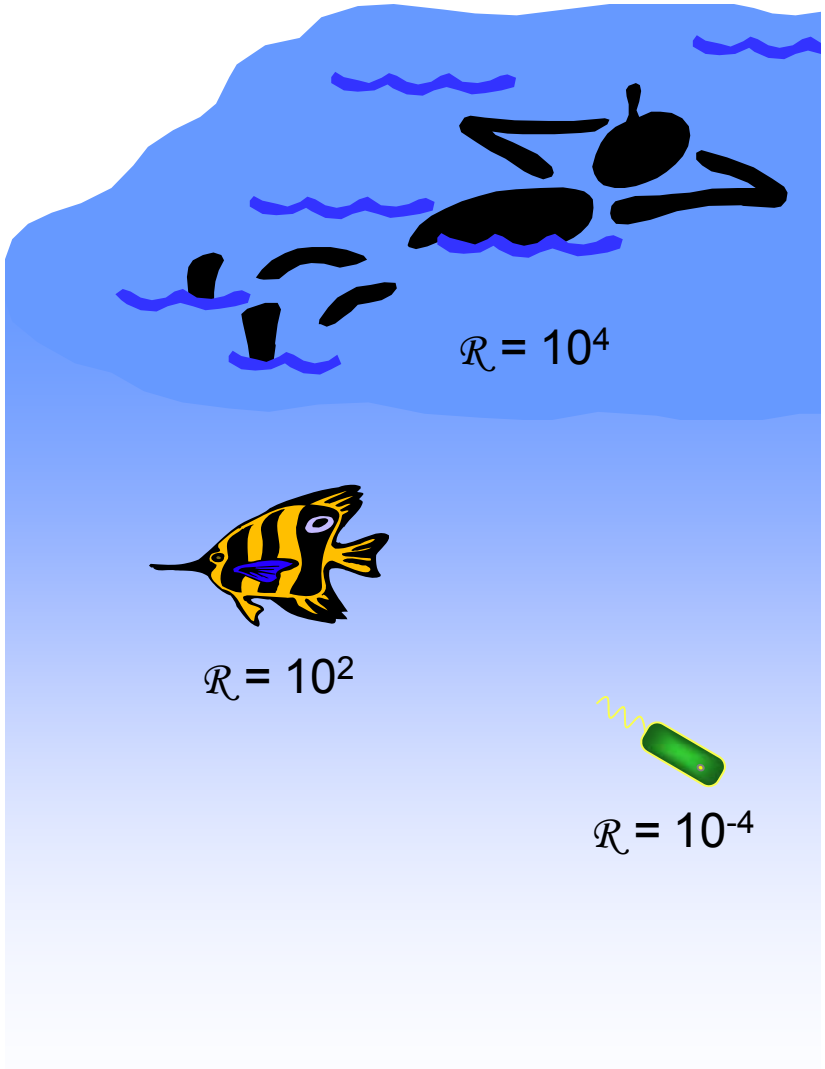

E. M. Purcell, *Am. J. Phys.* **1977,** *45*, 3-11

Designing Functional Nano/Microbots

Required Design Elements

- Movement Through Catalysis
- Cargo Loading, Transport, and Unloading
- Directional Movement Through Chemical Gradient (Chemotaxis)
- Emergent Collective Behavior Through Inter-Bot Communication via Chemical Signals

Scientific American, May, 2009

Platinum Blondes *& Hot Rods*

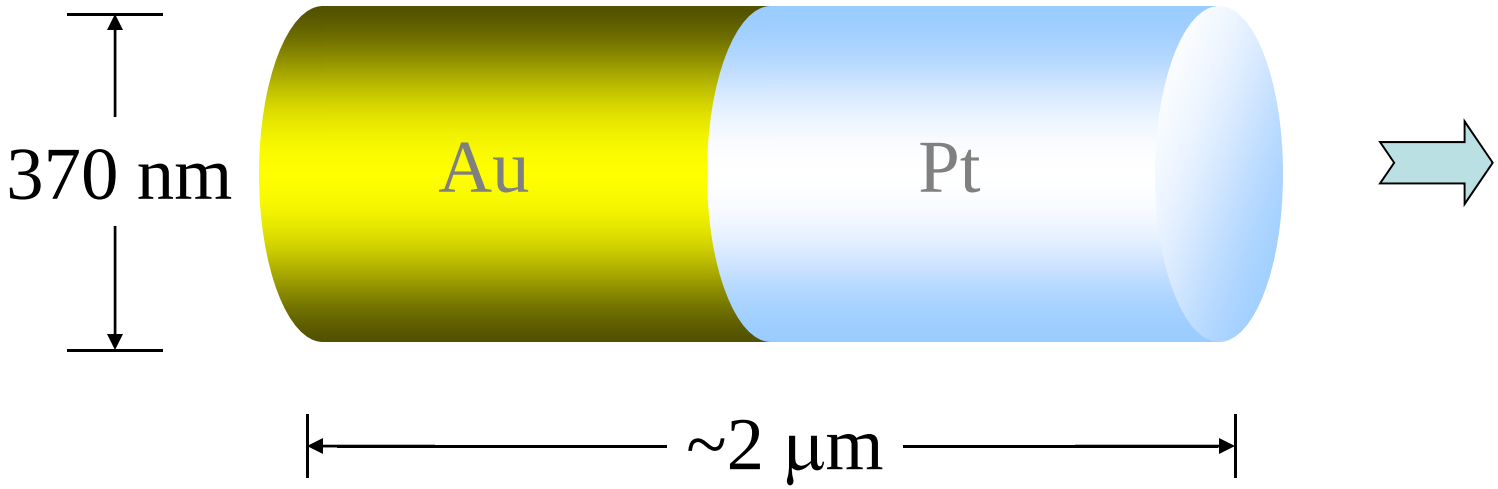

$$2H_2O_2(aq) \xrightarrow{Pt/Au} 2\,H_2O(l) + O_2(g)$$

J. Am. Chem. Soc., **2004**

Nanorod Synthesis

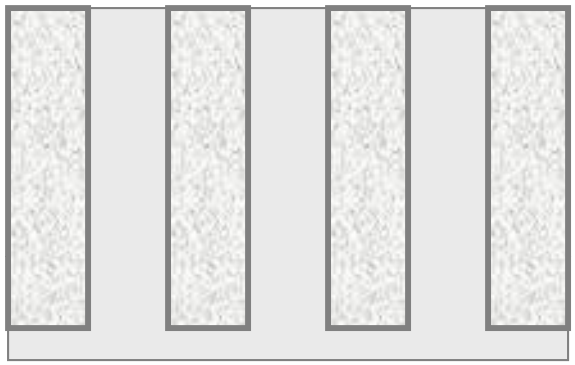

Aluminum oxide membrane

Ag evaporation

plating

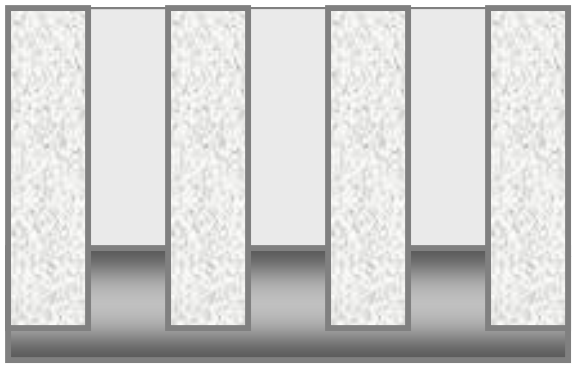

Ag-filled Al_2O_3 membrane

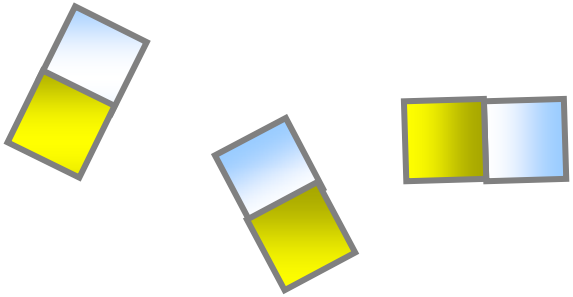

Free rods after etching

HNO_3

NaOH

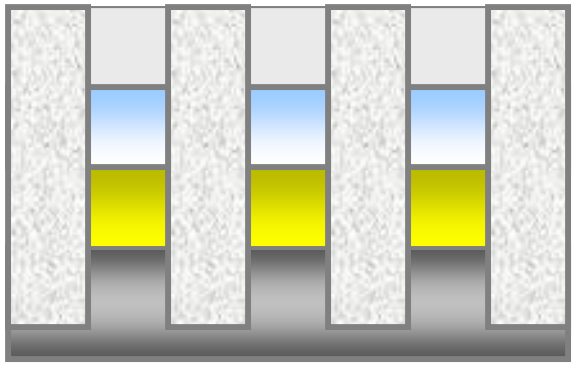

Electroplate Au and Pt

Mallouk et al.

Fabrication of Janus particles

Formation of monolayer

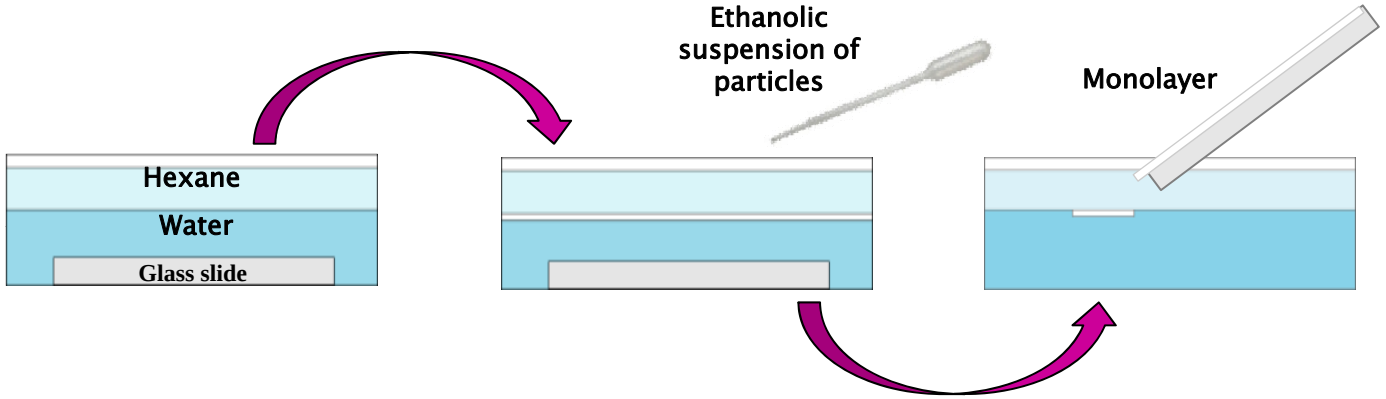

Metal deposition

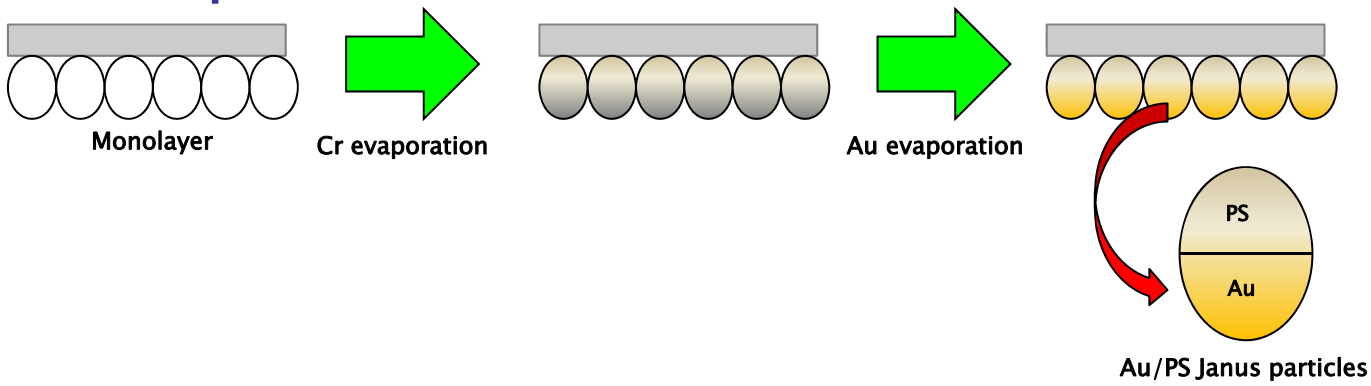

FESEM images of 1.5 μm polystyrene/gold Janus particles

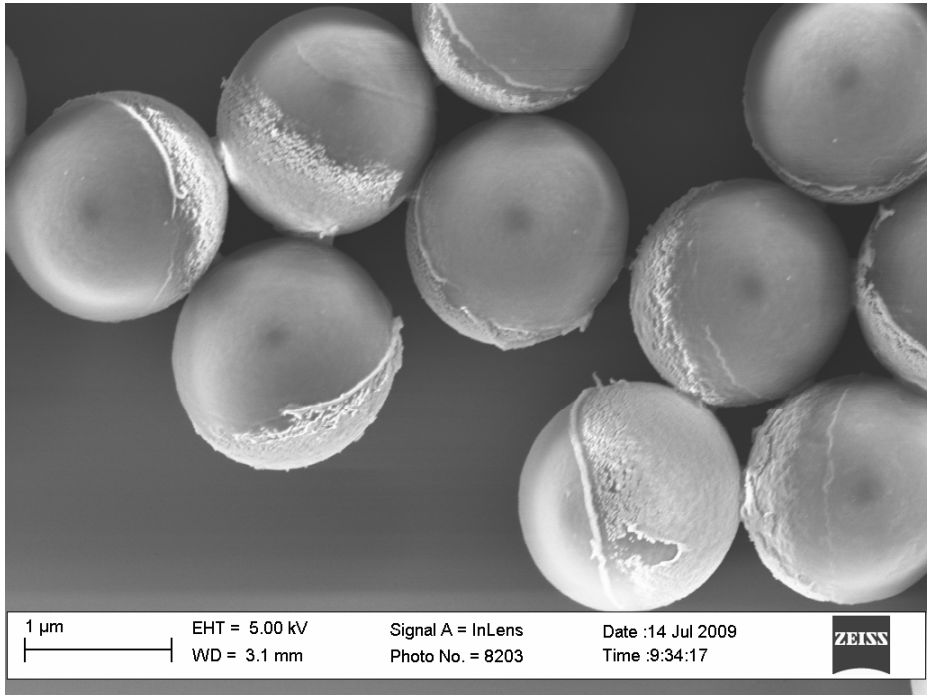

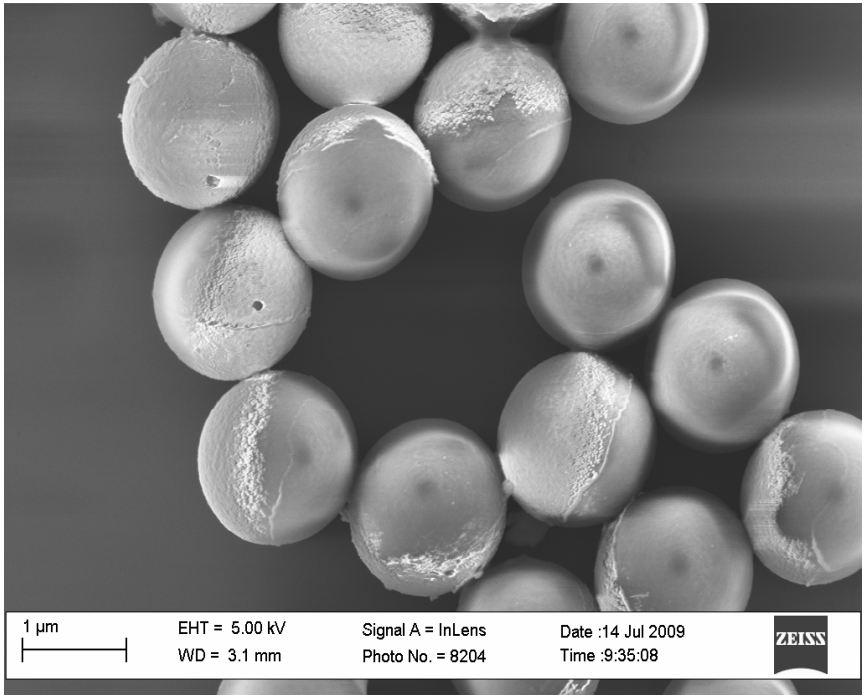

Allows selective loading and delivery of cargo from each face

Rod Movement Experiments

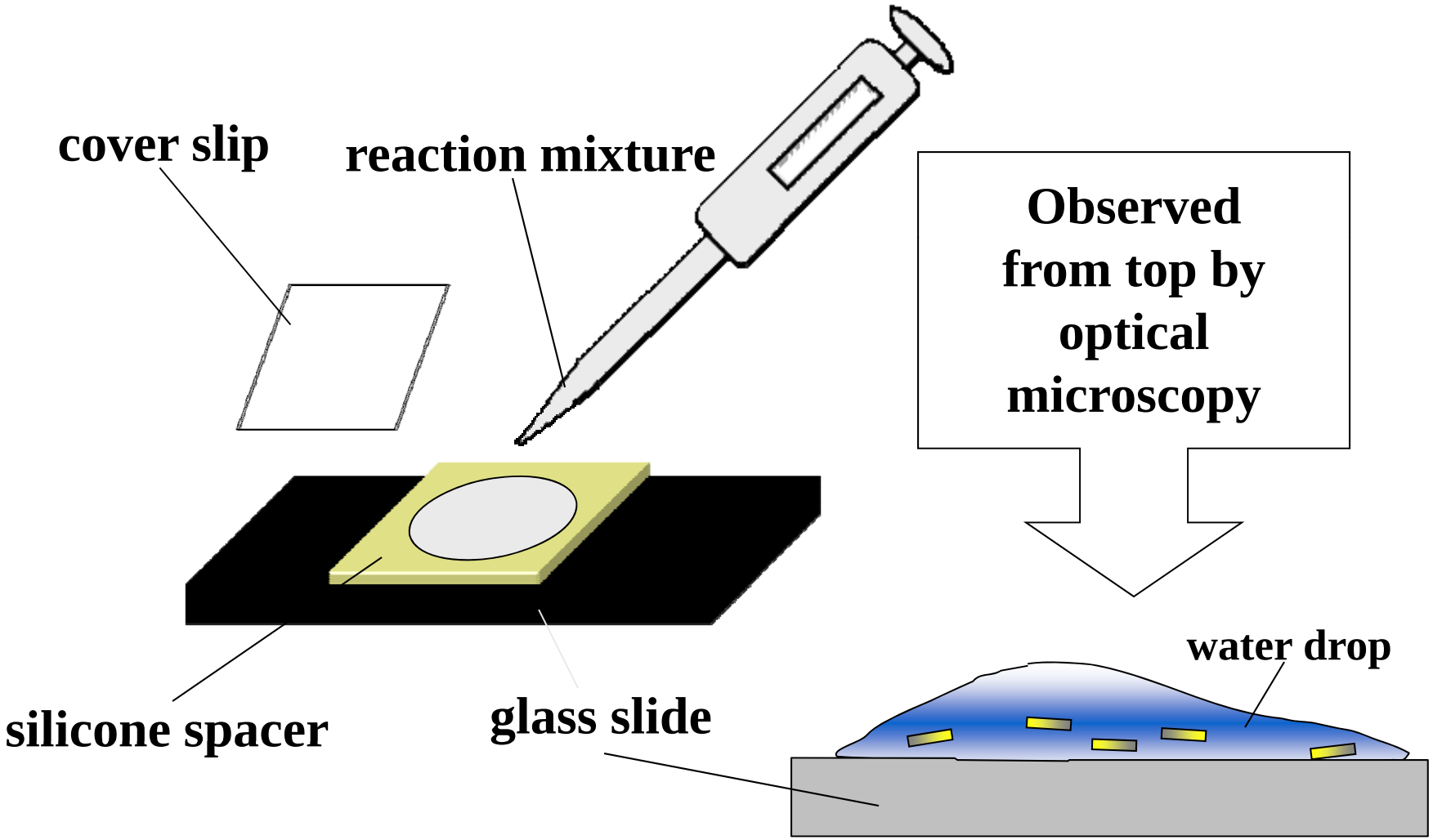

Electrokinetic Propulsion

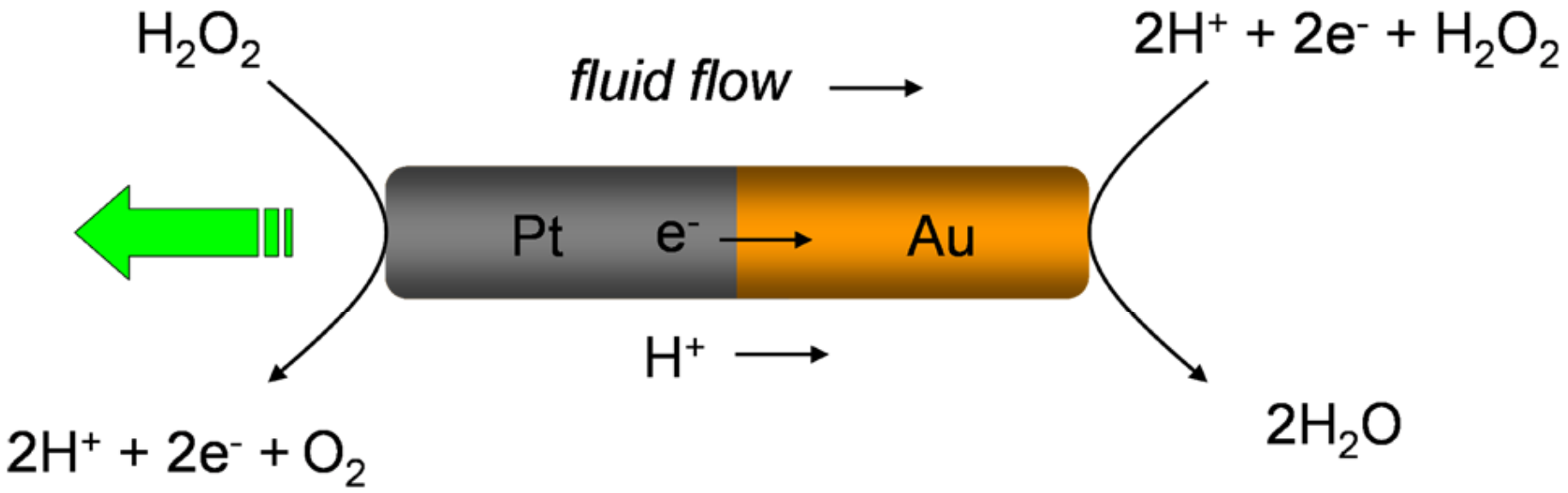

Autonomous Moving Nanorods (Real-Time)

2-μm Au/Pt rods in H_2O

… in 2.5% H_2O_2

real-time video at http://research.chem.psu.edu/axsgroup/

First demonstration of nano/micromotors powered by catalysis *outside biological systems*

RELATIVE SPEEDS

	Speed (km/h)	Body lengths per second
Cheetah	111	25
Human	37.5	5.4
Bacteria (flagellar)	1.5×10^{-4}	10
Au/Pt	**5.8×10^{-5}**	**10**
Brownian motion	6.6×10^{-7}	0.3

Absolute speed limited by body size

Directionality

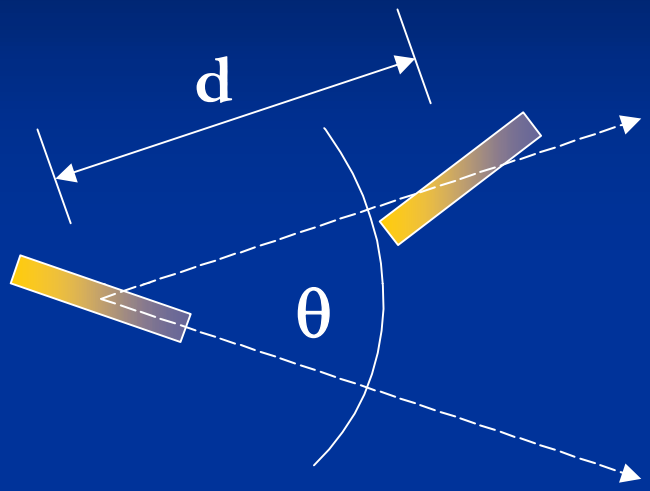

d = center-to-center displacement

θ = angle between direction particle is pointed and direction particle moves

Directionality Factor = cos θ

Net Forward (v_z) = cos θ × d

Speed vs. Directionality

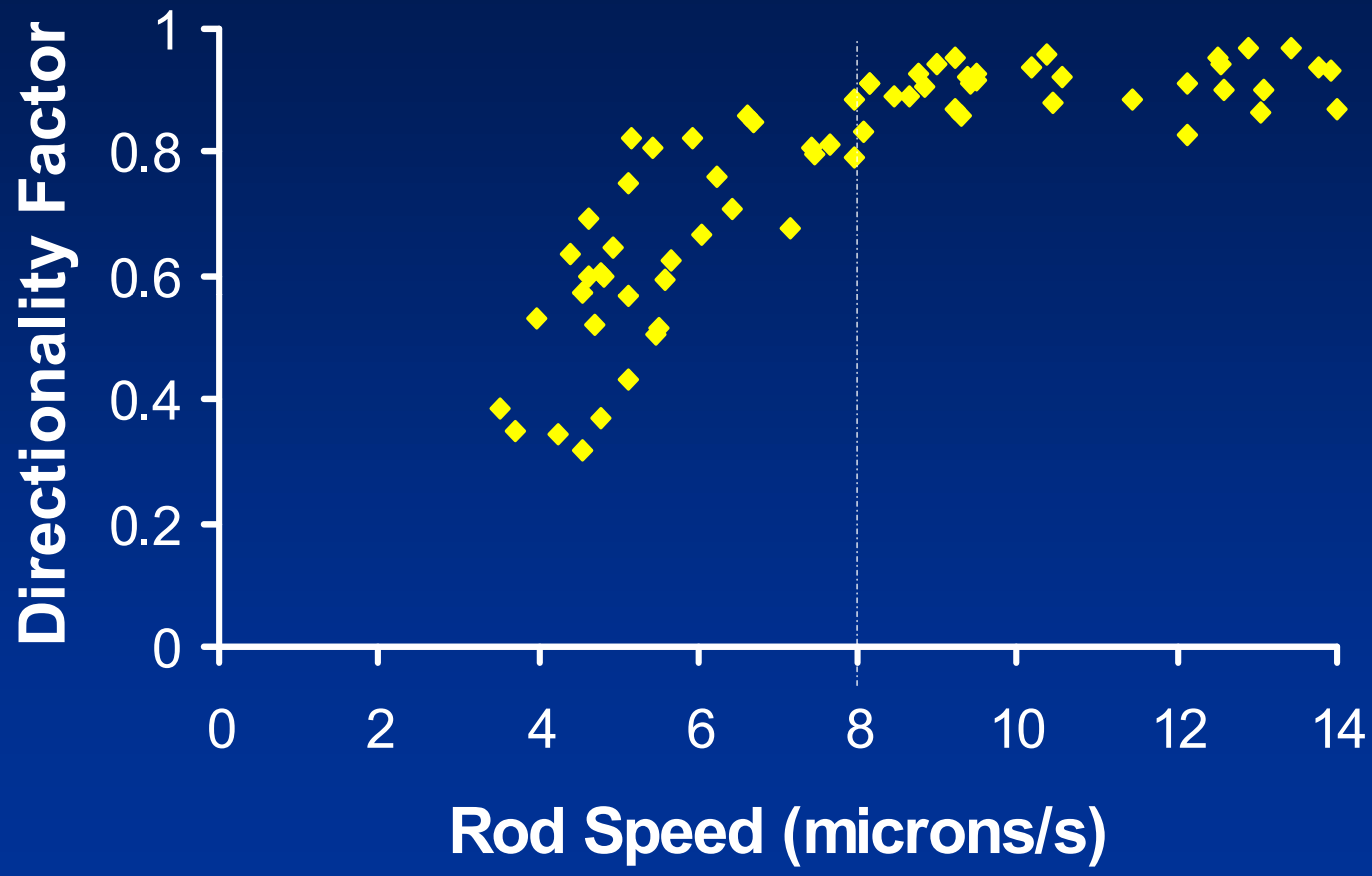

For 2.0 μm rods in 3.3% H_2O_2

H_2O_2 Concentration Effects

% H_2O_2	Average Speed (μm/s)	Directionality Factor	Net Forward (μm/s)
4.9	7.7 ± 0.9	0.78	6.60
3.3	7.9 ± 0.7	0.75	6.59
1.6	5.5 ± 0.6	0.65	3.84
0.33	5.0 ± 0.4	0.60	3.43
0.031	3.9 ± 0.5	0.19	0.92
pure H_2O	3.3 ± 0.5	0.01	0.04

WHAT DETERMINES O_2 PRODUCTION RATE?

1. Rate of diffusion of H_2O_2 to the catalyst surface

2. *Rate of H_2O_2 decomposition -*

   Depends on catalyst turnover rate and surface area

Faster Pt/Au motors incorporate carbon nanotubes (Wang)

CNT-Enhanced Catalytic Nanomotors

Wang, UCSD

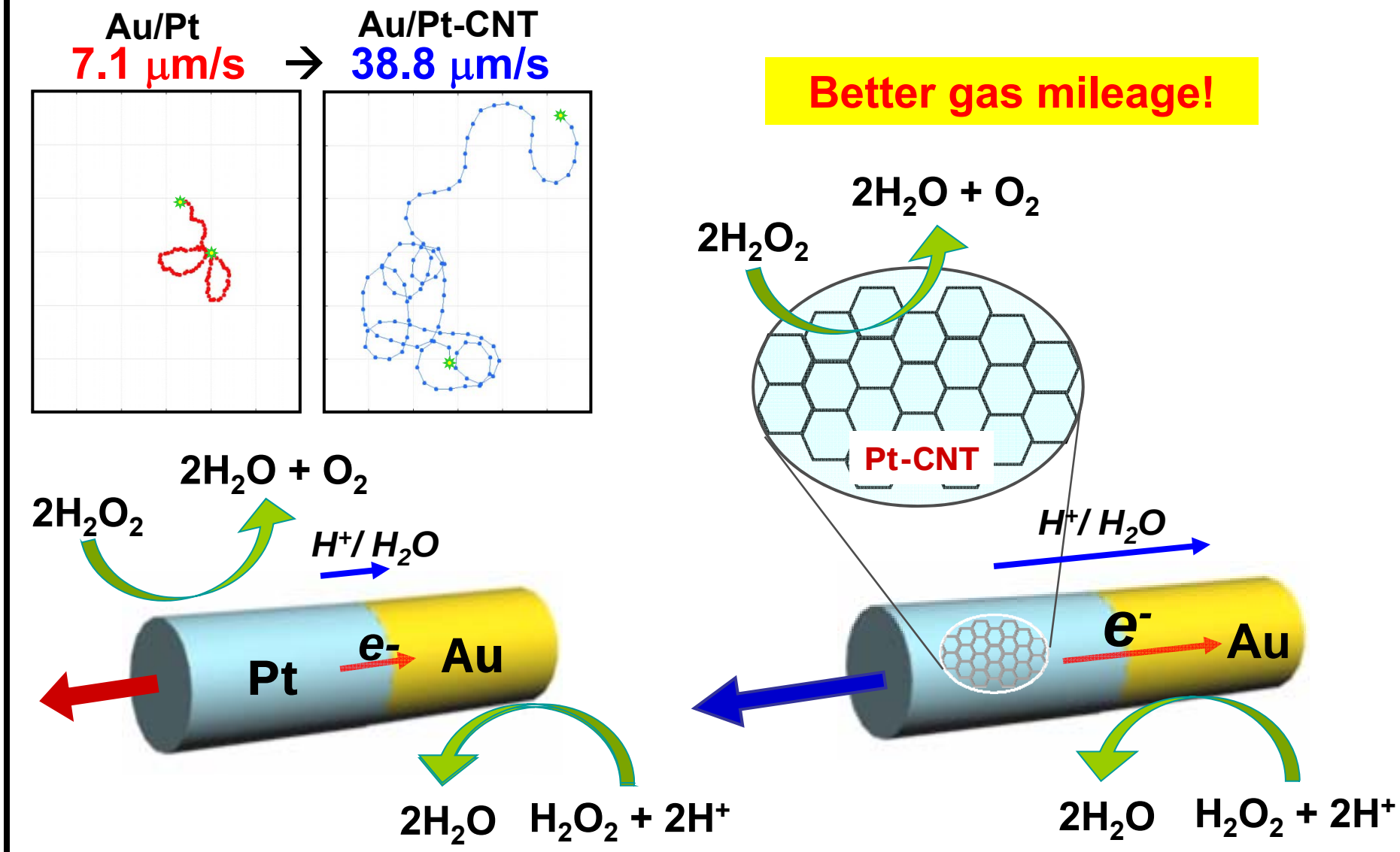

Higher velocity due to higher rate of peroxide decomposition at the CNT-Pt segment

TEMPERATURE-MODULATED MOVEMENT

Thermally modulating and activating the motion

On-demand acceleration and slowing down

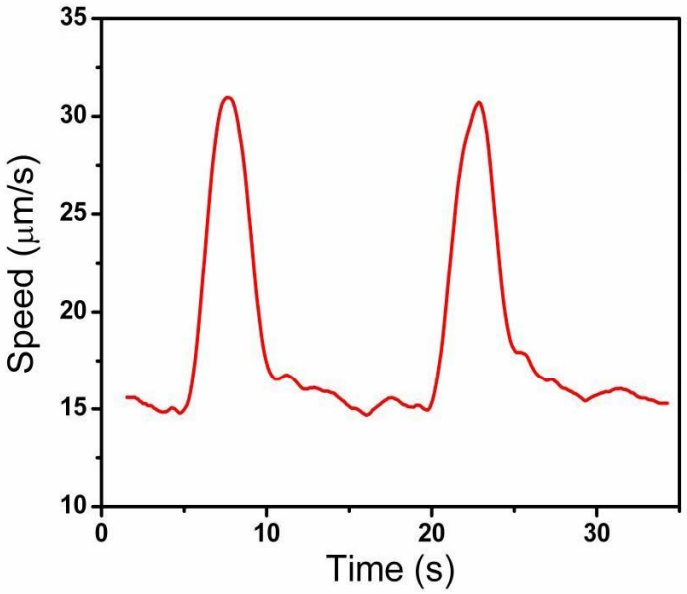

Pt-Au Nanomotors at room (A) and elevated (B)

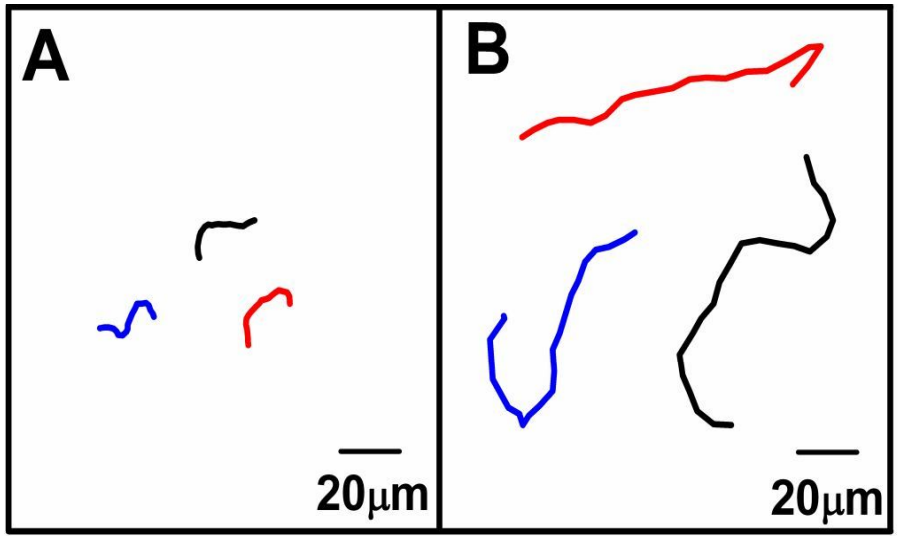

High temperature Electrochemical Propulsion

Faster kinetics of the fuel redox processes and lower solution viscosity associated with the heat pulse.

Wang, Small 2009

DIRECTION OF MOTION

3.3-um Au/Pt rod
(image capture)

Same rod
(video capture)

Moves Pt end forward: Excludes Bubble propulsion (momentum recoil)

Bubble Propulsion Catalytic Motors: Whitesides, Sanchez, Wang , Feringa

Electrokinetic Mechanism

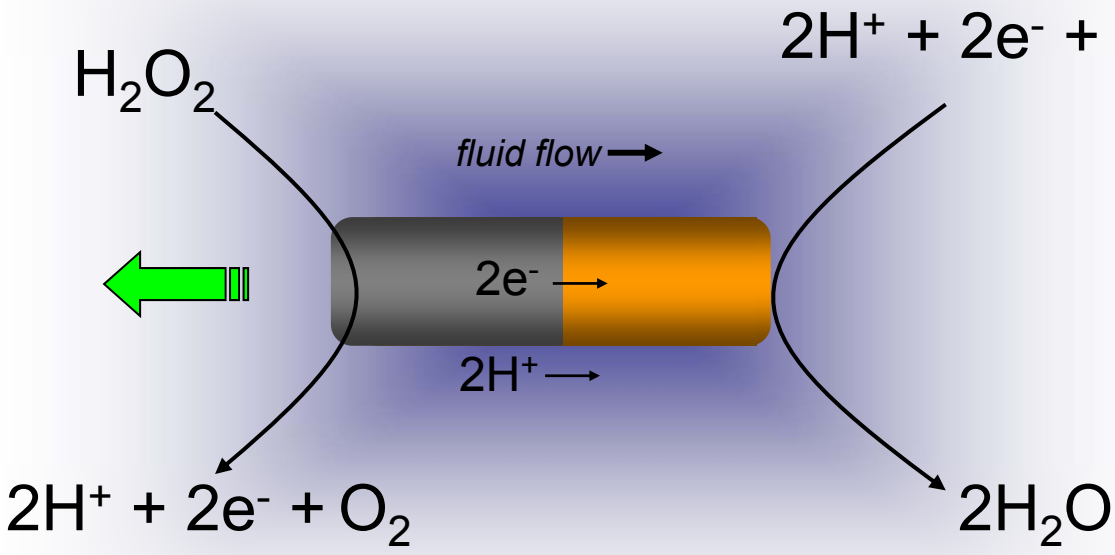

$$i_{e^-} = i_{H^+}$$

$$E = \frac{J_{H^+}}{\sigma}$$

$$v = \frac{\zeta \varepsilon E}{\mu} f$$

At Pt: $H_2O_2 \rightarrow O_2 + 2H^+ + 2e^-$

At Au: $H_2O_2 + 2H^+ + 2e^- \rightarrow H_2O$

J = current density
σ = conductivity
E = electric field

J. Am. Chem. Soc., **2006**

Measuring Current in Small Systems

- Pt/Au motor
  - Interdigitated Array
    - baseline: <0.00001 A/m^2
    - water: ~0.00001 A/m^2
    - 0.6% H_2O_2: 0.27 A/m^2
    - 3% H_2O_2: 0.53 A/m^2
  - Predicted Electric Field ($E=J/\sigma$)
    - J = 0.53 A/m^2
    - σ = 4.1 μS/cm
    - **E = 13.1 V/cm**

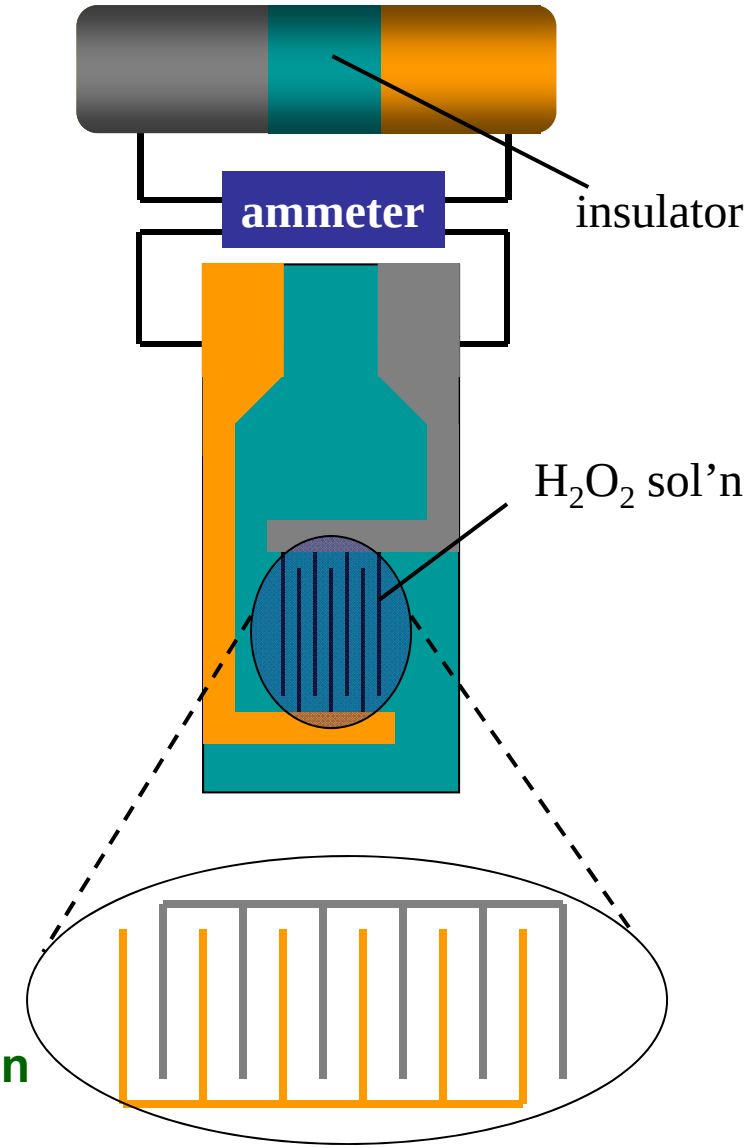

Allows Prediction of Speed and Direction of Motion For Different Bimetallic Pairs *(Langmuir, 2006)*

Tracking Data for Bimetallic Nanorods in 5 wt % Aqueous H_2O_2 Solution

Bimetallic Nanorod	Speed (μm/s)	Directionality	Leading end (observed)	Leading end (predicted)
Rh-Au	23.8 ± 2.9	0.73 ± 0.15	Rh	Rh
Pt-Au	20.0 ± 3.8	0.84 ± 0.04	Pt	Pt
Pd-Au	15.3 ± 2.0	0.92 ± 0.05	Pd	Pd
Pt-Ru	30.2 ± 4.0	0.65 ± 0.11	Pt	Pt
Au-Ru	24.0 ± 2.0	0.90 ± 0.05	Au	Au
Rh-Pt	17.0 ± 3.0	0.79 ± 0.13	Rh	Rh
Rh-Pd	16.2 ± 1.8	0.84 ± 0.14	Rh	Rh
Pt-Pd	13.6 ± 2.3	0.63 ± 0.10	Pt	Pt
Ni-Au	4.75 ± 1.1	0.33 ± 0.12	Ni	Ni

Langmuir, 2006

Effect of Ethanol on the Catalytically Generated Current Between a Platinum and a Gold Electrode

% Ethanol (v/v)	Current density[a] ($\times 10^2$ A/m^2)	Axial velocity (μm/s)
0	2.61(3)	19
10	1.67(1)	8.8
20	1.21(2)	7.2
33	0.90(1)	5.6
90	0.278(3)	2.4
H_2O[b]	0.0043(8)	-

[a]Current density calculated from measured current divided by the area of exposed platinum (2.62×10^{-4} m^2).
[b]H_2O is the baseline current density in pure deionized water without added H_2O_2 or ethanol.

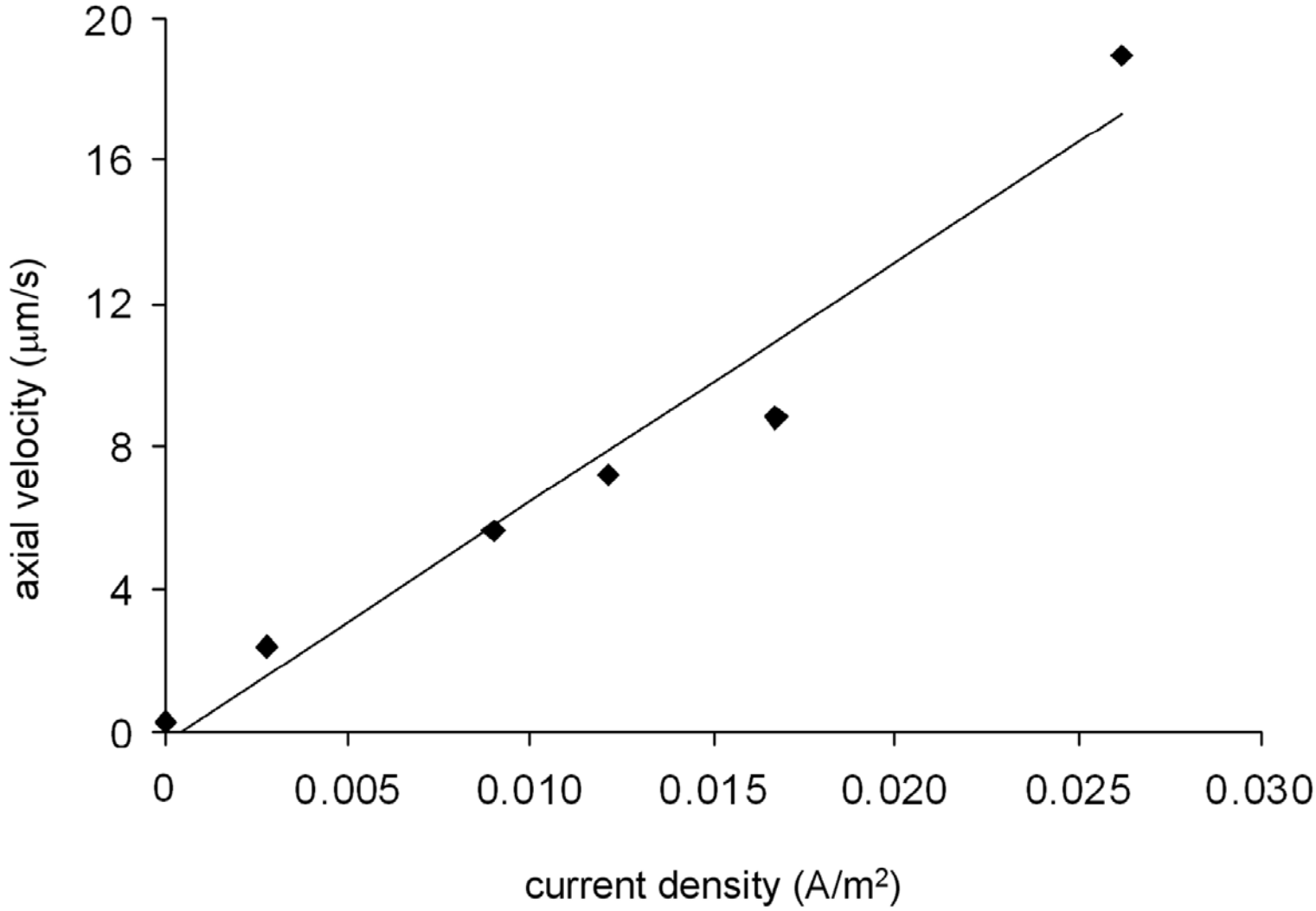

Plot of axial velocities of Pt/Au rods vs. current density in ethanol/H_2O_2 solutions

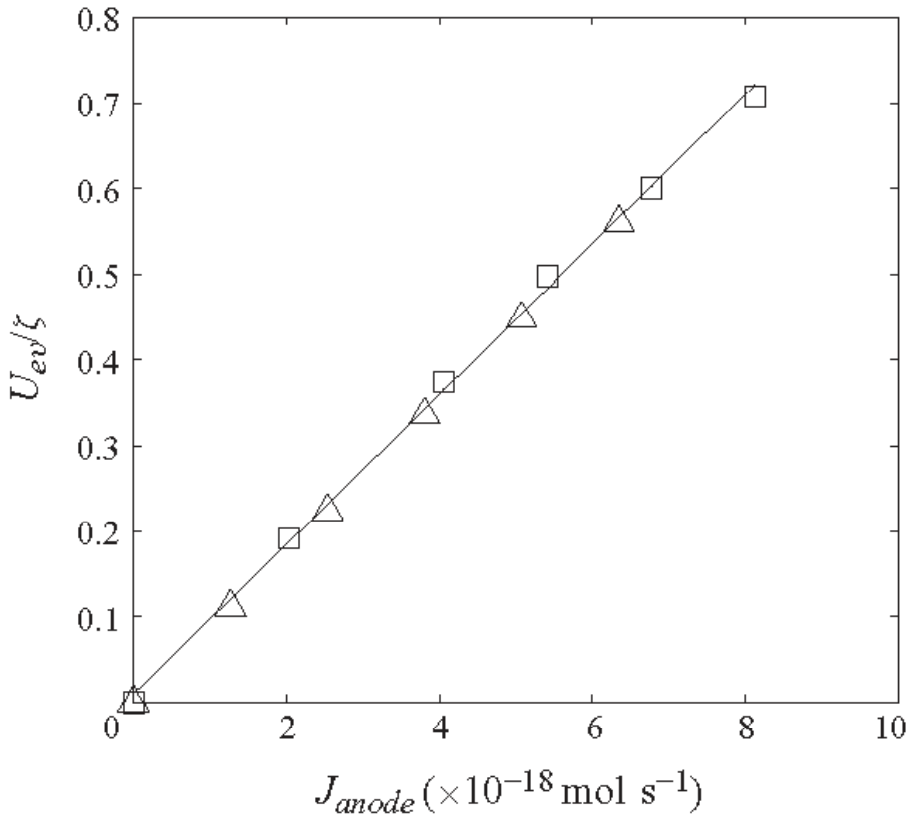

FIGURE 10. Electroviscous velocity normalized by zeta potential (units of μm s^{-1} mV^{-1}) as a function of total proton flux out of anode surface J_{anode} (defined in the text) for data of Moran *et al.* (2010) (△) and current data (□). These plots support the prediction of (3.61) that the ratio of velocity to zeta potential should scale linearly with the proton flux. Also note that the slope of the old and new data is essentially the same; this is expected because the constants in the scaling relationship (λ_D, h, D_+, etc) are unchanged from the old to the new simulations.

Posner, J. Fluid. Mech. (2011)

Rod Speed vs. Conductivity

$$v = \frac{\zeta \varepsilon E_x}{\mu} f$$

$$v = \frac{\zeta \varepsilon}{\mu} \frac{J}{\sigma} f$$

As conductivity *increases*, velocity should *decrease*!

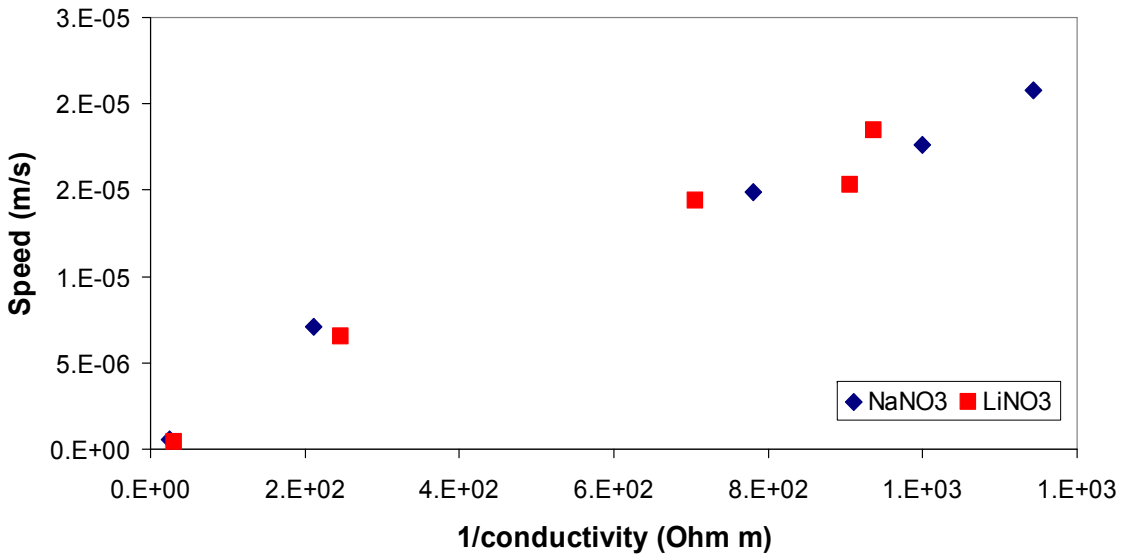

slowing due to decreased conductivity

PtAu rods; 3% H_2O_2

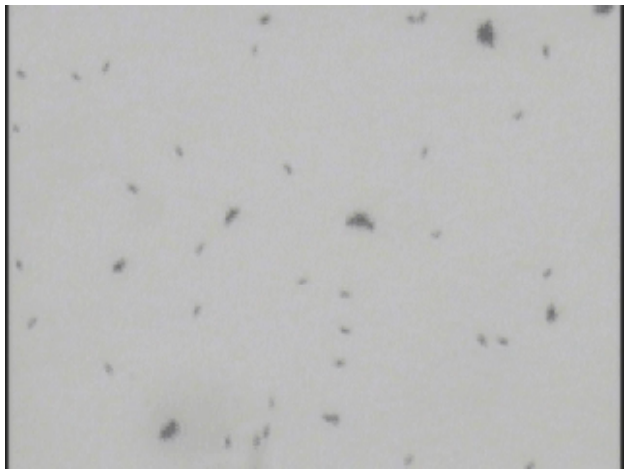

PtAu rods; 3% H_2O_2; 3 mM $NaNO_3$

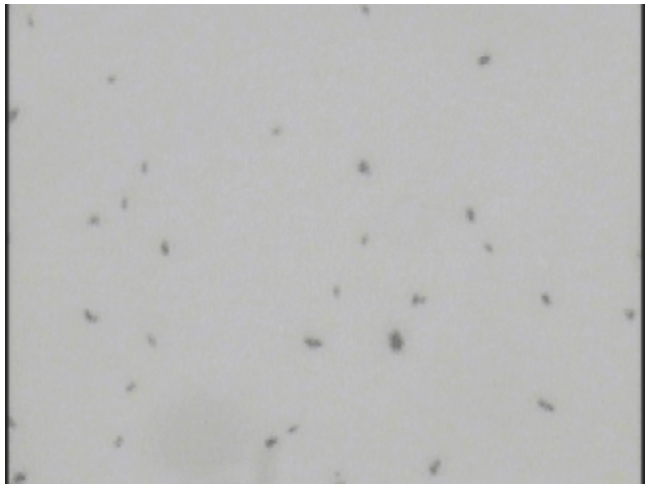

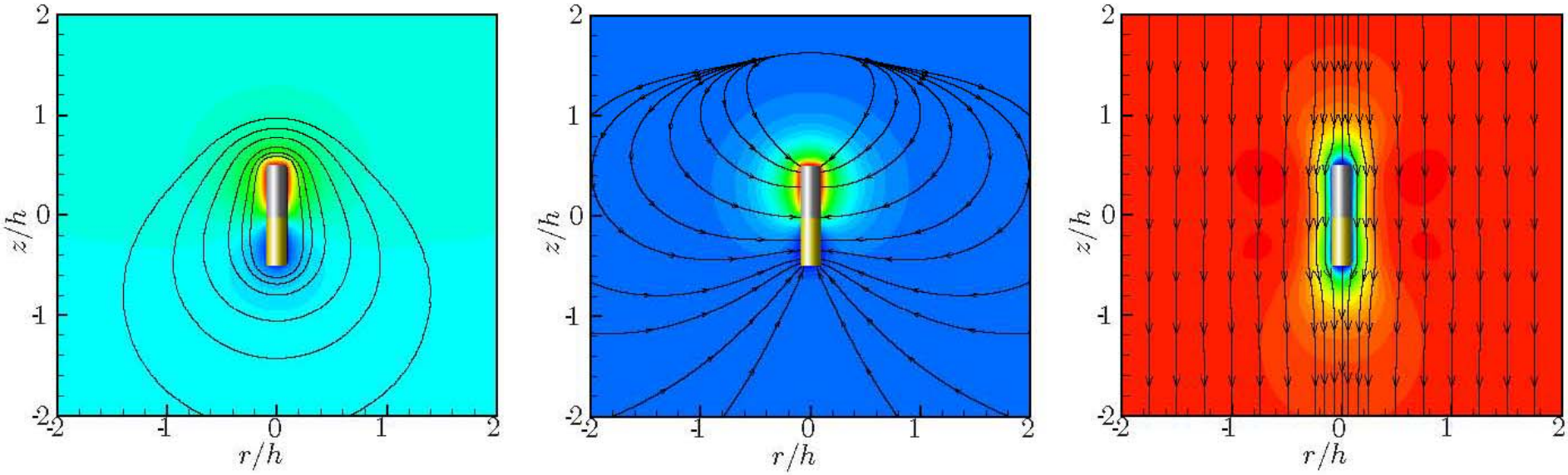

(Left) Simulation-generated plots of normalized proton concentration c^* (colors) and electrical potential ϕ^* (contour lines)

(Middle) Charge density ρ_e/ρ_{e0} (color) and electric field (streamlines)

(Right) Reaction induced charge auto-electrophoresis (RICA) velocity magnitude (colors) and streamlines (black lines) for the case $\zeta = -10$ mV and dimensionless flux $j/j_d = 0.8$.

The reactions lead to an asymmetry in the proton concentration such that an excess of protons builds up at the anode and protons are depleted at the cathode. The excess of protons results in positive charge density at the anode and the generation of electric field pointing from the anode to the cathode.

Posner, J. Fluid. Mech. (2011)

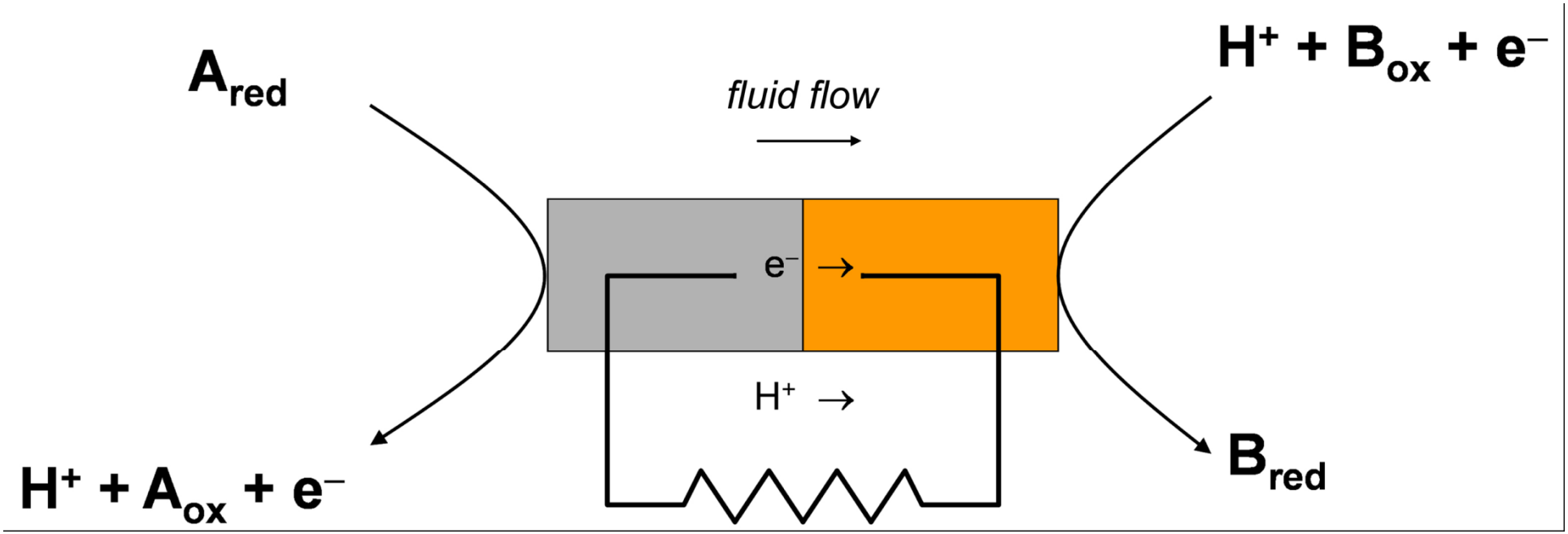
A_{red}
fluid flow
$H^+ + B_{ox} + e^-$
e^-
H^+
$H^+ + A_{ox} + e^-$
B_{red}

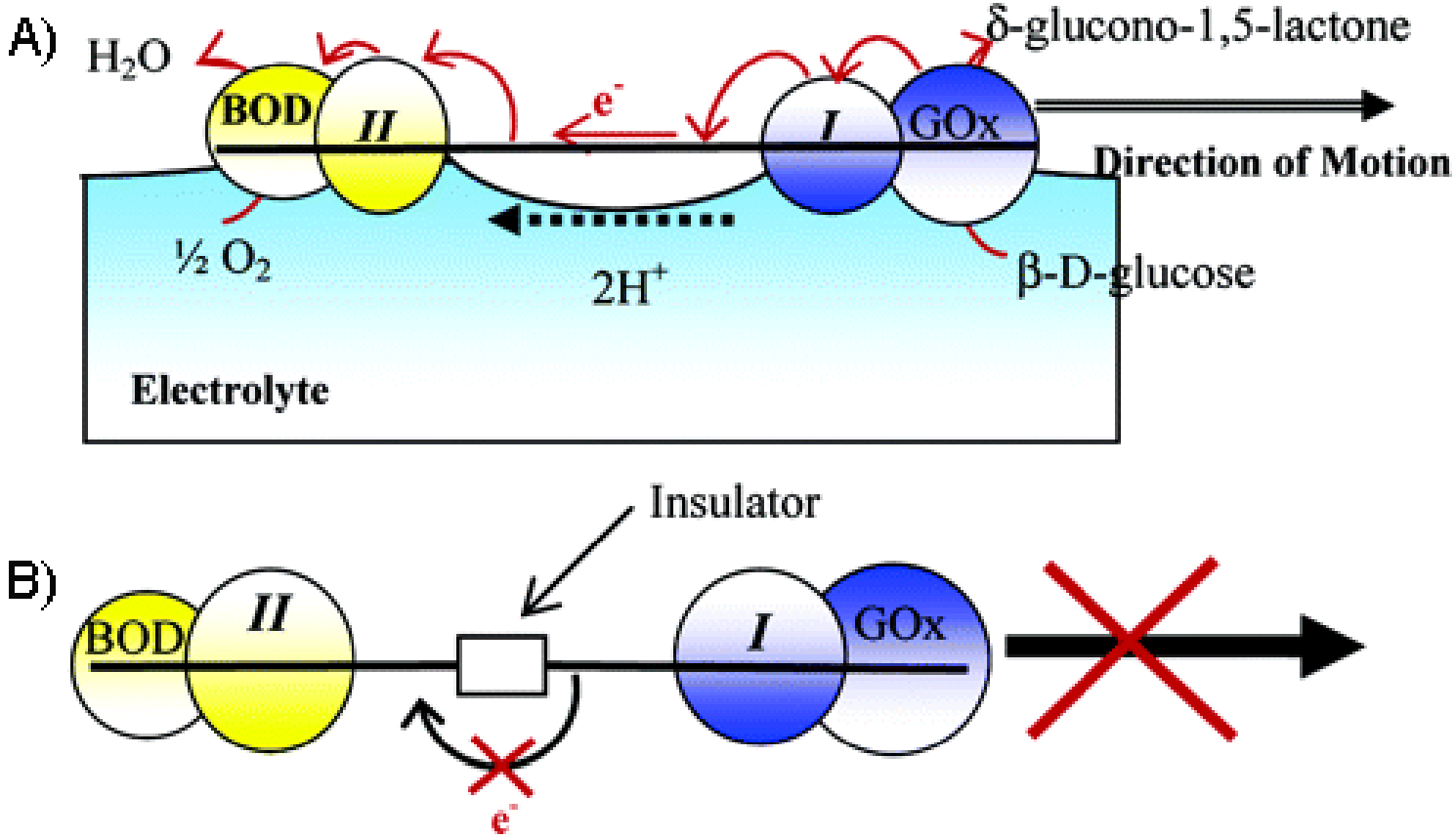

(**A**) A self-propelled bioelectrochemical motor consisting of a carbon fiber functionalized with glucose oxidase (GOx) and redox polymer ***I*** on one end and bilirubin oxidase (BOD) and redox polymer ***II*** on the opposite end. When the fiber is placed on a pH 7 buffer solution containing 10 mM glucose, electrons flow along the path *glucose* → *GOx* → ***I*** → *carbon fiber* → ***II*** → *BOD* → O_2, and the fiber is propelled at the solution-O_2 interface by the ion flow accompanying the flow of electrons. (**B**) When an insulator is introduced between the two electrocatalytic fiber ends, the fiber does not move.

N. Mano , A. Heller, *J. Am. Chem. Soc.* **2005**

Relevance to Biological Systems

- Examples of motility mechanisms:
  - flagellar systems (ATP motors) (*e. coli*)
  - polymerization systems (*listeria*)
  - **unknown systems** (*synechococcus*)[a]
- Our system may help understand how synechococcus bacteria swim

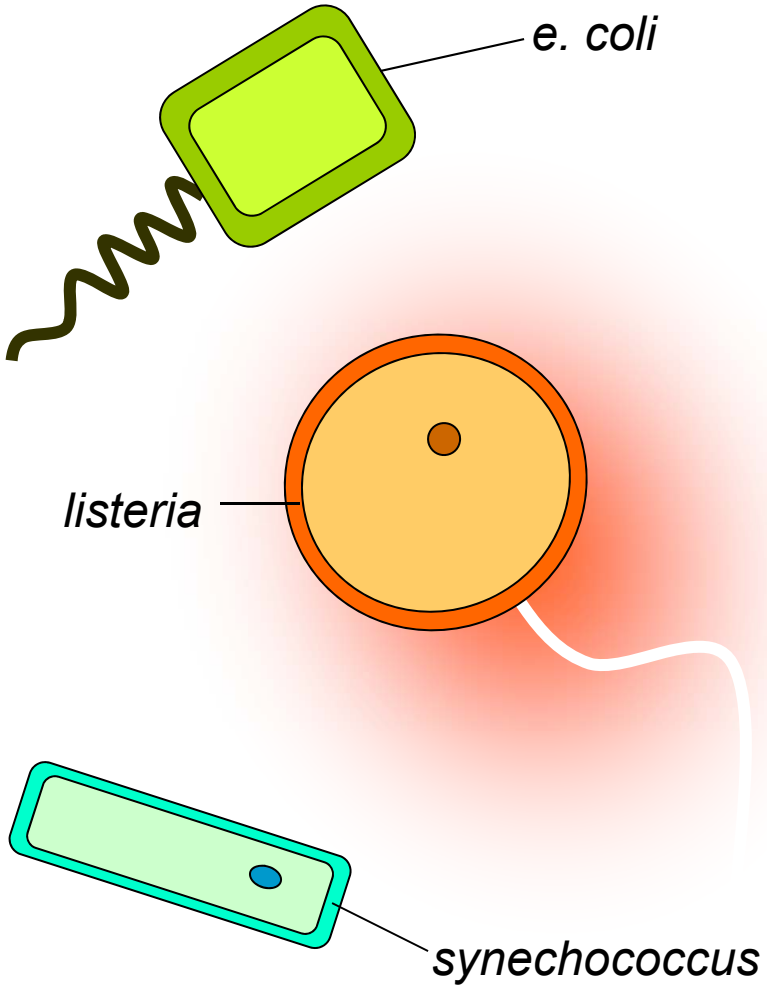

[a] Waterbury and Willey, *Science,* **1985,** *230,* 74-76.

Design of Magnetic Motors

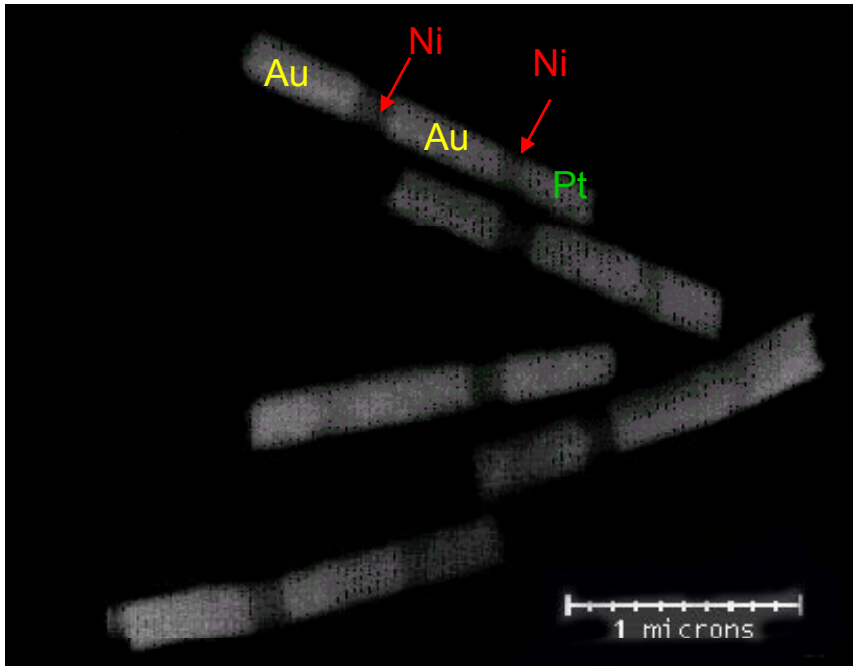

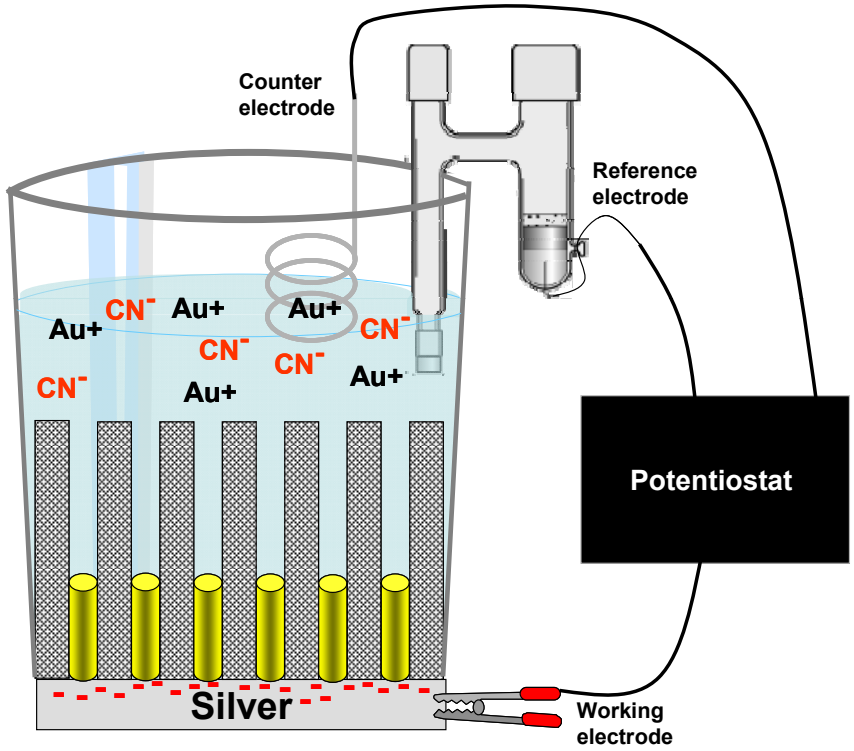

~1.5μm striped rods after release. Concavity permits designation of metal order

Following Whitesides (**2003**)

***Angew. Chem.*, 2005**

Autonomous Magnetized Moving Rods Response to Magnet

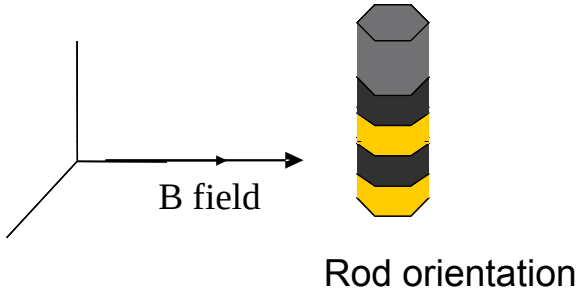

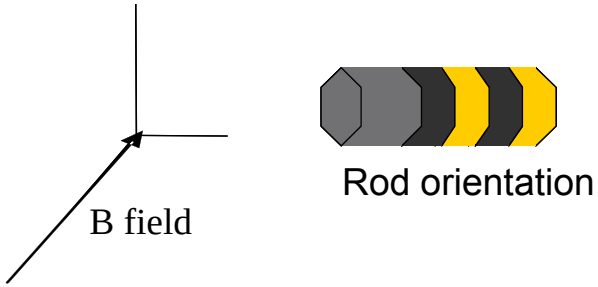

~1.5μm striped rods moving in dilute solution of H_2O_2

Angew. Chem., 2005

Rod size and magnetic moments similar to magnetotactic bacteria

Effects of the Field

	Not magnetized 0% H_2O_2	No field 5% H_2O_2	In field 5% H_2O_2
Directionality (0.1 sec)	0.0	0.5	0.4
Net forward (μm/sec)	0.0	2.9	2.4
Directionality (2 sec)	-	0.6	0.8
Rotational diffusion coefficient (deg^2/sec)	200	2000	60

Demonstrating Micron Control

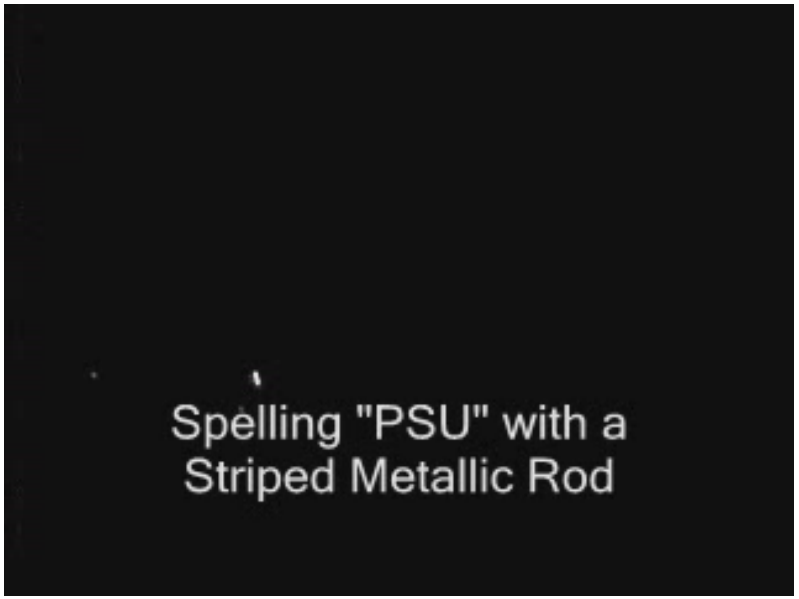

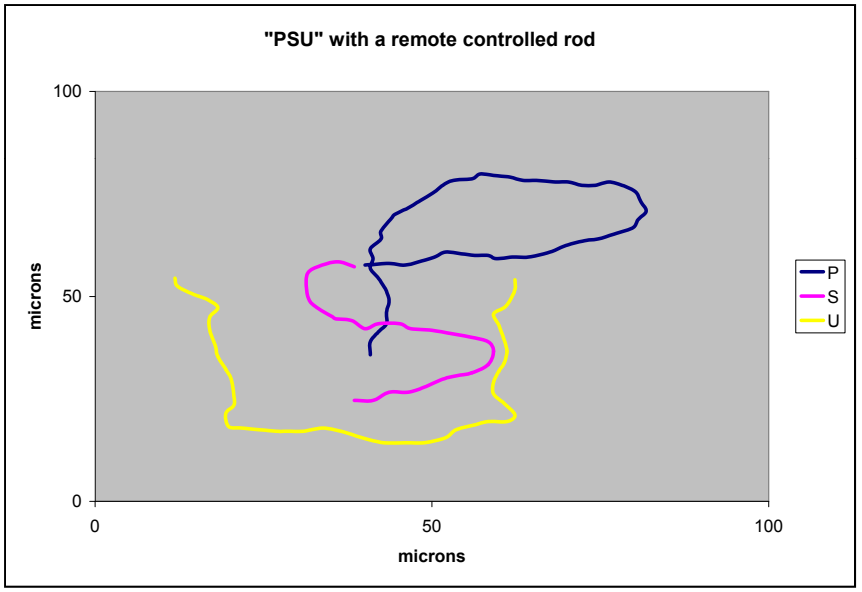

Spelling “PSU” by hand, rotating a stack of NdFeB magnets to steer the magnetized rods while in a dilute solution of hydrogen peroxide

Other Magnetically Guided Catalytic Motors: Wang, Sanchez

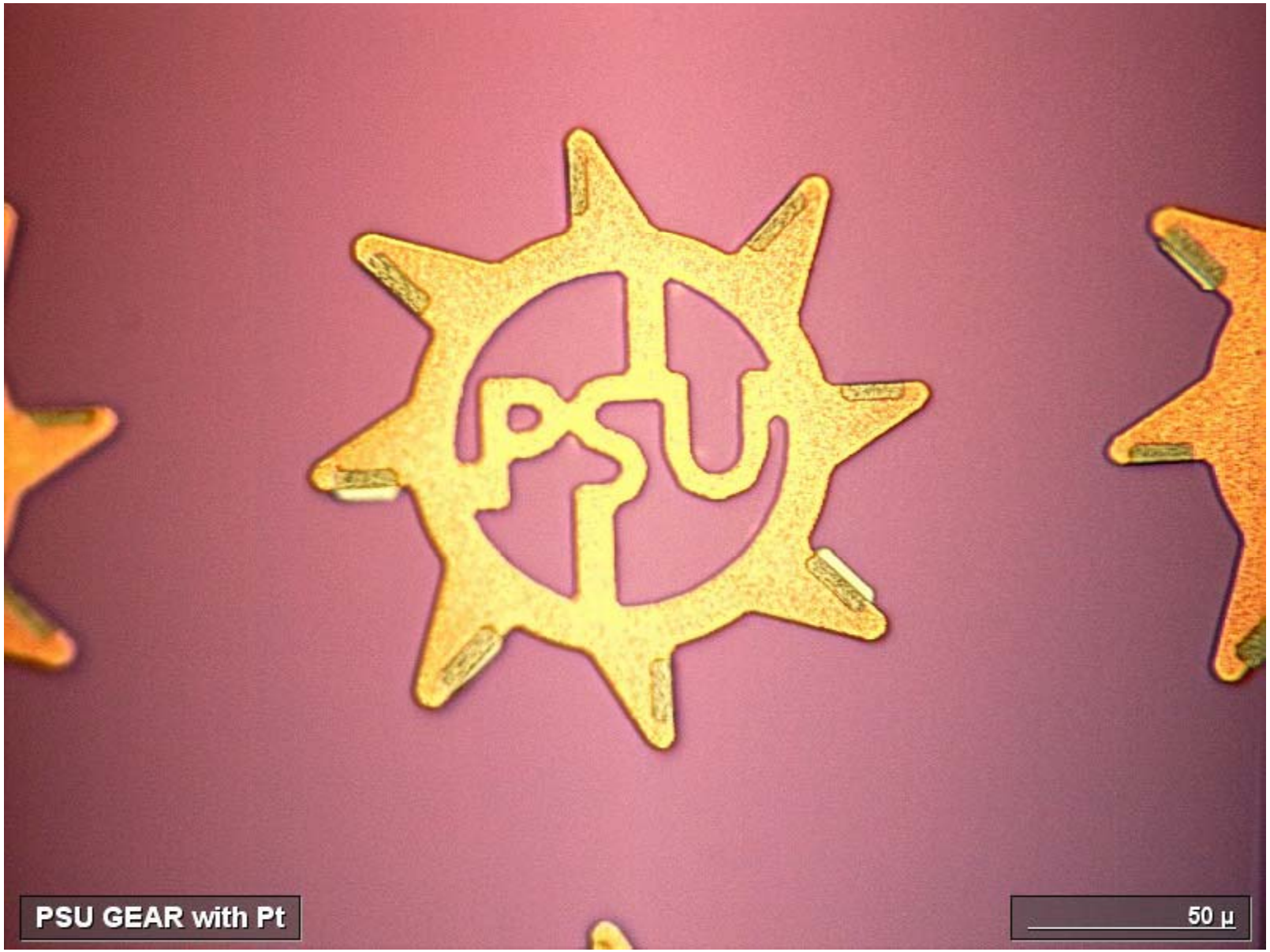

SMALL, 2005

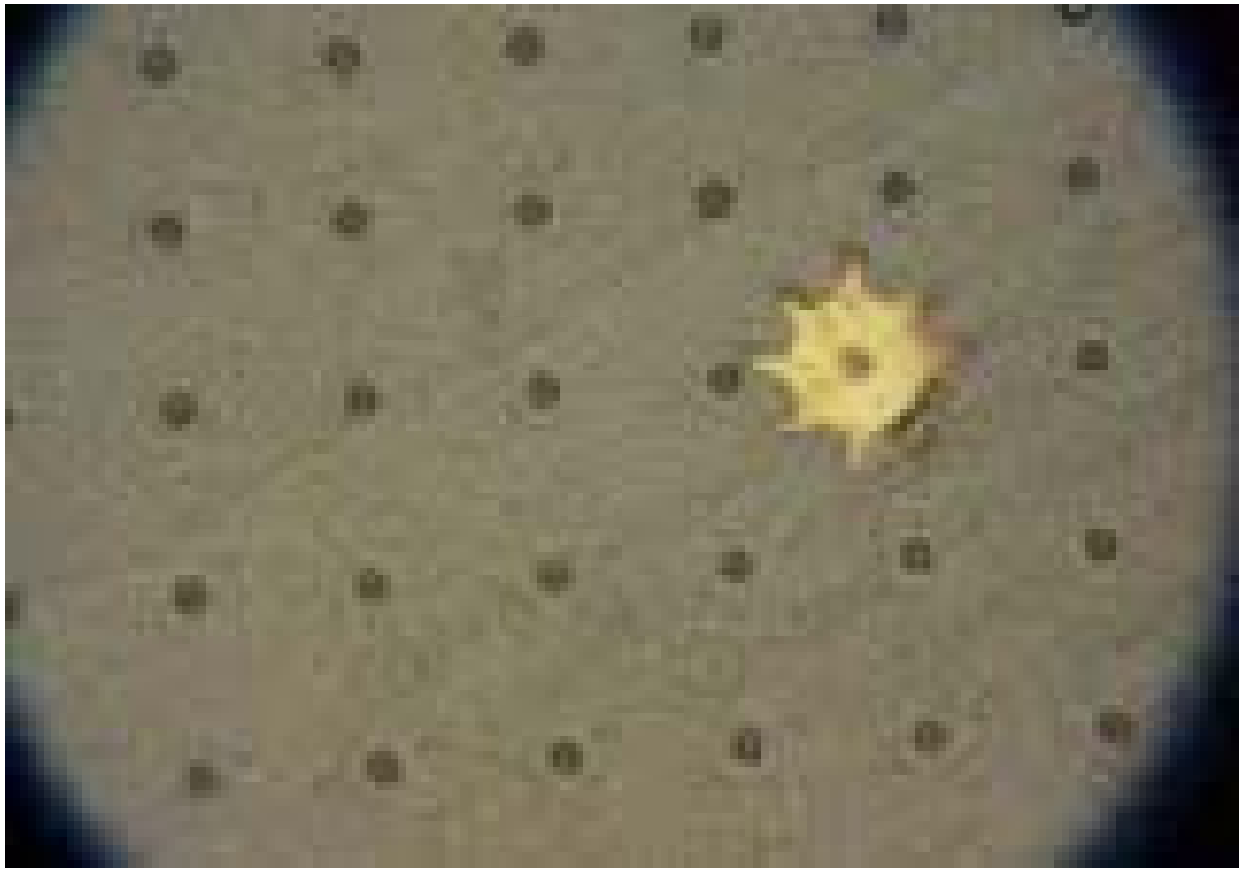

real-time video at http://research.chem.psu.edu/axsgroup/


Fabricated Gear System-10x
0.1 mm

Designing Functional Nano/Microbots

Required Design Elements

- Movement Through Catalysis
- Cargo Loading, Transport, and Unloading
- Directional Movement Through Chemical Gradient (Chemotaxis)
- Emergent Collective Behavior Through Inter-Bot Communication via Chemical Signals

Transporting Cargo: The Vision

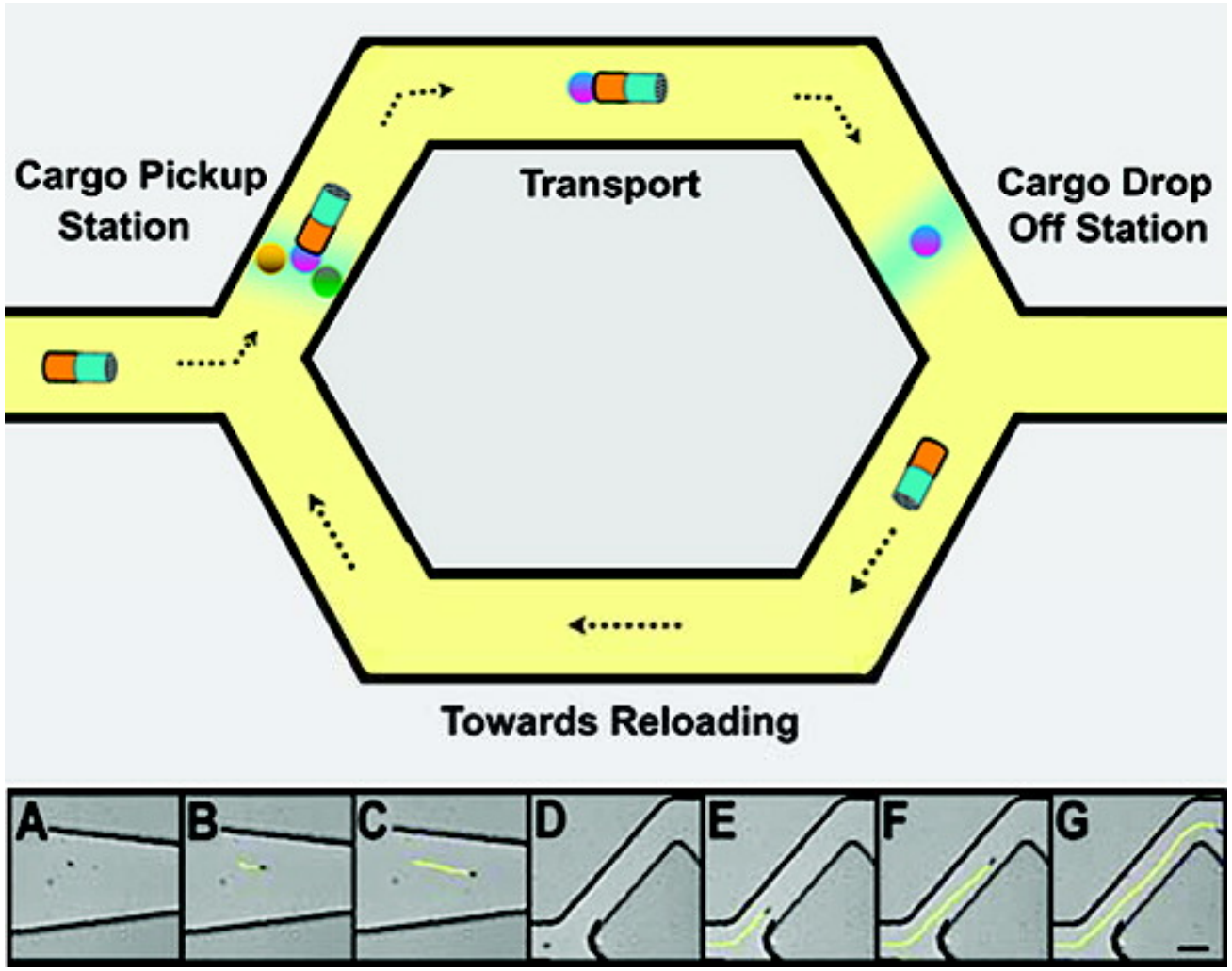

Wang, *ACS Nano* **(2009)**

Attaching Payload to Nano/Micromotors

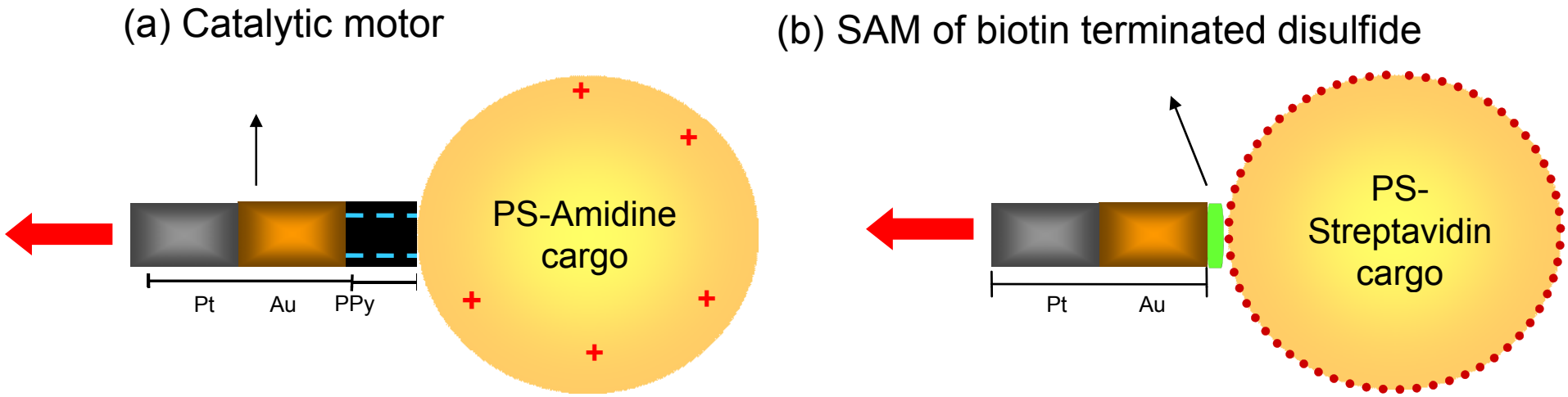

Cargo attachment by:
(a) electrostatic interaction between the negative polypyrrole (PPy) end of a platinum/gold/polypyrrole motor and a positively charged polystyrene (PS) amidine micro-sphere
(b) biotin-streptavidin binding between the gold tips of platinum/gold rods functionalized with a biotin-terminated disulfide and streptavidin-coated cargo

Nano Lett., 2008

Other Cargo-carrying Catalytic Motors: Wang, Sanchez

Pt-Au-PPy with Amidine Microspheres

Rod: 3 μm; Cargo: 2 μm

1000 x Dark Field Reflection Microscopy

Experimentally observed doublet speeds versus theoretical expectations based on calculations.
The equivalent sphere radius R_{eq} of a rod (Pt-Au-PPy) or a rod-sphere doublet is the radius of a sphere which has the same drag coefficient.

R_{cargo} (μm)	R_{eq} doublet calculated by CDL-BIEM (μm)	Velocity ratio predicted by R_{eq}	Experimentally observed velocity ratio ($U_{doublet} / U_{rod}$)		
			I	II	III
0	0.46 - 0.53	NA	NA	NA	NA
0.38	0.59 - 0.65	0.78 - 0.81	0.80 ± 0.03	0.79 ± 0.01	0.76 ± 0.04
0.60	0.76 - 0.81	0.61 - 0.66	0.67 ± 0.01	0.67 ± 0.01	0.63 ± 0.03
1.05	1.14 - 1.18	0.40 - 0.45	0.53 ± 0.01	0.54 ± 0.00	0.49 ± 0.01

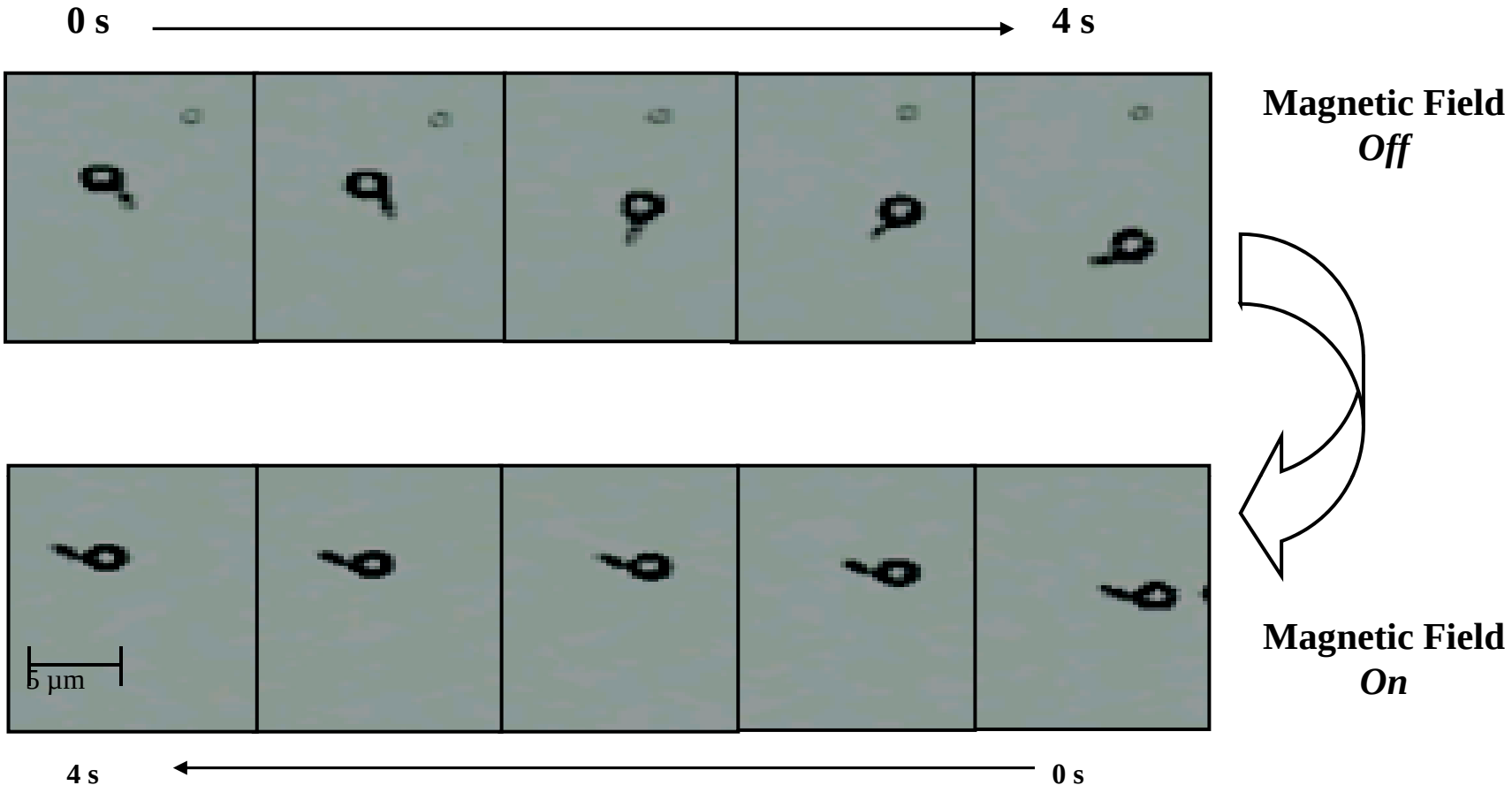

Optical microscopy images of a Pt-Ni-Au-Ni-Au-PPy motor pulling 1.05 µm radius cargo showing the trajectory over 4 sec

Nano Lett., 2008

From Motors to Micropumps

Motor

- Suspended motor moves itself.

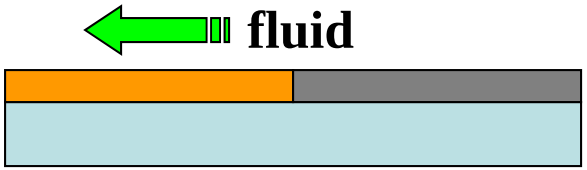

Micropump

- Immobilized motor moves surrounding fluid
- Channel-free directed fluid flow

Catalytically Induced Fluidic Pumping-Marangoni Convection

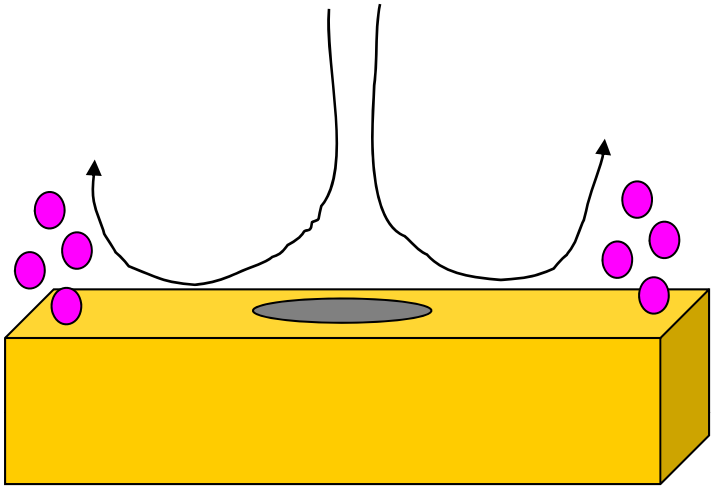

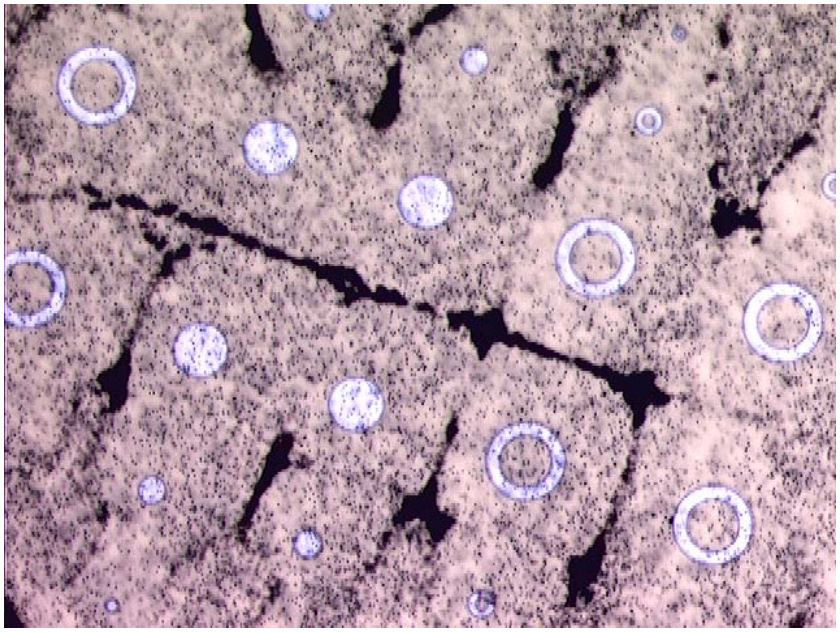

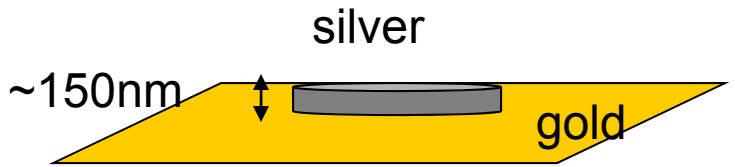

Microfluidics By Catalysis:

Real-time convective-motion of 2 μm gold rods on Ag patterned gold surface at 500x*

Real-time pattern formation of 1 μm polystyrene spheres on Ag patterned gold surface at 500x*

*0.5% w/w aqueous solution of hydrogen peroxide

Microfluidics By Catalysis

Convection and pattern formation not unique to gold and polystyrene!

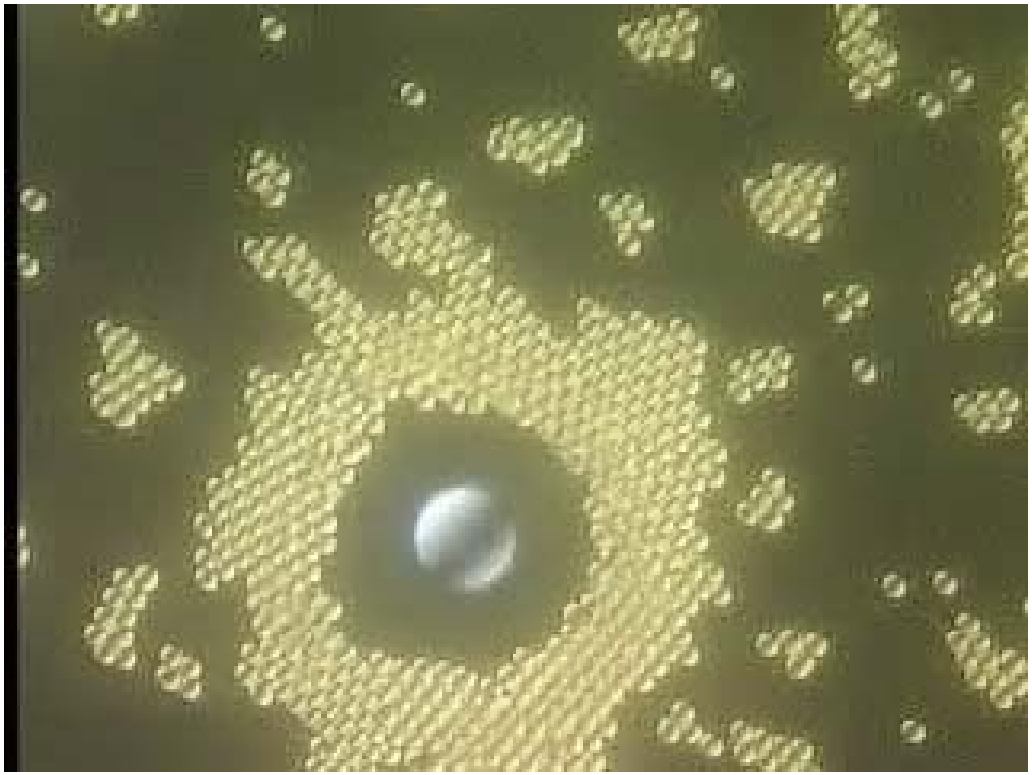

Real-time movie of silica spheres 2.3 μm in diameter exhibiting pattern formation on Ag patterned gold surface at 500x

Colloid Behavior as a Function of the Surface Charge

Real-time convective-motion of amidine terminated polystyrene (2 μm) spheres on Ag patterned gold surface at 500x

Real-time pattern formation of 1 μm polystyrene spheres on Ag patterned gold surface at 500x*

Why are polystyrene spheres of the same density behaving differently when only the colloid surface properties differ?

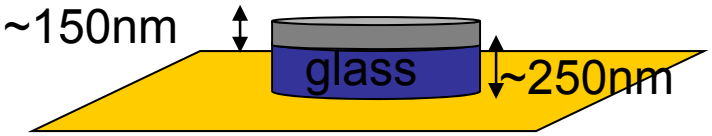

Evidence In Support of Electrokinetics

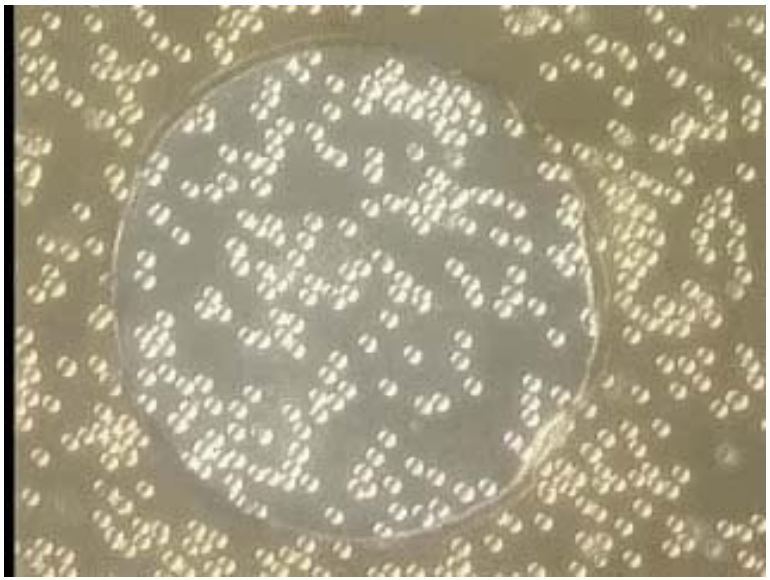

Real-time movie of silica spheres 2.3 μm in diameter pattern formation is now quenched on Ag patterned gold surface at 500x

Real-time movie of gold rods 2 μm in length convection is now quenched on Ag patterned gold surface at 500x

It is possible to turn off the convection/pattern formation by electrically isolating the silver from the gold!

Possible Model

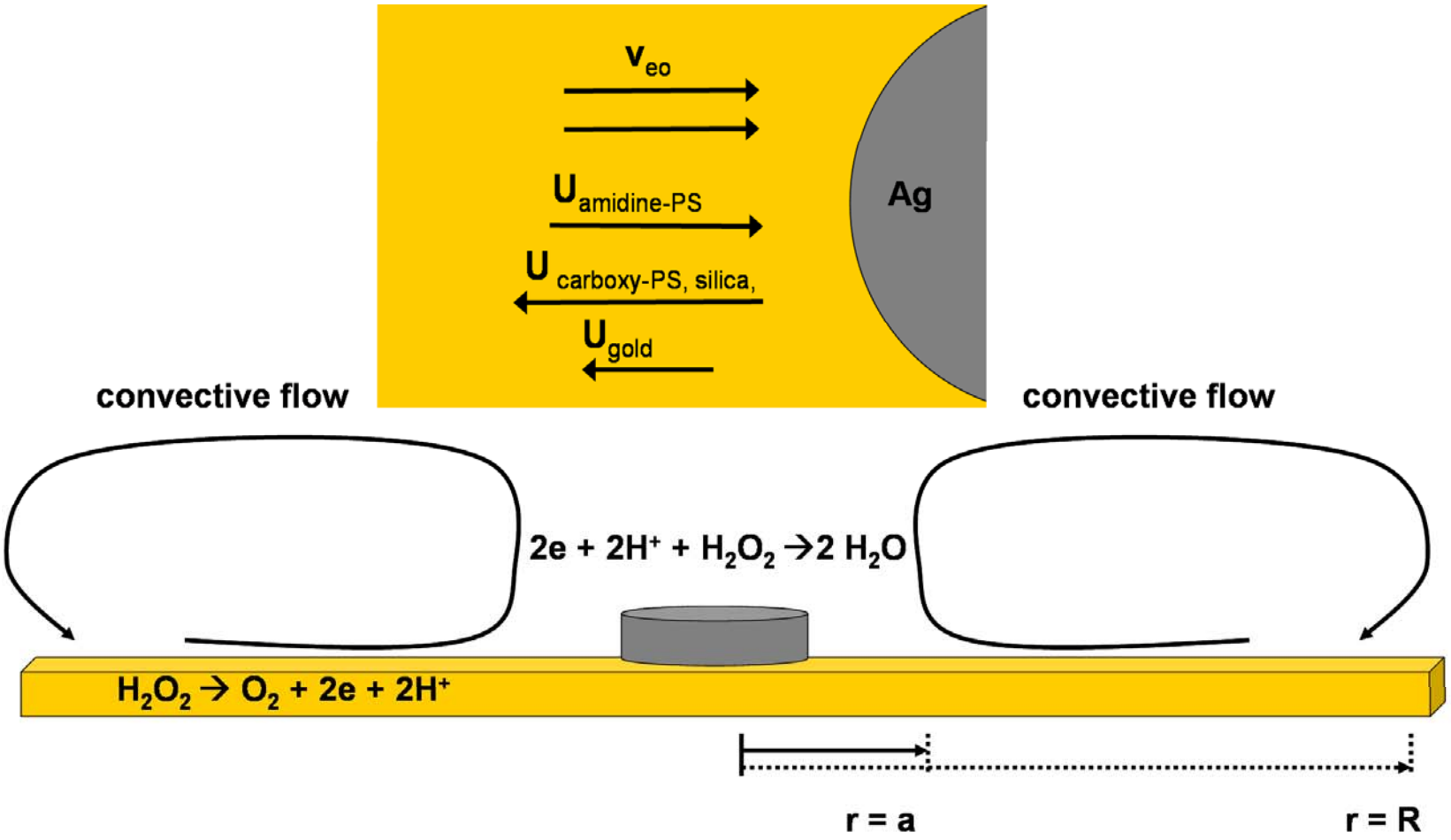

Here silver carries out the reduction of hydrogen peroxide (cathode) and gold the oxidation of hydrogen peroxide (anode). The proton gradient establishes an electric current.

J. Am. Chem. Soc., **2005**

BUBBLE POWERED SELF-PROPELLED MICROBOTS

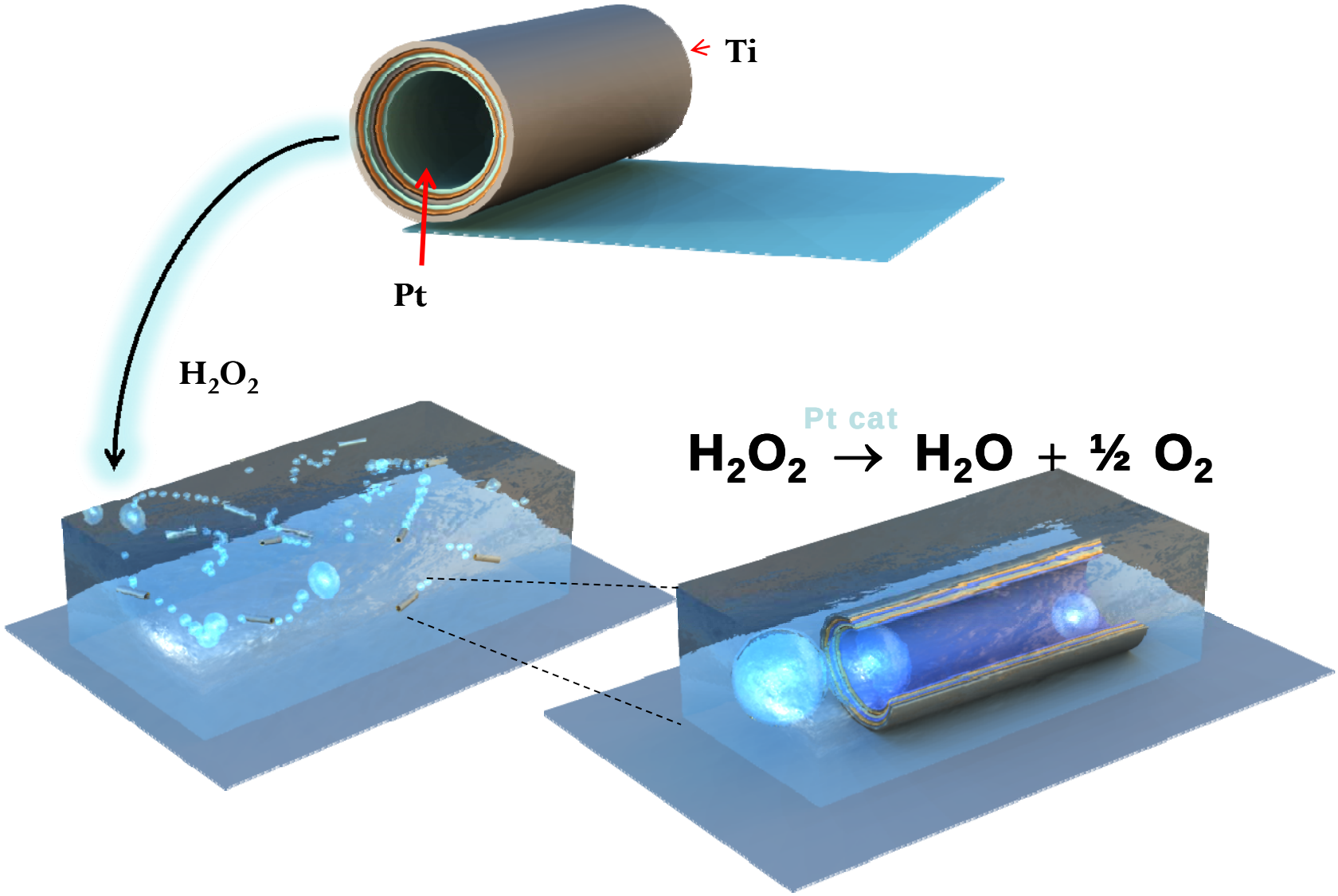

AUTONOMOUS TRAJECTORIES FROM TUBULAR MICROJETS

Solovev *et al., Small,* **5**, 1688 (2009)

DEPENDENCE ON FUEL CONCENTRATION

Bubble recoil mechanism

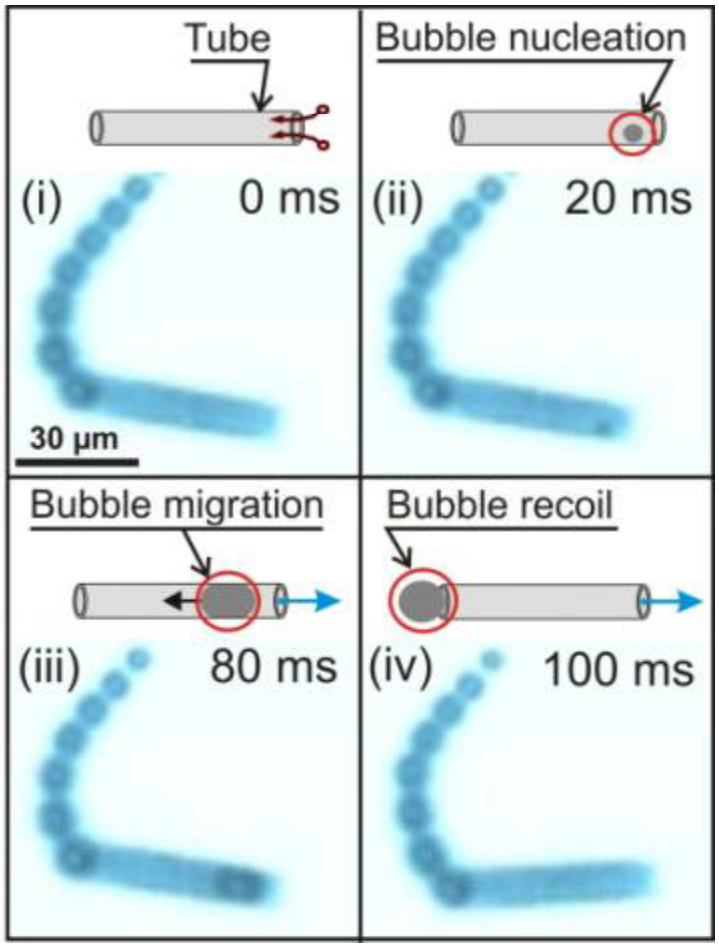

OPTIMUM FUEL CONDITIONS

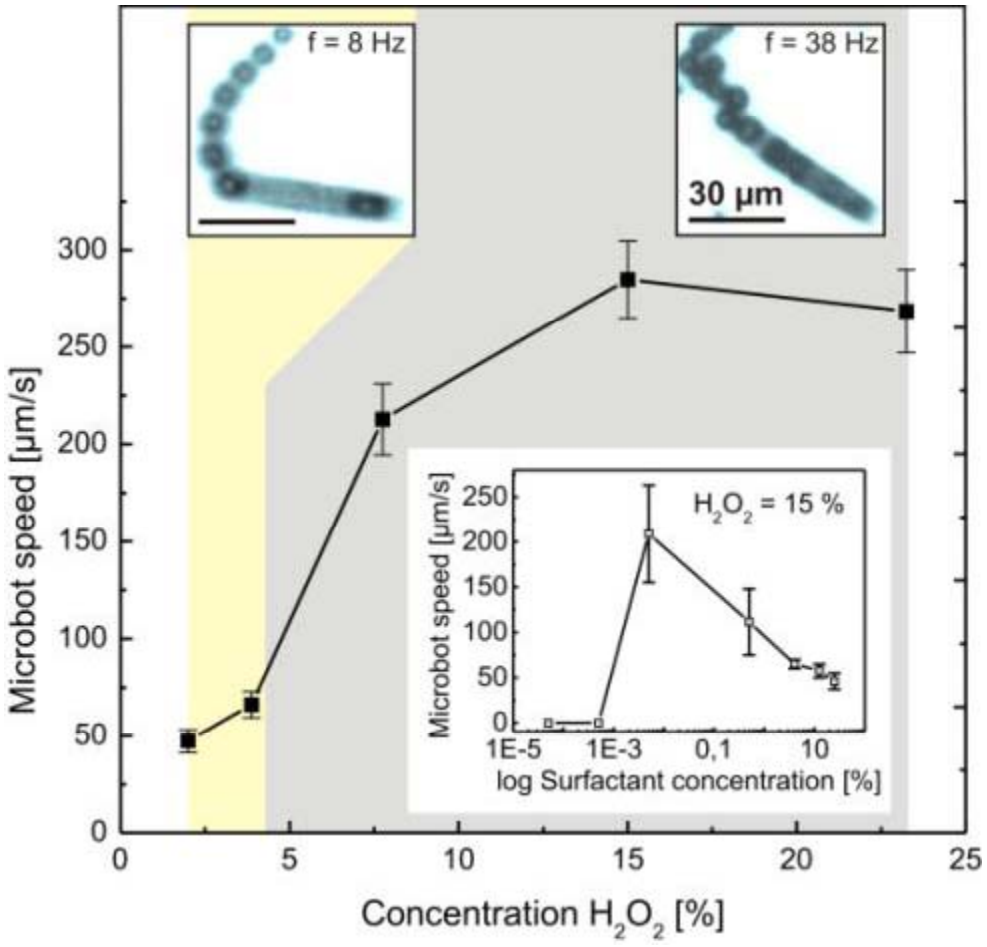

Solovev et al. *Adv. Funct. Mater*. **20**, 2430 (2010)

CONTROLLED MOTION OF TUBULAR MICROJETS

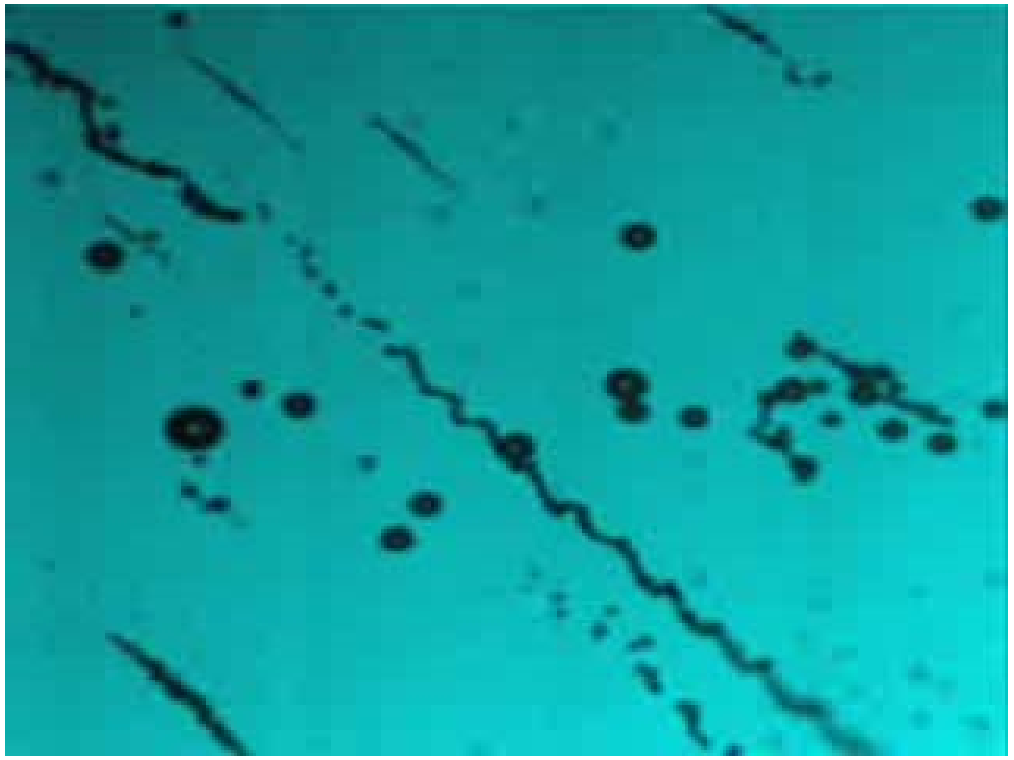

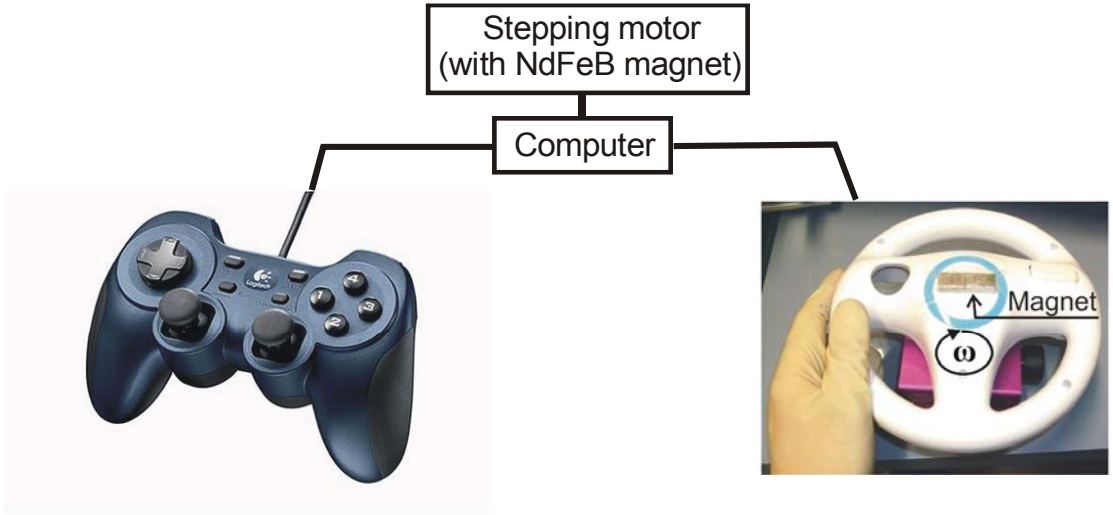

PICK-UP, TRANSPORT AND DELIVERY OF CARGO

1. EASY loading, transport of different micro-objects.

2. POWERFUL MICROENGINE

3. Delivery in specific targets.

Solovev *et al., Adv.Funct. Mat.* ***20****, 2430 (2010)*

SCALABILITY OF JET ENGINES

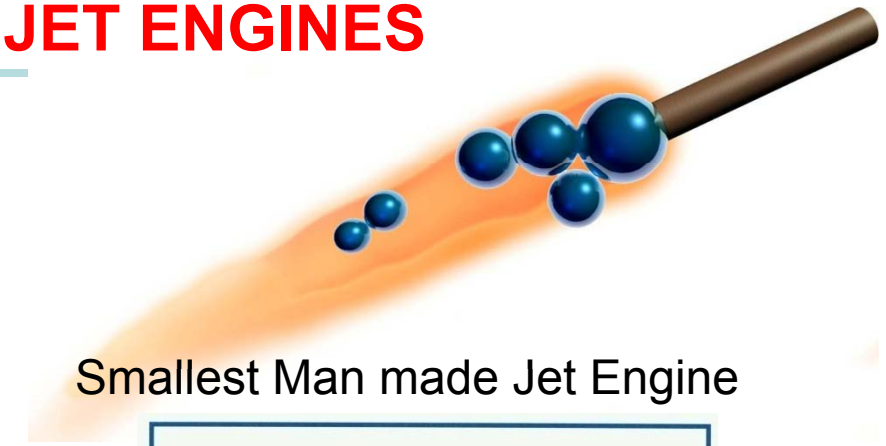

Biggest Man made Jet Engine

Smallest Man made Jet Engine

GUINNESS WORLD RECORDS

CERTIFICATE

The smallest man-made jet engine measures just 600nm across and weighs 1 picogram (10 ^ -15 kg). It was produced by Alex A. Solovev, Samuel Sanchez, Yongfeng Mei and Oliver G. Schmidt at the Leibniz Institute for Solid State and Materials Research (IFW Dresden) and demonstrated in Dresden, Germany, in September 2010

GUINNESS WORLD RECORDS LTD

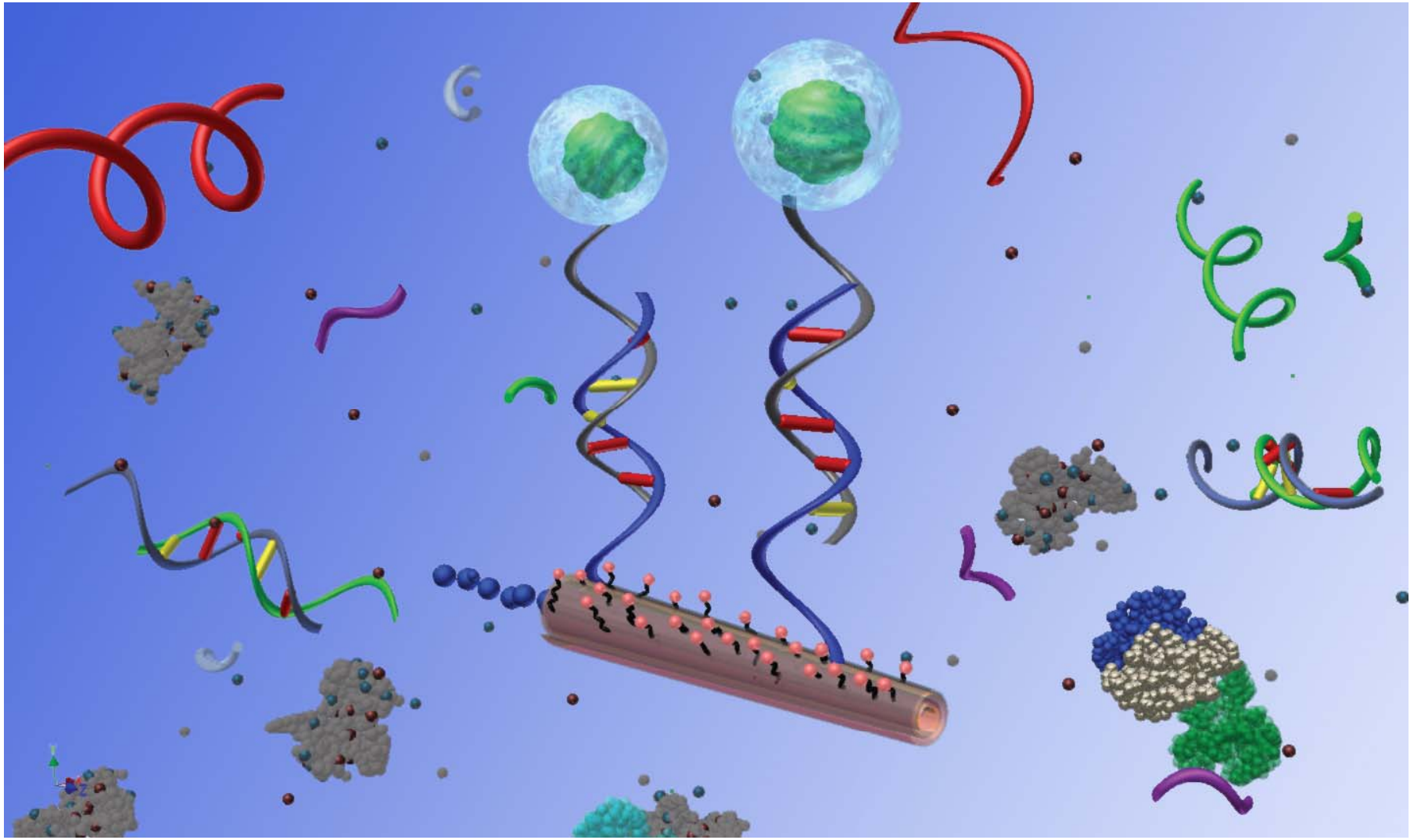

The micromachine-based target isolation concept offers numerous potential bioanalytical applications

Wang, Nano Lett. 2011

Wang, Angew. Chem. 2011

Selection and Isolation of Cancer Cells in Biological Fluids

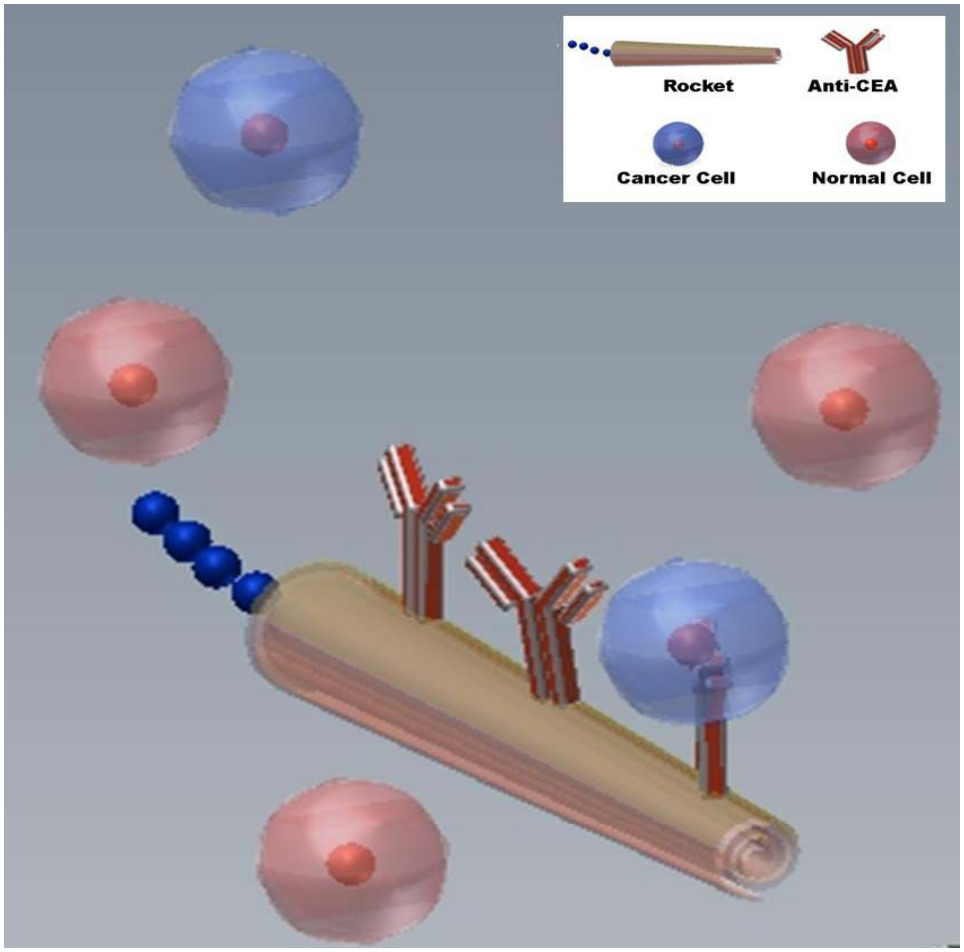

Immuno-micromachine for isolating CTCs

Capture and transport of a CEA + pancreatic cancer cell by an anti-CEA mAb modified rocket

Designing Intelligent Nano/Microbots: Synthetic Active Matter

1. Introduction to Synthetic Active Matter
2. Powering Active Particle and Fluid Motion
3. *Collective Behavior of Autonomous Nano/Microbots*

AYUSMAN SEN

Department of Chemistry, Penn State University
E-mail: asen@psu.edu

Designing Functional Nano/Microbots

Required Design Elements

- Movement Through Catalysis
- Cargo Loading, Transport, and Unloading
- Directional Movement Through Chemical Gradient (Chemotaxis)
- Emergent Collective Behavior Through Inter-Bot Communication via Chemical Signals

Quorum-Sensing Autonomous Nano/Microbots

- Bots Secrete Ions
- Electric Field Results from Different Diffusion Rates of the Cations vs. Anions
- Bots Move in Response to the Electric Field
- Bots Move Cooperatively in Response to Neighbors' Ion Gradients

Angew. Chem., 2009

DIFFUSIOPHORETIC MOTION OF PARTICLES BASED ON A GRADIENT OF ELECTROLYTE CONCENTRATION: ELECTROPHORESIS TENDS TO DOMINATE OVER CHEMOPHORESIS

$$U = \underbrace{\left(\frac{dLn(C)}{dx}\right)\left(\frac{D_C - D_A}{D_C + D_A}\right)\left(\frac{k_B T}{e}\right)\frac{\varepsilon\left(\zeta_p - \zeta_w\right)}{\eta}}_{\text{Electric Field}} + \underbrace{\left(\frac{dLn(C)}{dx}\right)\left(\frac{2\varepsilon k_B^2 T^2}{\eta e^2}\right)\left\{Ln\left[1-\tanh^2\left(\frac{e\zeta_W}{4k_B T}\right)\right] - Ln\left[1-\tanh^2\left(\frac{e\zeta_P}{4k_B T}\right)\right]\right\}}_{\text{Chemophoretic Term}}$$

U is the particle speed, dLn(C)/dx is the electrolyte gradient
D_C and D_A are the diffusion constants of the cation and anion components
k_b is the Boltzmann constant, T is the temperature, e is the elementary charge
ε is the solution permittivity, η is the dynamic viscosity of the solution,
ζ_P is the zeta potential of the particle,
ζ_W is the zeta potential of the wall (ζ_W = 0 away from the wall)

Speed proportional to ion gradient and charge on the particle
Under low Reynolds number conditions (R~10^{-5}),
the mass and radius of the particle are *not* important

J. L. left. Lowell and D. *C.* Prieve *J . Fluid Mech.* (1982), *vol.* 117, *pp.* 107-21.
D. *C.* PrieveJ. L. Anderson, J.P. Ebel and M. E. Lowell, *J. Fluid Mech.* (1984), *vol.* 148, *pp.* 247-269.

Quorum-Sensing Autonomous Nano/Microbots

- Bots Secrete Ions
- Electric Field Results from Different Diffusion Rates of the Cations vs. Anions
- Bots Move in Response to the Electric Field
- Bots Move Cooperatively in Response to Neighbors' Ion Gradients

Angew. Chem., 2009

Photochemistry of Silver Chloride

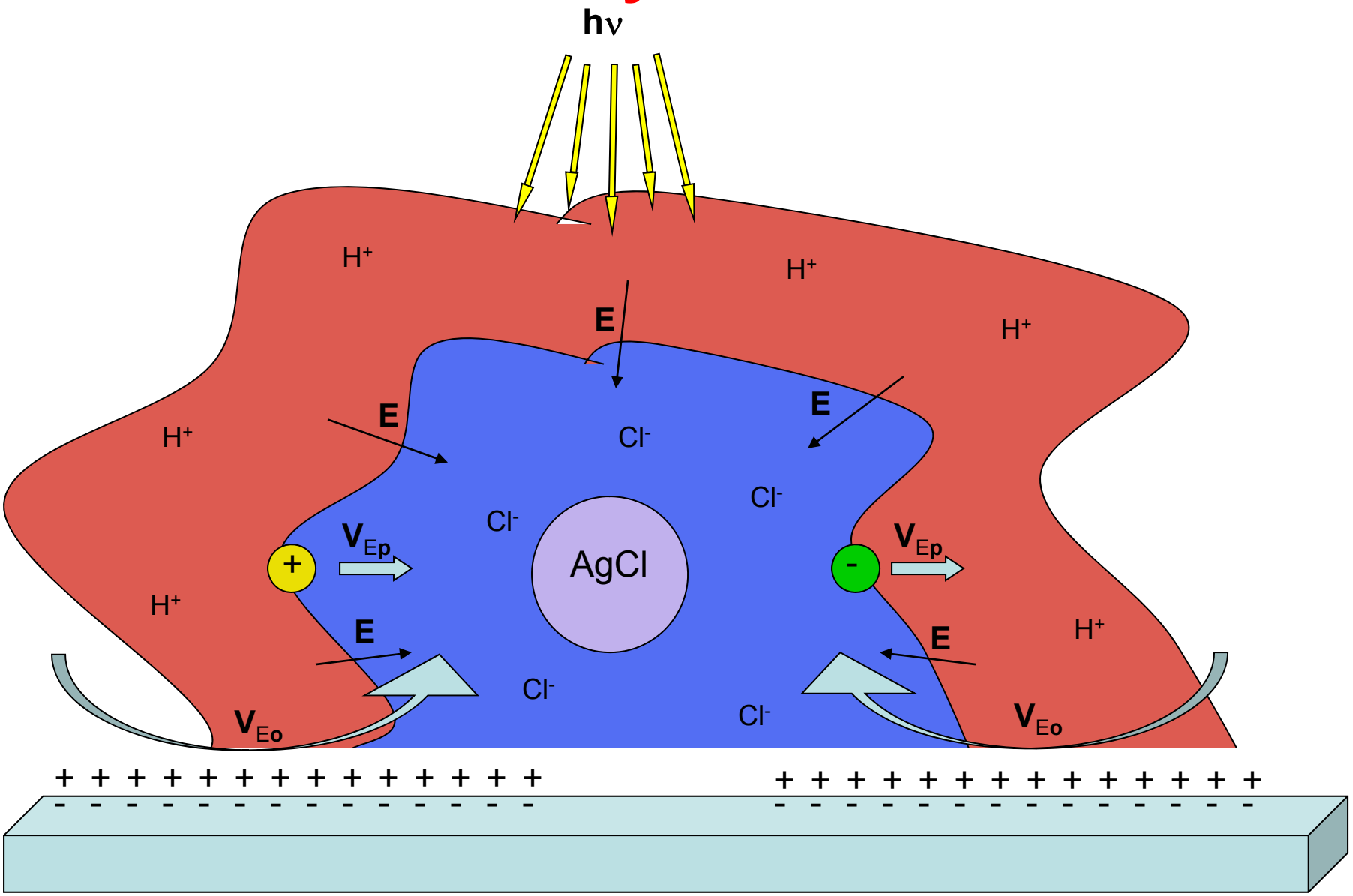

$$4\,AgCl + 2\,H_2O \xrightarrow{h\nu,\ Ag^+} 4\,Ag + 4\,H^+ + 4Cl^- + O_2$$

Emergent Collective Behavior Through Communication via Chemical Signals

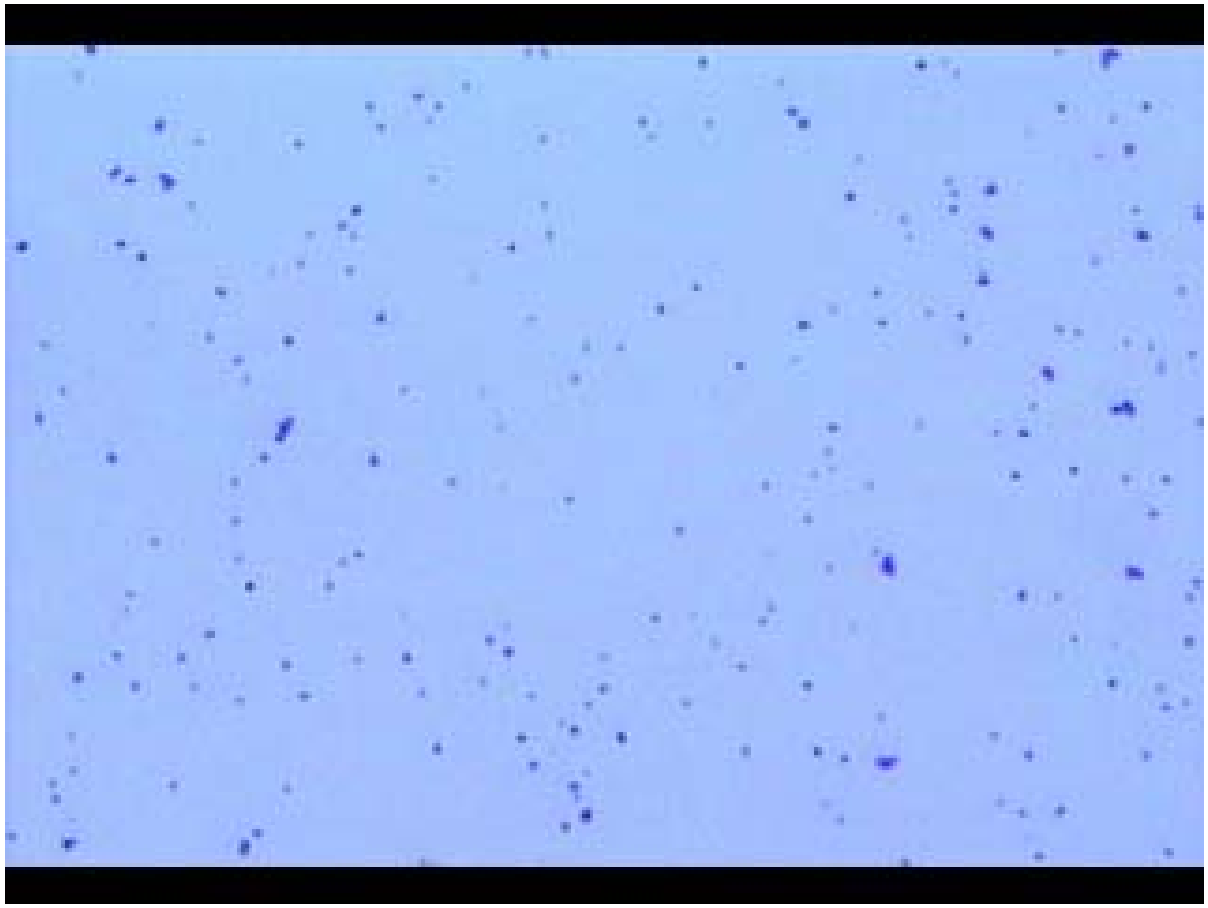

Silver chloride particles in deionized water undergo Brownian motion in visible wavelength light. After 2 sec, the UV light is switched on. Large schools of colloids form at longer times.
Video plays in real time.

Emergent Collective Behavior Through Communication via Chemical Signals

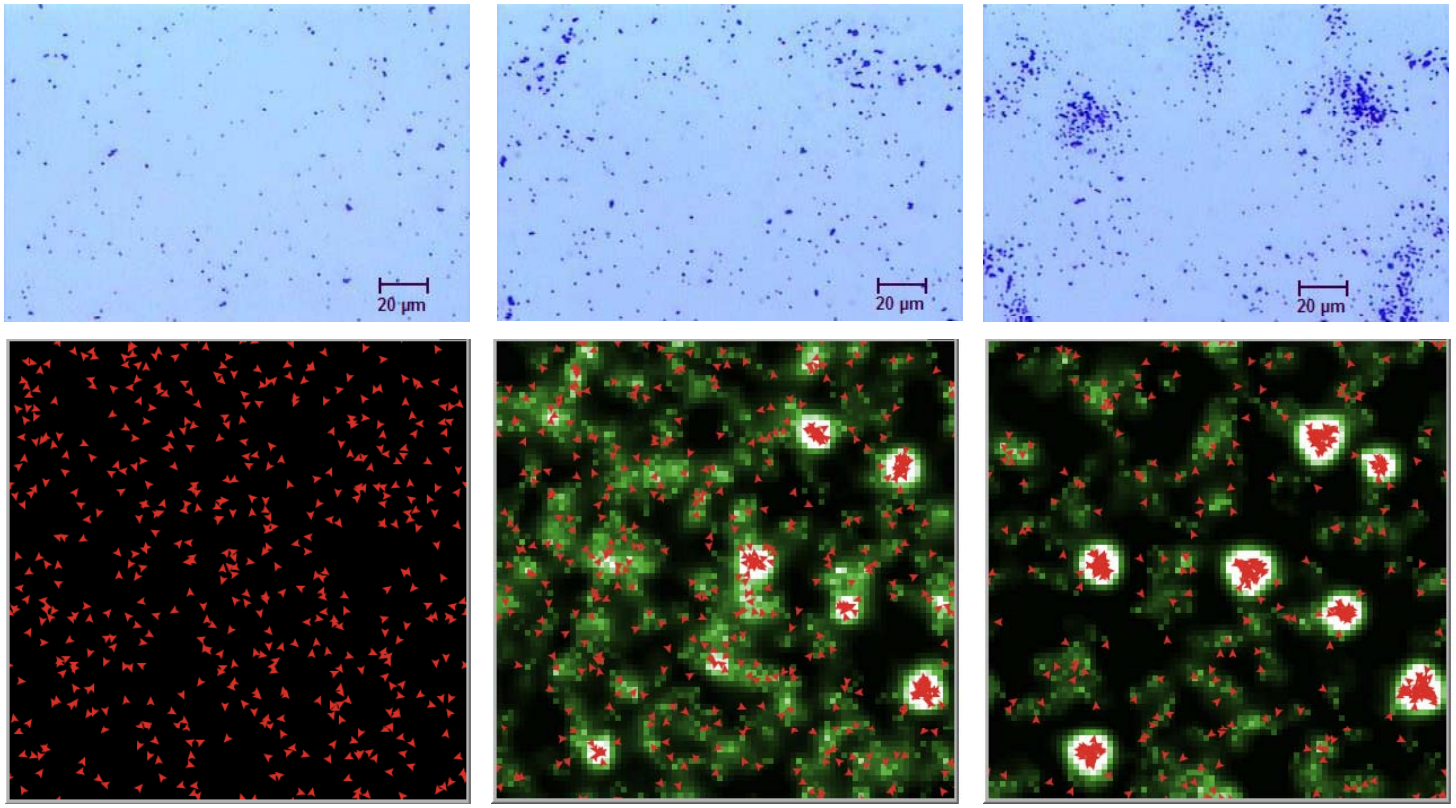

(a-c) AgCl particles in deionized water (a) before UV illumination, (b) after 30 s of UV exposure, and (c) after 90 s.
(d-f) Simulation of AgCl particles in deionized water after (d) 0 timesteps, (e) 250 timesteps, and (f) 750 timesteps.

Change in concentration at a given lattice site with time

$$\underbrace{C_{x,y}(t+\Delta t)}_{New\ \ Conc.} = \underbrace{(1-b)}_{Bulk\ \ Loss}\left\{\underbrace{C_{x,y}(t)}_{Original\ \ Conc.} + \underbrace{an_{x,y}}_{Chemical\ \ Production} + \underbrace{D\left[C_{x+1,y}(t)+C_{x-1,y}(t)+C_{x,y+1}(t)+C_{x,y-1}(t)-4C_{x,y}(t)\right]}_{Diffusion}\right\}$$

Chemical gradient across a lattice site in x and y directions

$$\psi_x = C_{x+1,y}(t) - C_{x-1,y}(t)$$

$$\psi_y = C_{x,y+1}(t) - C_{x,y-1}(t)$$

Probability of hopping in a given direction,
in addition **to user-defined Brownian hop probability, λ_B**

$$\lambda_x(t) = \alpha\left|\psi_x\right|$$

$$\lambda_y(t) = \alpha\left|\psi_y\right|$$

The modified NetLogo program was run for 1000 time steps with schooling defined as 4+ particles occupying a single lattice site

A Typical Simulation Of Particle Collective Behavior

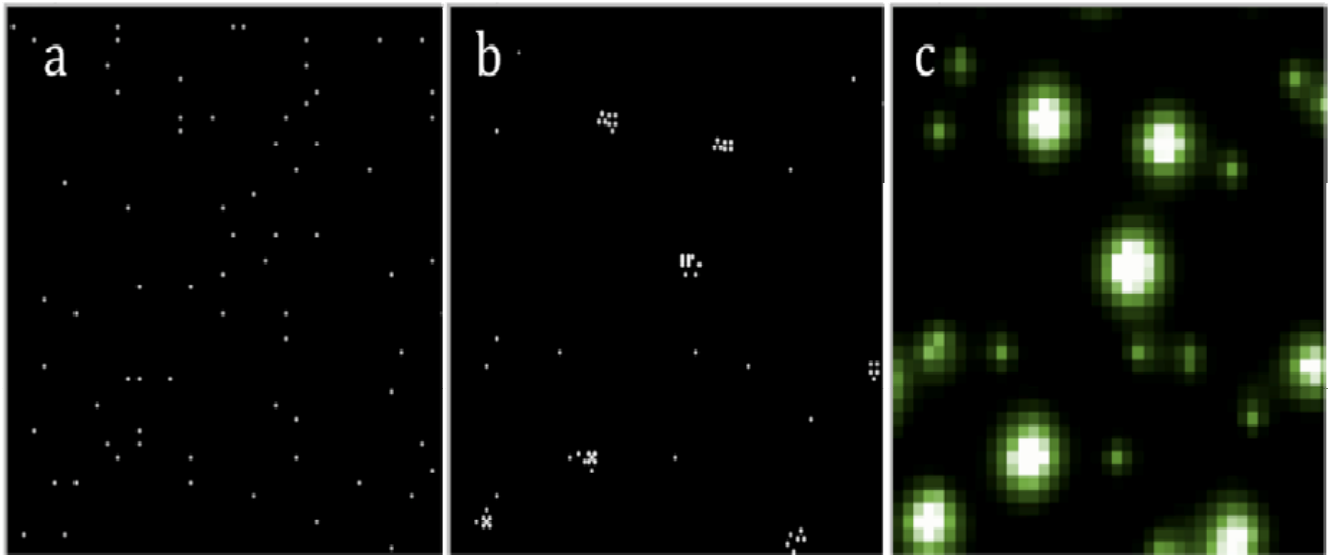

(a) Initially randomly distributed particles.
(b) Particles after 2000 times-steps.
(c) A plot of the chemical values of every lattice site at 2000 time-steps.

Brighter shades of green approaching white indicate higher chemical concentrations.

U. Wilensky, 1997. NetLogo: http://ccl.northwestern.edu/netlogo/ models/Slime

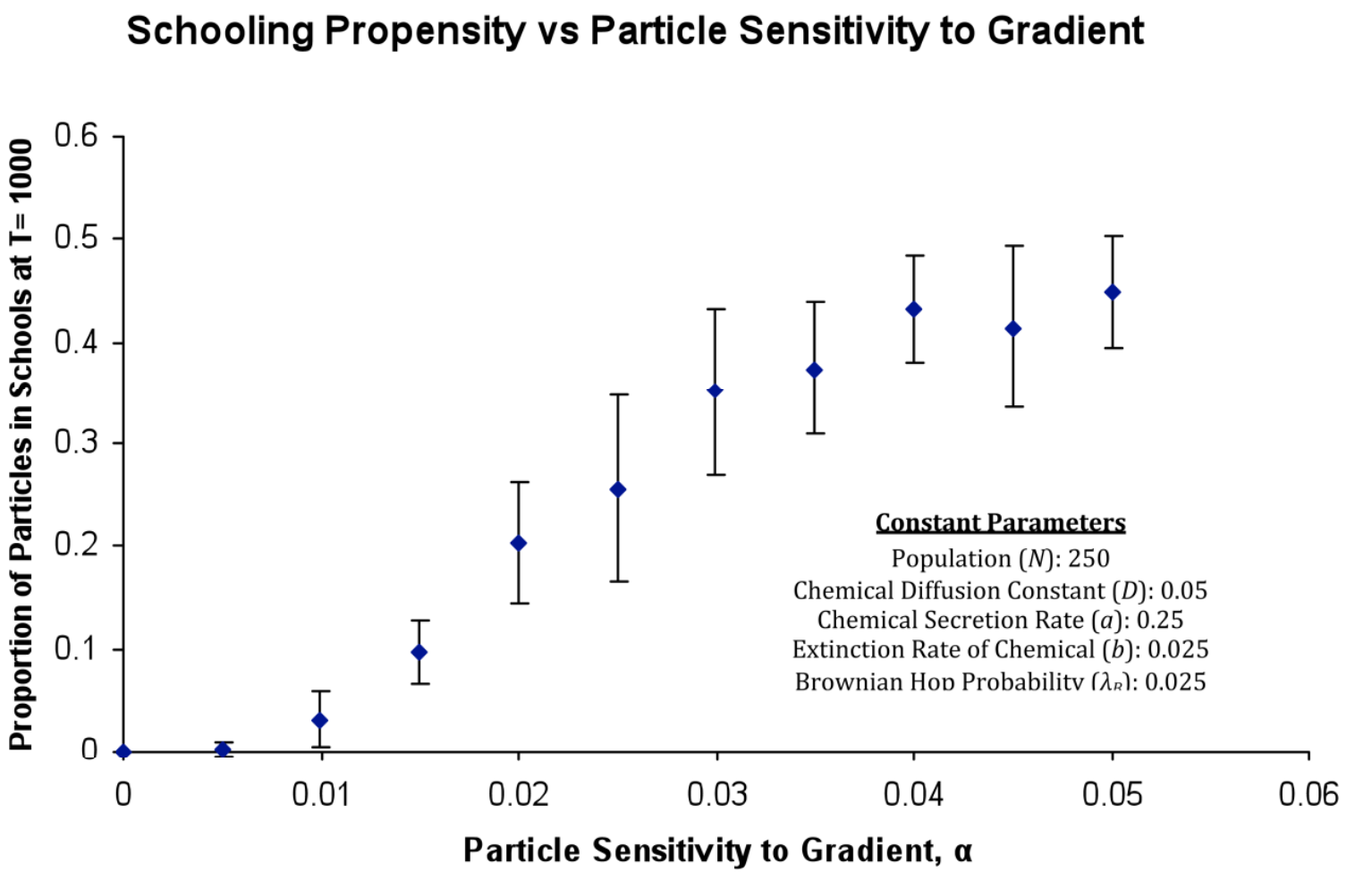

Faraday Discuss., 2009

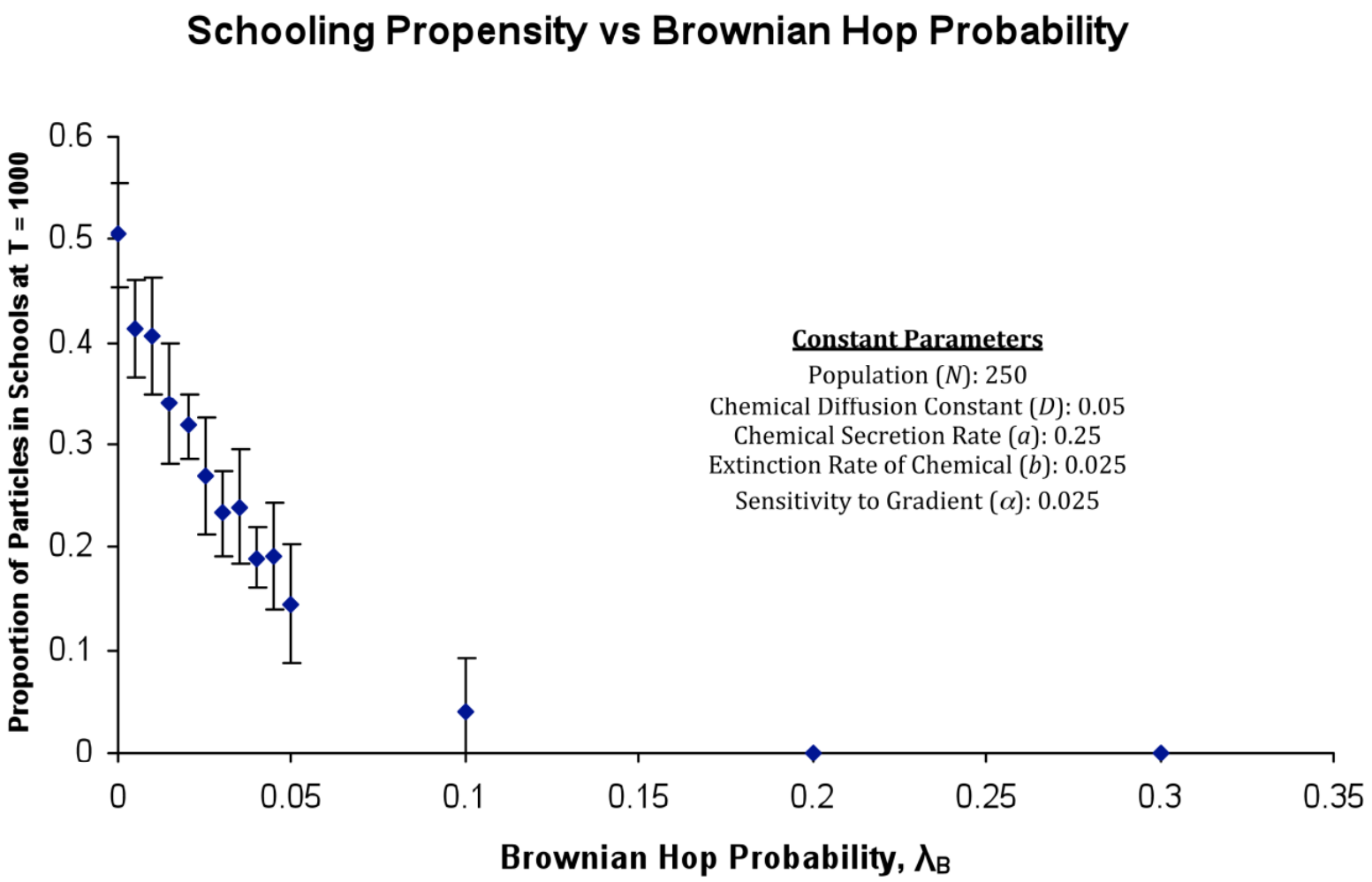

Faraday Discuss., 2009

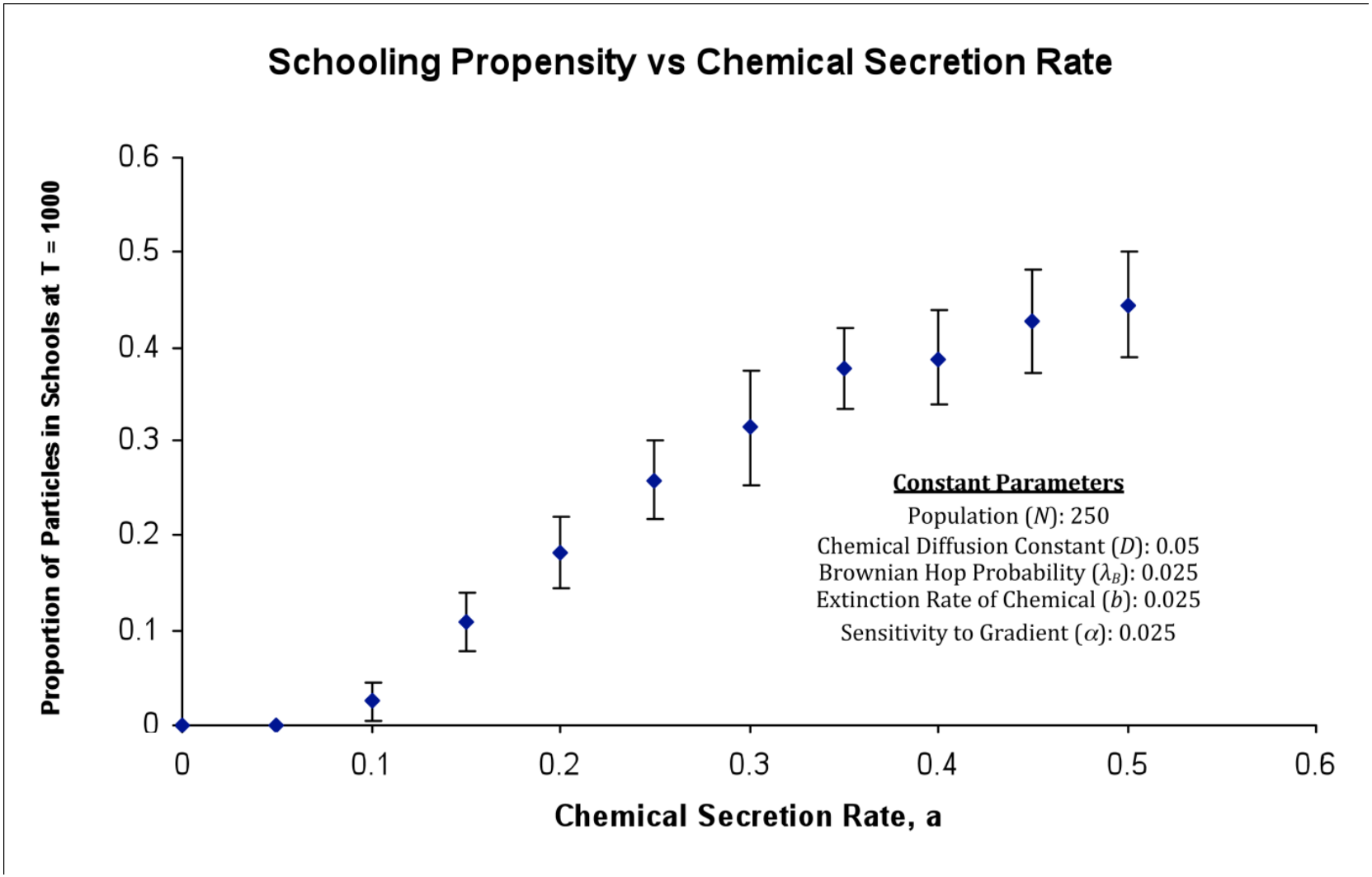

Faraday Discuss., 2009

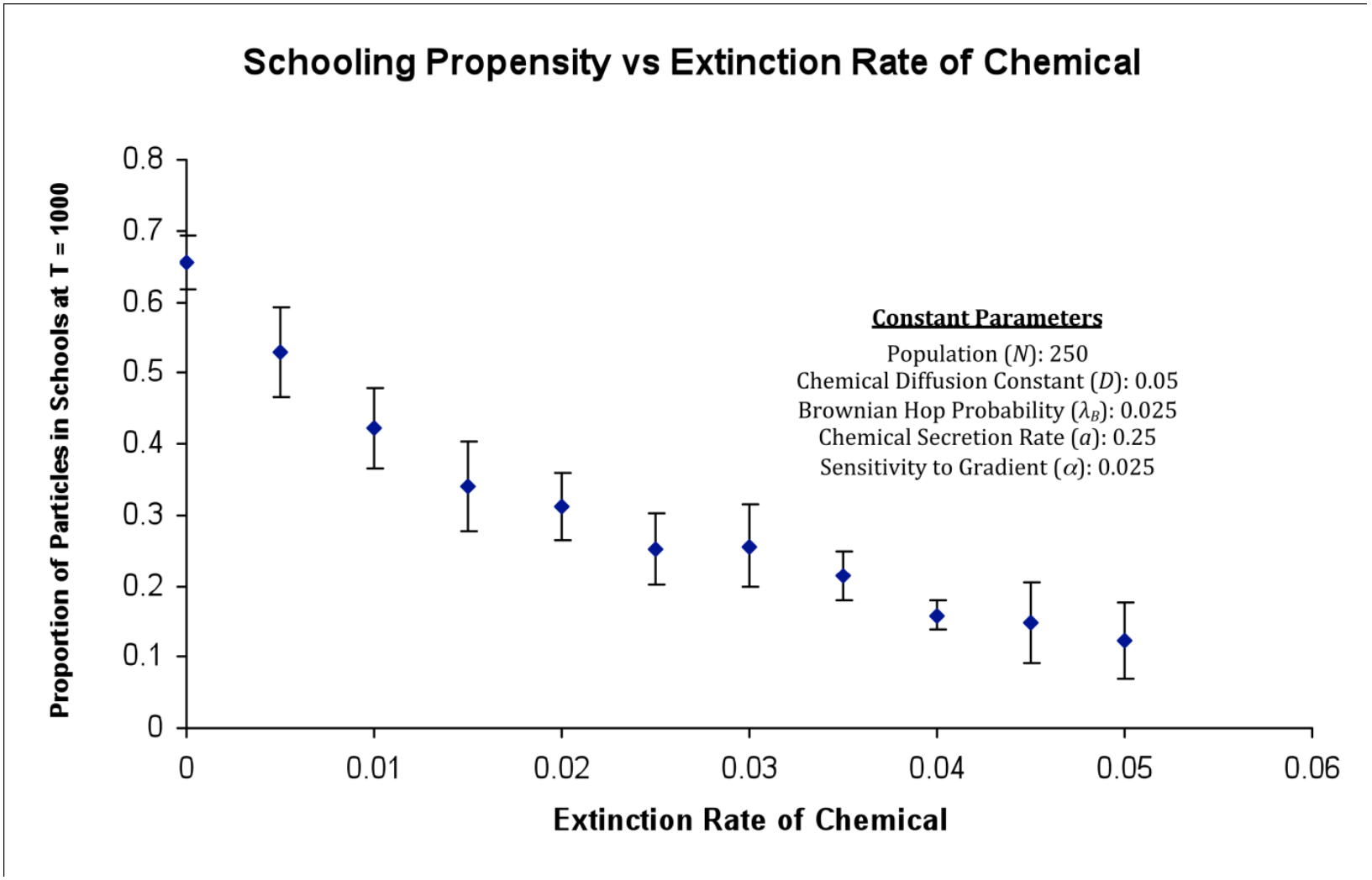

Faraday Discuss., 2009

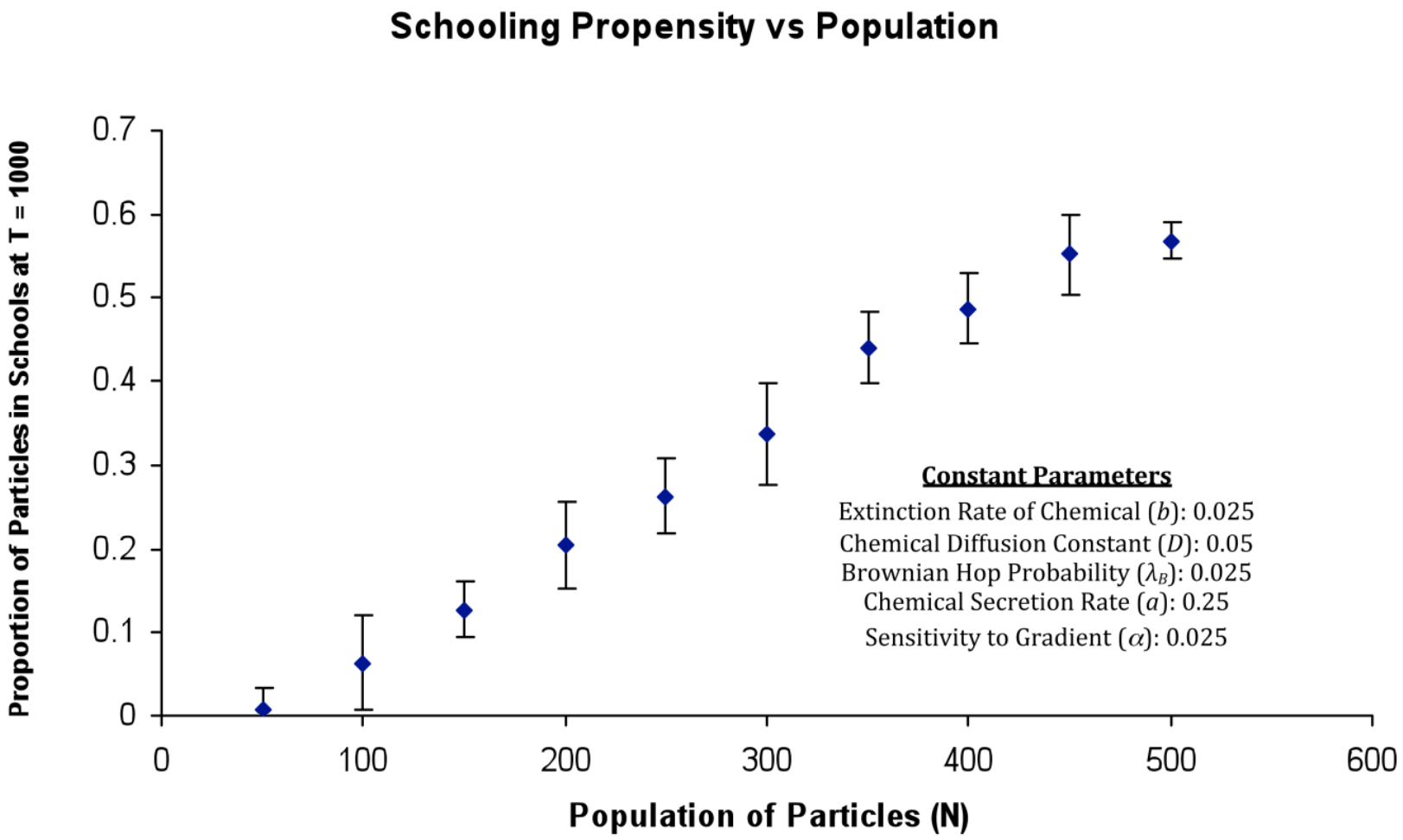

Faraday Discuss., 2009

Predator-Prey: Silica Spheres Actively *Seeking Out* and Surrounding Phototaxing AgCl Particles

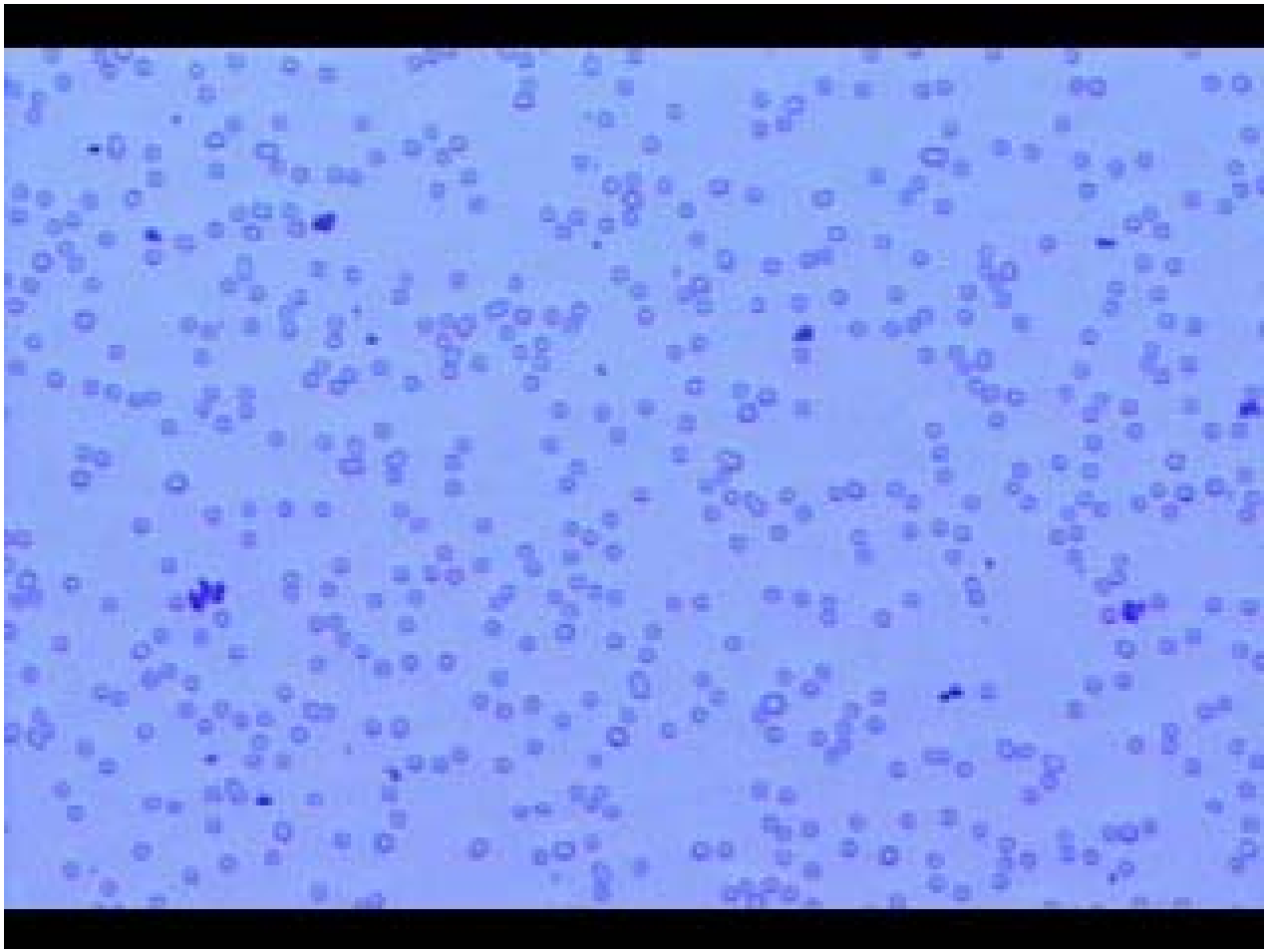

Silver chloride particles (dark objects) with silica particles.
When the UV light is switched on at 3 seconds,
silver chloride particles begin to move and also attract silica particles.
Video plays in real time.

Collective Particle Behavior

New Design Principles

- Two or more different particle types can move autonomously to organize themselves *spatially*

- Allows coordinated movement of dissimilar particles that are *not* attached to each other making it easier to transport and deliver cargo at designated areas

Angew. Chem., 2009

Microfireworks with Silver Chloride Particles

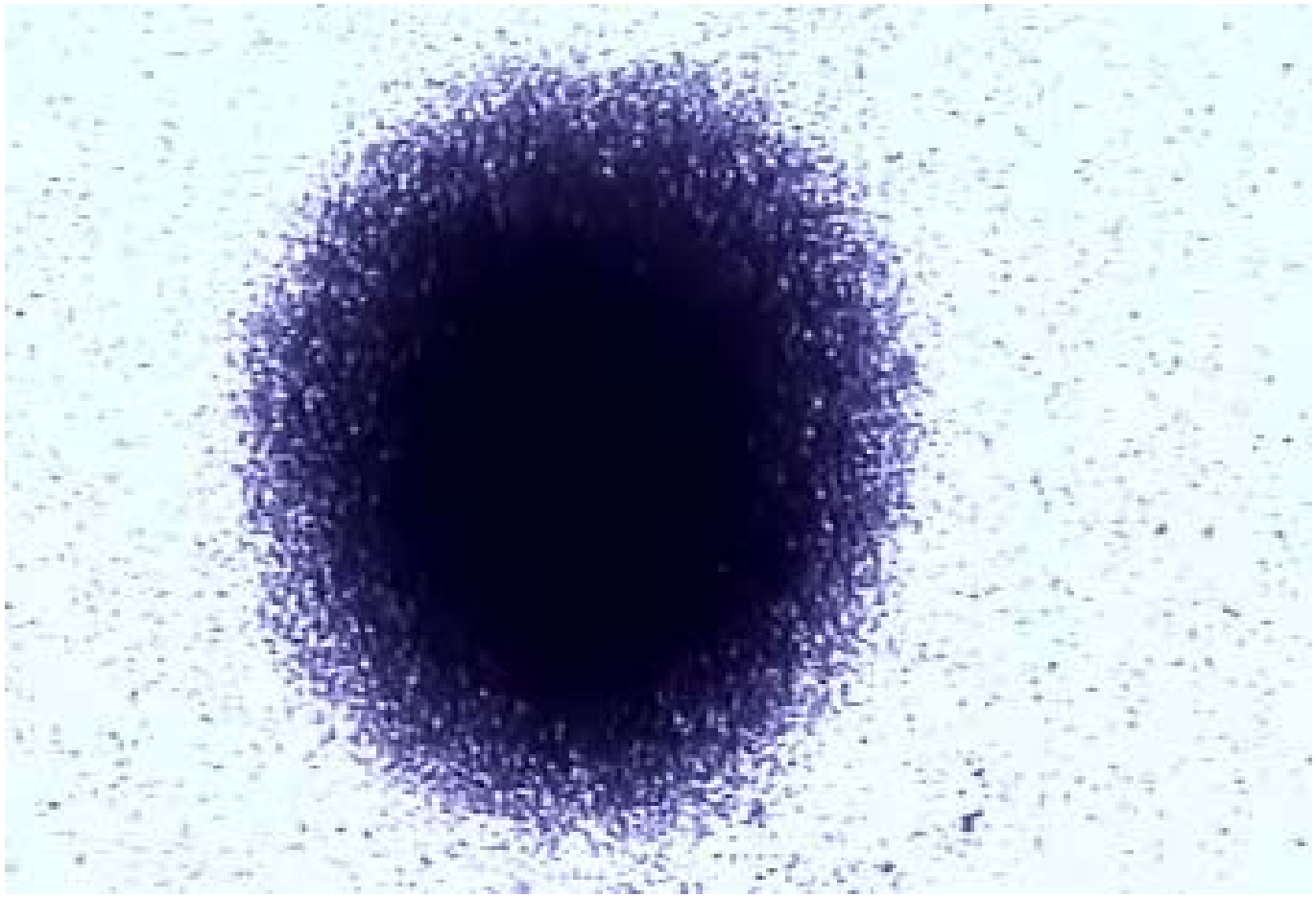

Real time video
The UV light is alternately turned on and off

***Angew. Chem.*, 2009**

Oscillatory Behavior and Emergent Synchronization of Particles Under Redox Conditions

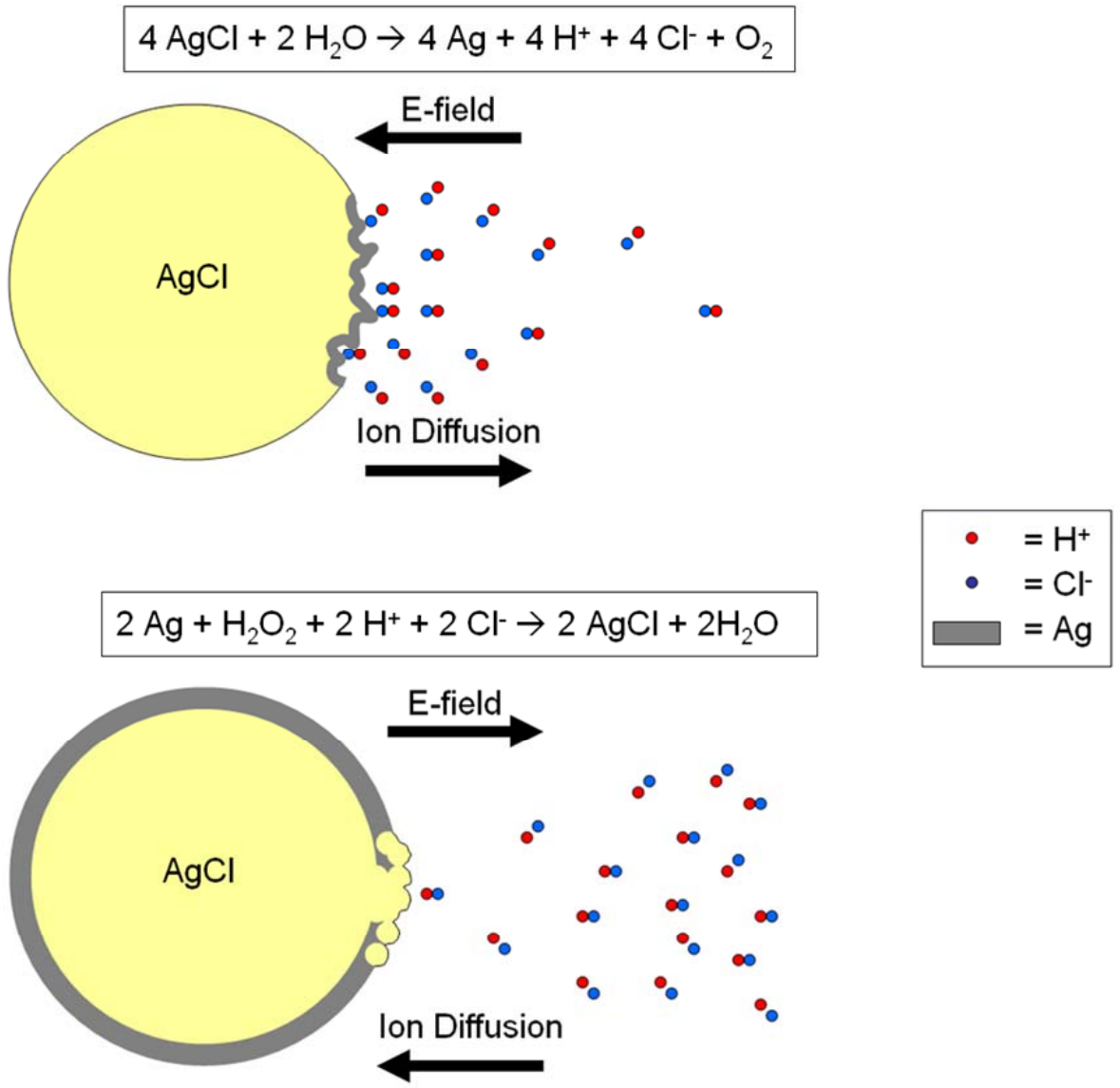

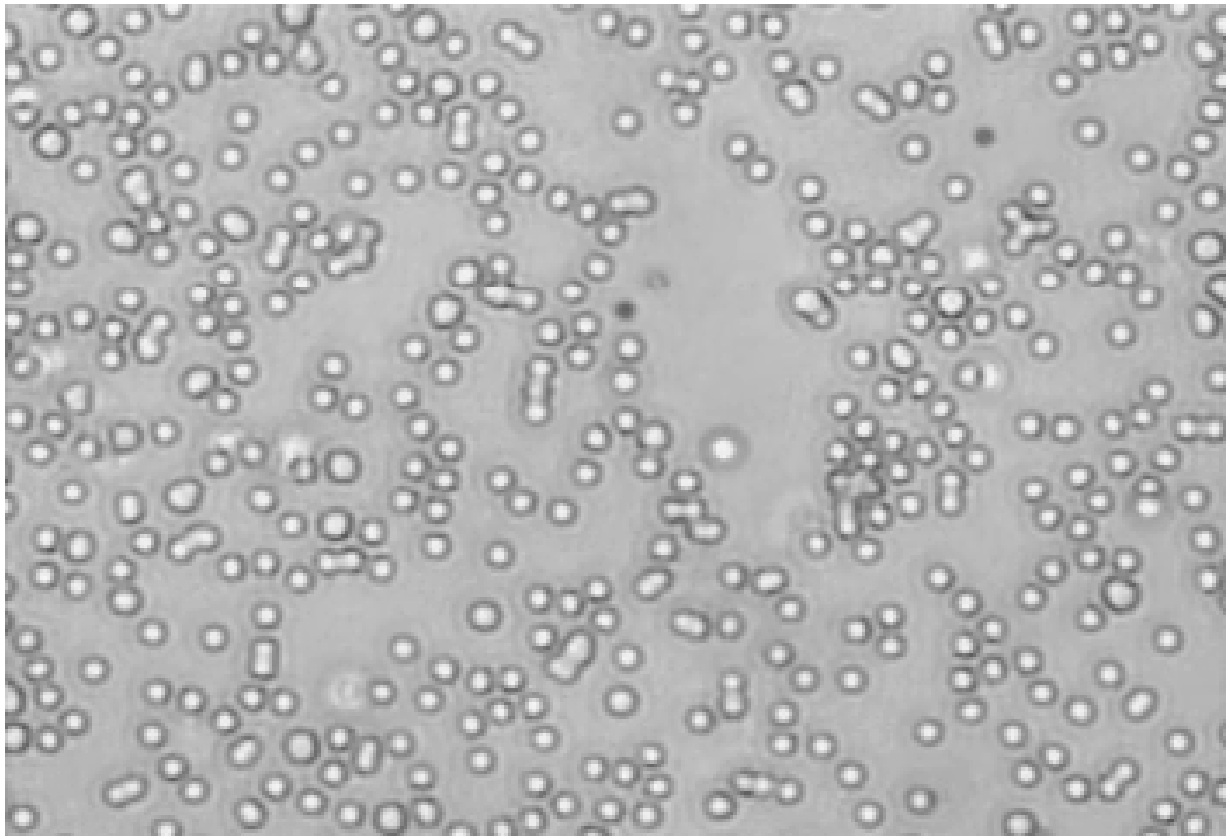

A solution containing AgCl particles (darker objects), silica tracer spheres (lighter objects), and 1% (v/V) H_2O_2 in water. The particles are illumined with UV light over a microscope slide. The AgCl particles are seen to move through solution, and alternately bind and release the silica tracer particles. The video is 194 μm in width. Movie plays in real-time.

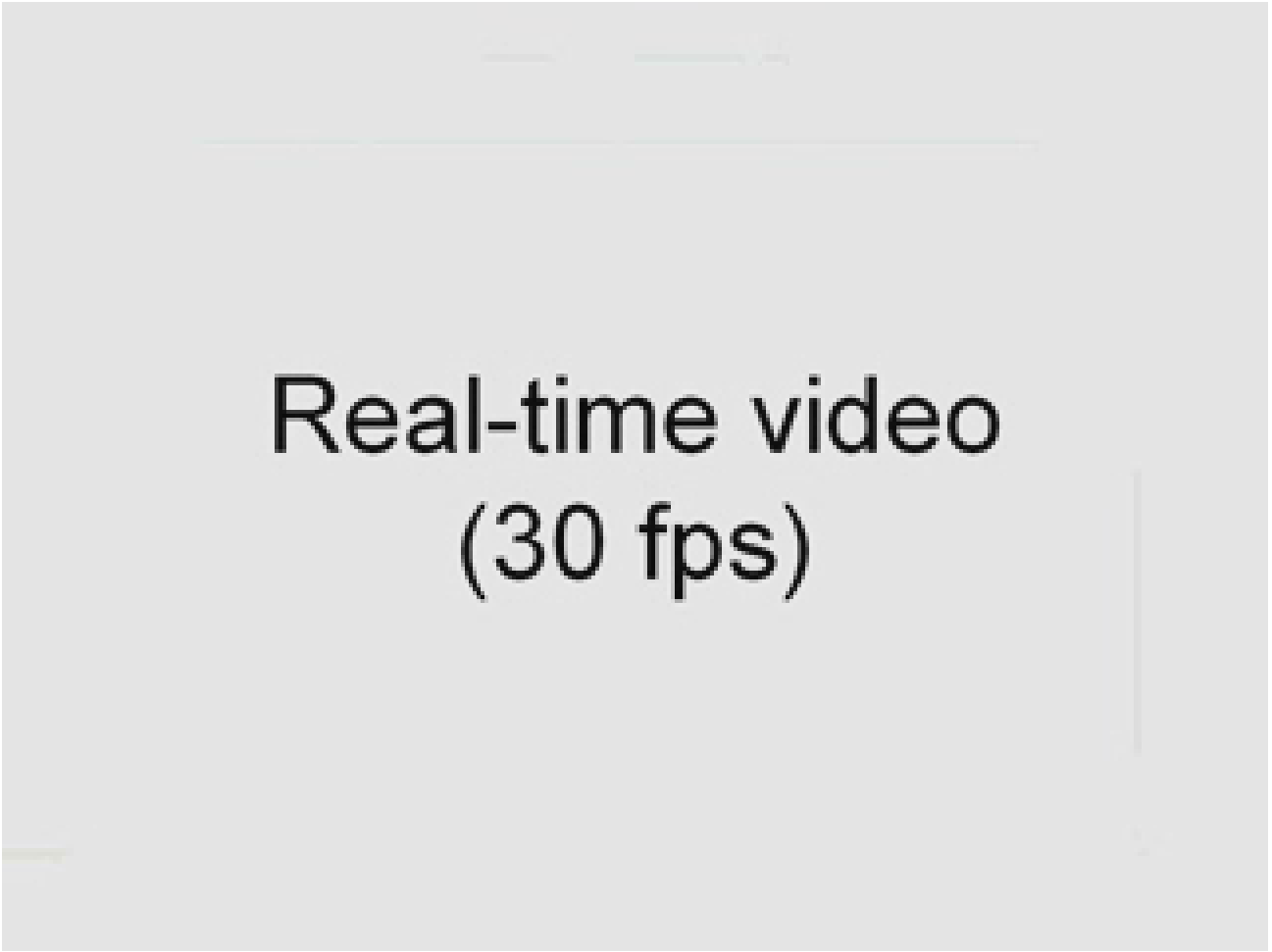

A UV-illuminated aqueous solution containing 2.3 μm silica tracer particles, 0.33 mM HCl, and 0.17% (v/V) H_2O_2 is imaged above an array of 9 μm diameter silver disks with 11 μm spacings.
As a traveling wave of tracer particle motion passes the array, the disks appear to flash on and off as their color alternates between reflective silver and darkened AgCl.

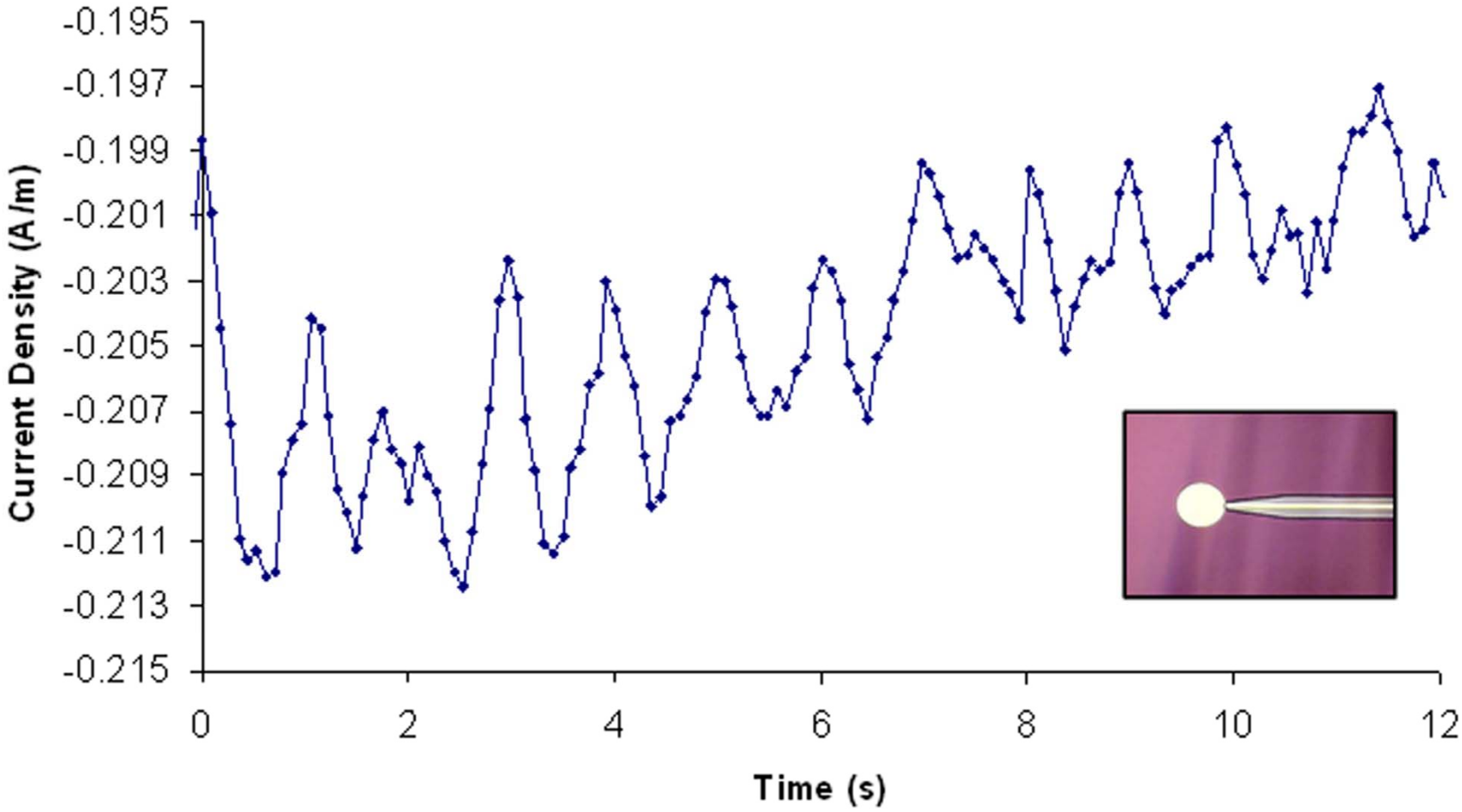

Current from a 90 μm silver disk patterned on a SiO_2 wafer in the presence of 0.17% (v/V) H_2O_2, 0.17 mM HCl and silica tracer spheres, under UV illumination. After a few seconds of illumination, current oscillations are recorded which match the oscillations of tracer particles. Negative currents are oxidative with respect to the silver surface. **Inset**, the 90 μm diameter silver disk connected to an insulated silver wire that monitored the reaction current on the disk surface.

Real Time Video:
Solution containing AgCl particles and 1% H_2O_2 in water under UV illumination

Designing Functional Nano/Microbots

Required Design Elements

- **Movement Through Catalysis**
- **Cargo Loading, Transport, and Unloading**
- **Directional Movement Through Chemical Gradient (Chemotaxis)**
- **Emergent Collective Behavior Through Inter-Bot Communication via Chemical Signals**

***Scientific American*, May, 2009**

DIFFUSIOPHORETIC MOTION OF PARTICLES BASED ON A GRADIENT OF ELECTROLYTE CONCENTRATION: ELECTROPHORESIS TENDS TO DOMINATE OVER CHEMOPHORESIS

$$U = \underbrace{\left(\frac{dLn(C)}{dx}\right)\left(\frac{D_C - D_A}{D_C + D_A}\right)\left(\frac{k_B T}{e}\right)\frac{\varepsilon\left(\zeta_p - \zeta_w\right)}{\eta}}_{\text{Electric Field}} + \underbrace{\left(\frac{dLn(C)}{dx}\right)\left(\frac{2\varepsilon k_B^2 T^2}{\eta e^2}\right)\left\{Ln\left[1-\tanh^2\left(\frac{e\zeta_W}{4k_B T}\right)\right] - Ln\left[1-\tanh^2\left(\frac{e\zeta_P}{4k_B T}\right)\right]\right\}}_{\text{Chemophoretic Term}}$$

U is the particle speed, dLn(C)/dx is the electrolyte gradient
D_C and D_A are the diffusion constants of the cation and anion components
k_b is the Boltzmann constant, T is the temperature, e is the elementary charge
ε is the solution permittivity, η is the dynamic viscosity of the solution,
ζ_P is the zeta potential of the particle,
ζ_W is the zeta potential of the wall (ζ_W = 0 away from the wall)

Speed proportional to ion gradient and charge on the particle
Under low Reynolds number conditions (*R*~10^{-5}),
the mass and radius of the particle are *not* important

Movement Due to External Salt Gradient: Oil Reservoir Salinity: 50,000 – 150,000 ppm

Directions of Particle and Fluid Flow Components in Diffusiophoresis

Assumption: Particle and underlying substrate are negatively charged, and $D_- > D_+$ (e.g. NaCl)

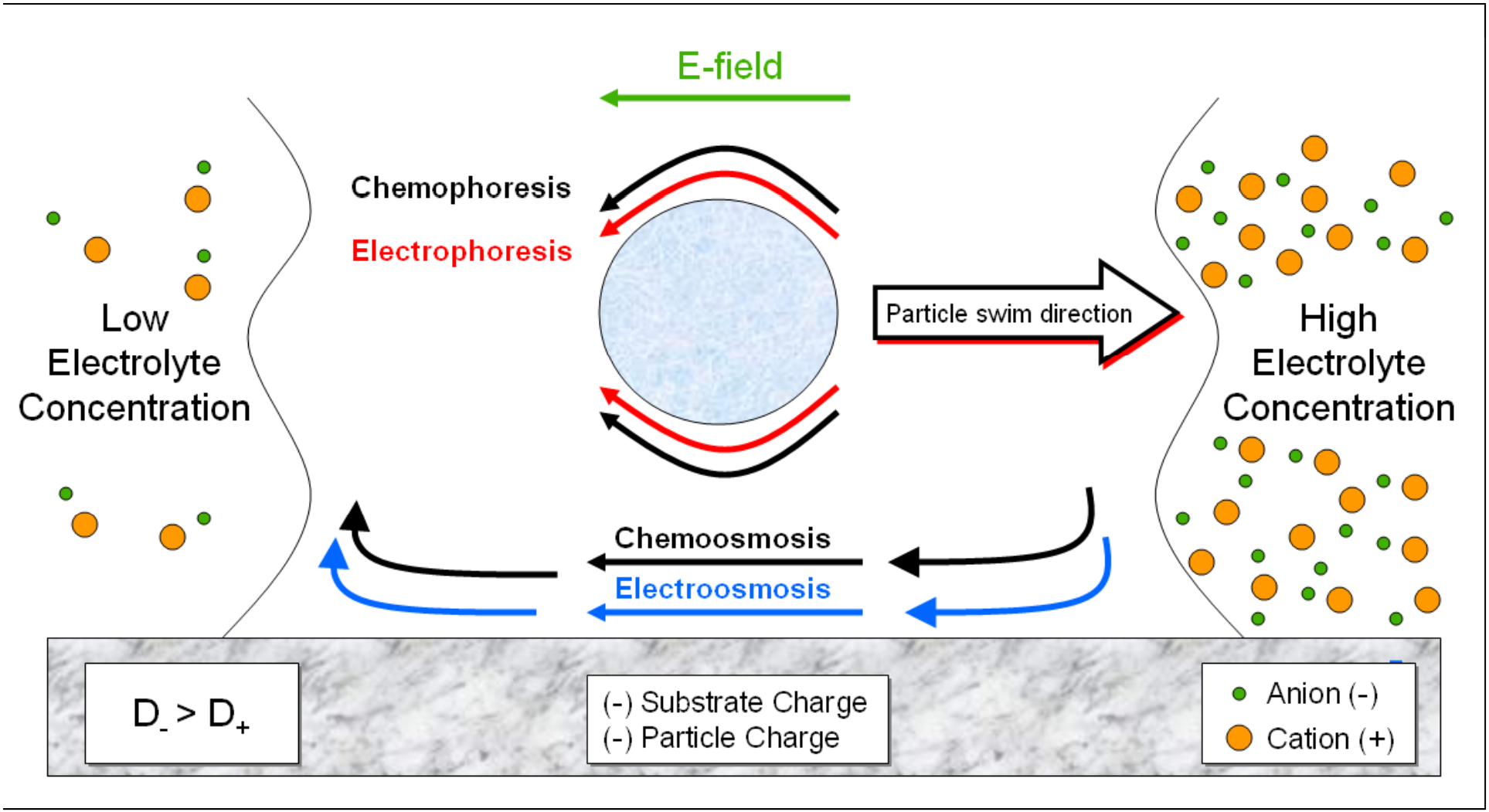

DIFFUSIOPHORETIC MOTION OF PARTICLES BASED ON A GRADIENT OF ELECTROLYTE CONCENTRATION

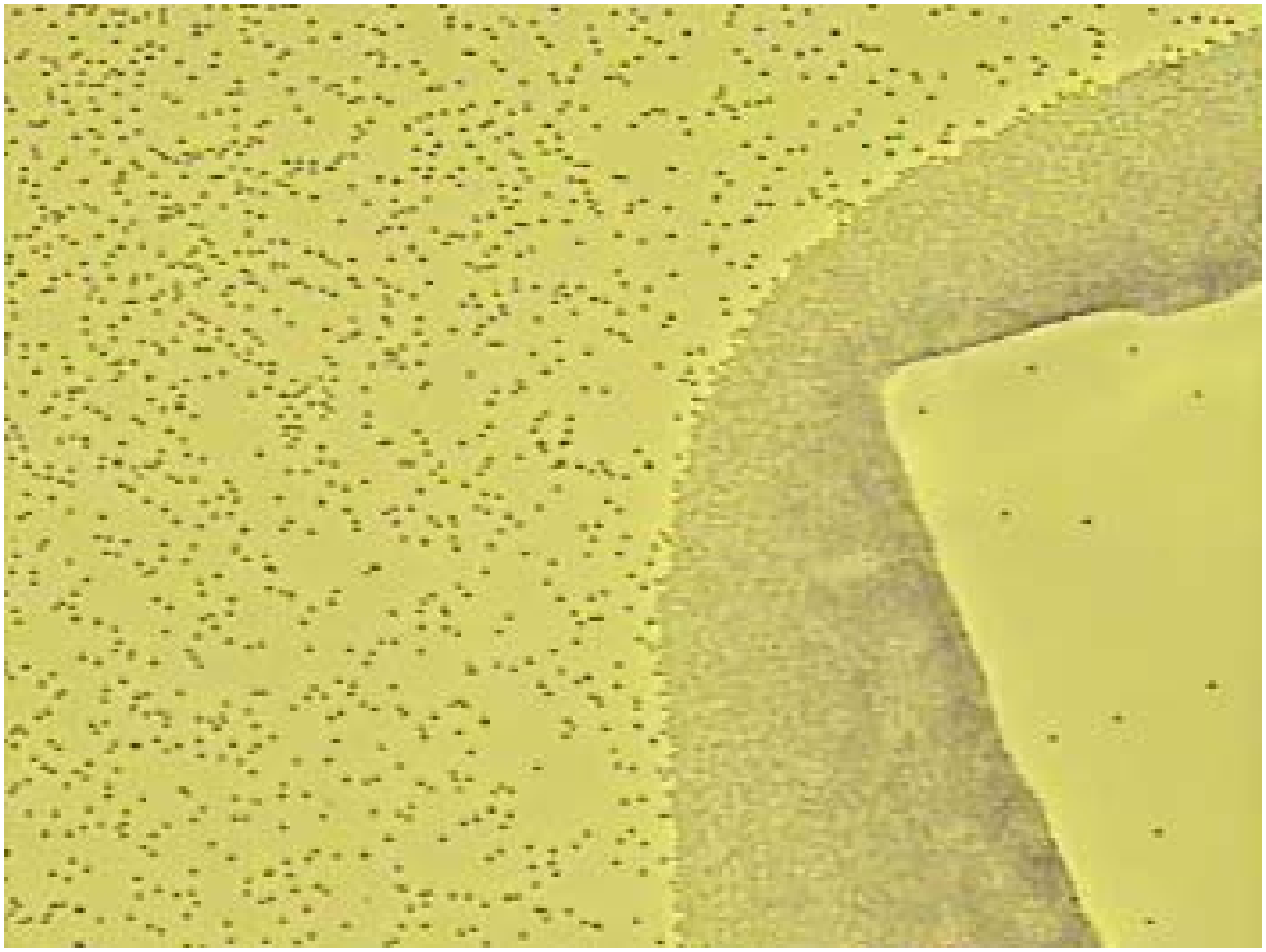

Migration of silica microspheres (d = 2.3 μm) towards a gel containing 1 mM NaCl

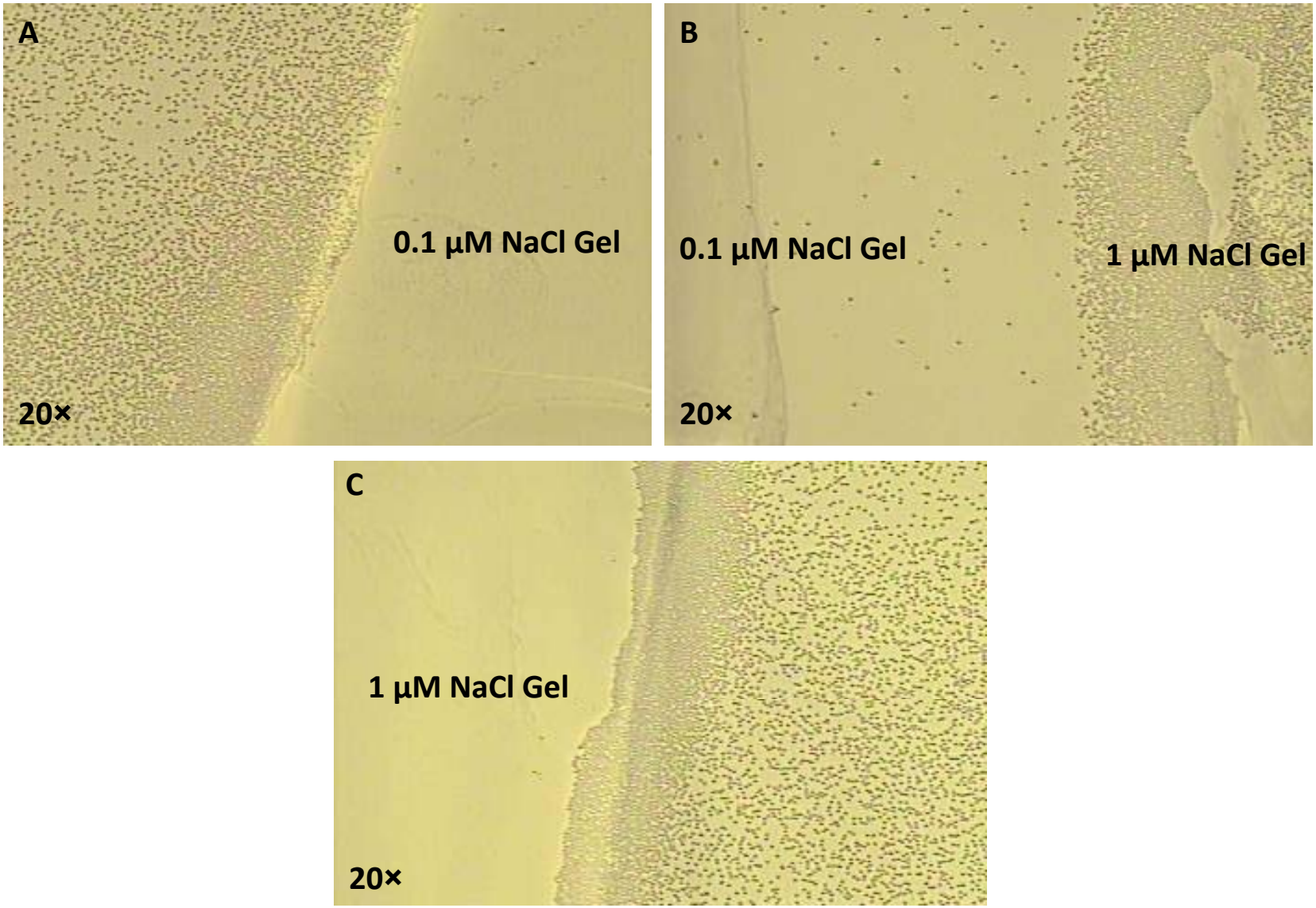

Migration of silica microspheres (d = 2.3 µm) in competing concentration gradients of NaCl solution

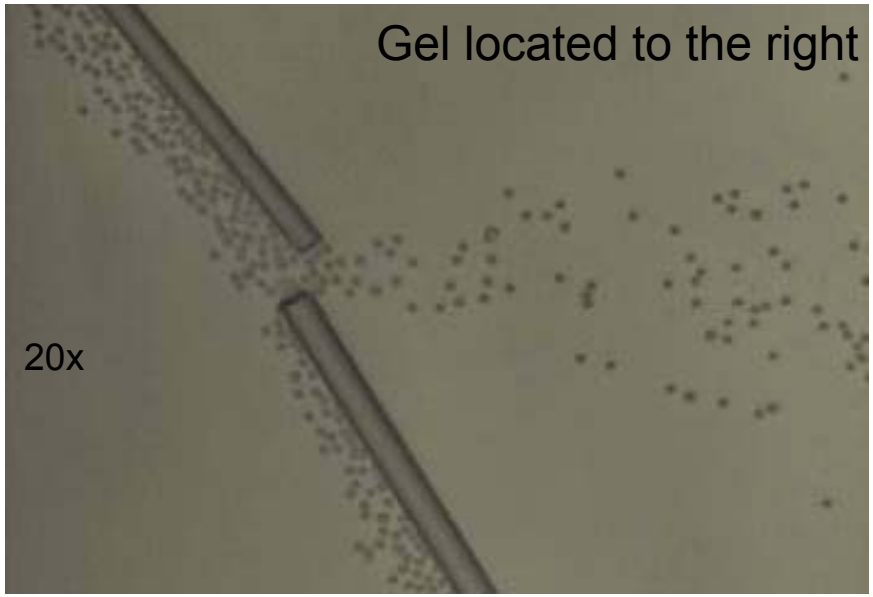

Silica microspheres (d = 2.3 μm) navigating past glass fiber barriers in response to an agarose gel containing 1 mM NaCl (located to the right of the field of vision in both images)

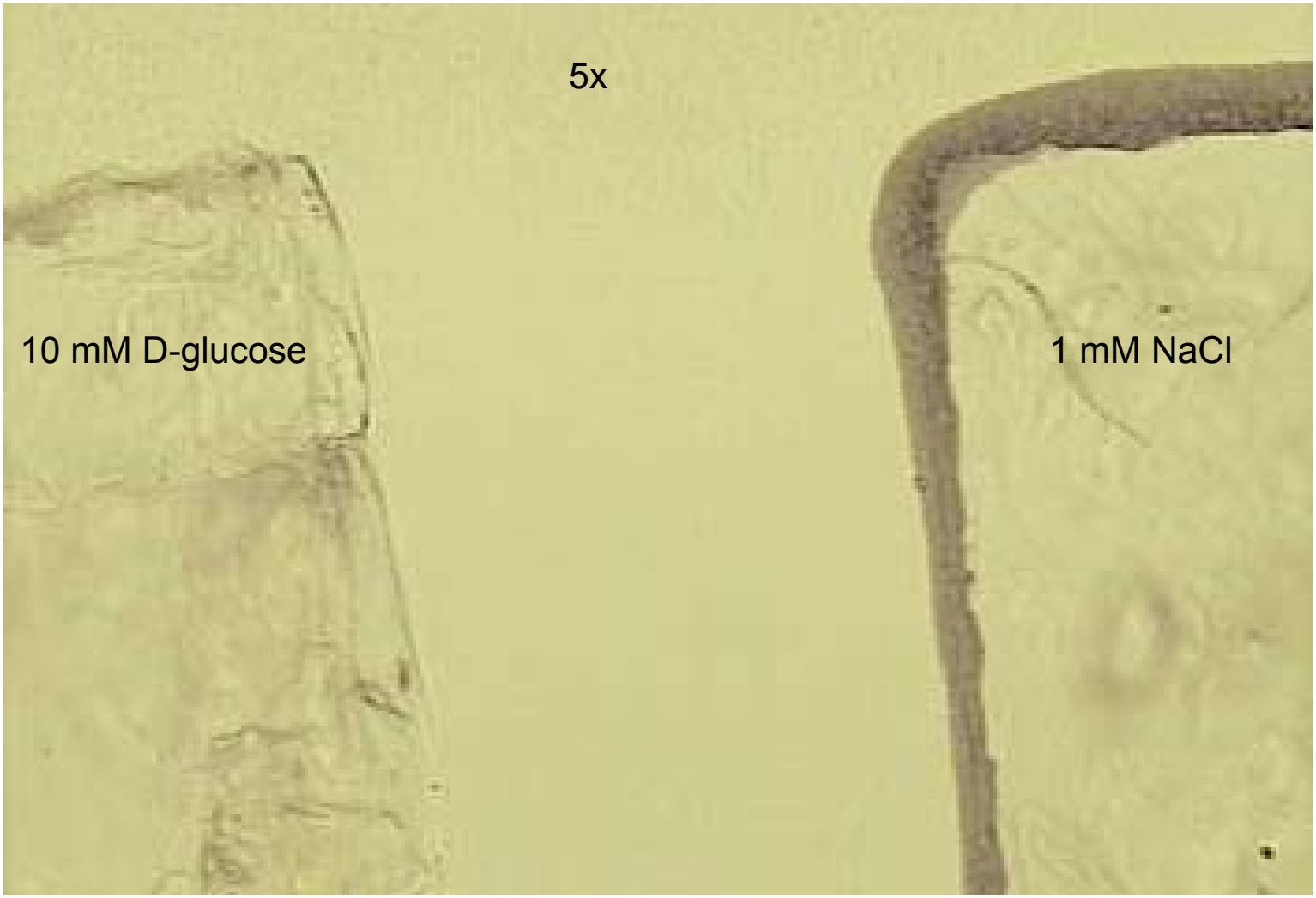

Silica tracer particles (d = 2.34 μm) preferentially migrate towards NaCl-leaching gel.
Gels contain 10 mM D-glucose (left) and 1mM NaCl (right).

Silica Particles in The Presence of an Agarose Gel Soaked in 1 mM NaCl

Particles			Along the Gradient		Orthogonal to Gradient	
			Average Velocity (x)	SD	Average Velocity (y)	SD
2.34µm	~200 µm from gel	1 mM NaCl	1.32	0.27	-0.056	0.21
		1 mM KCl	0.97	0.16	-0.024	0.15
0.90µm	~200 µm from gel	1 mM NaCl	1.32	0.32	-0.020	0.26
		1 mM KCl	0.93	0.29	-0.049	0.23

Speed: µm/sec

Experimental Setup for Particle Movement in an Electric Field

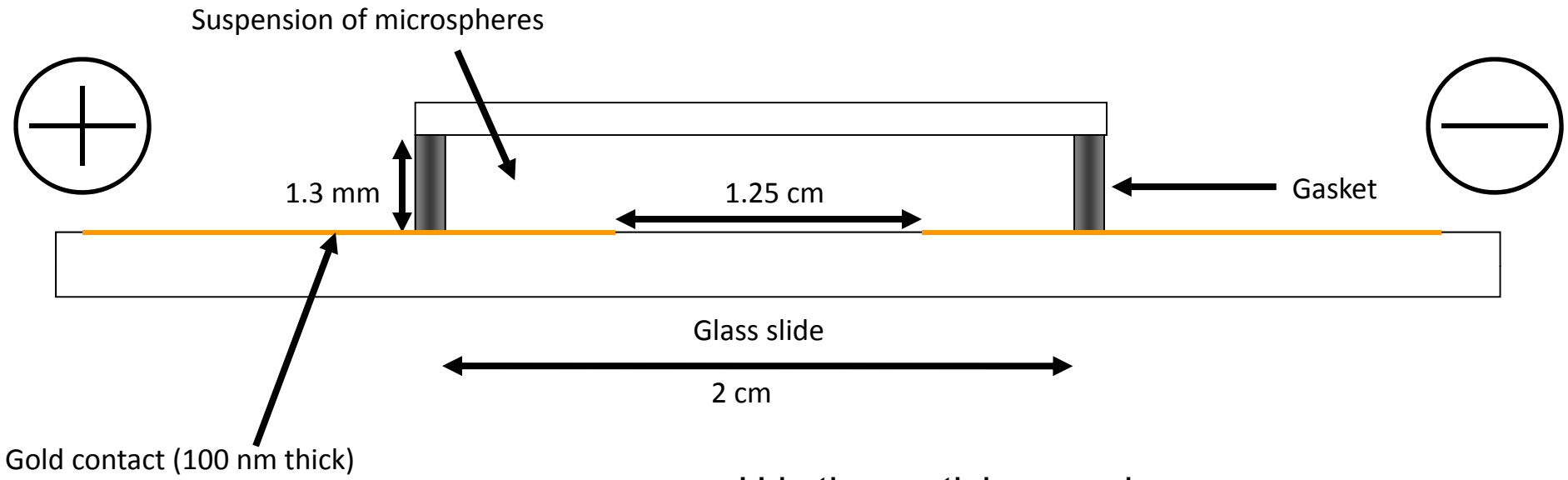

$$U = \frac{\varepsilon\left(\zeta_P - \zeta_W\right)}{\eta} E$$

U is the particle speed
ε is the solution permittivity
E is the applied electric field
η is the dynamic viscosity of the solution,
ζ_P is the zeta potential of the particle,
ζ_W is the zeta potential of the wall (ζ_W = 0 away from the wall)

Comparison of Movement in an Applied Electric Field to Diffusiophoretic Migration

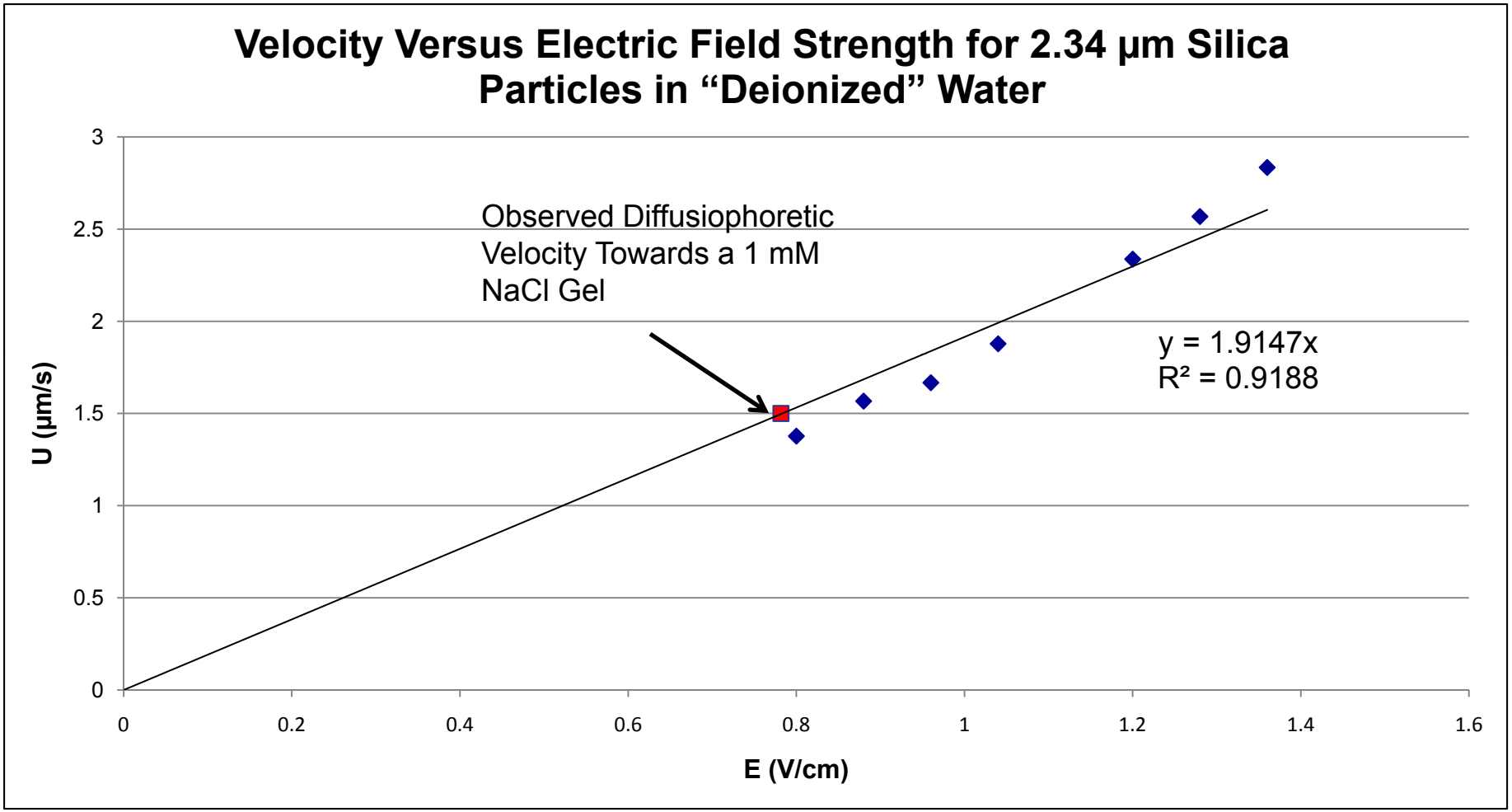

Microfluidic Setup

Channel width: 240 μm
Channel height: 100 μm
Flow rate: 350 μm/s
Particle: Fluorescent Carboxylated polystyrene; 100 nm radius

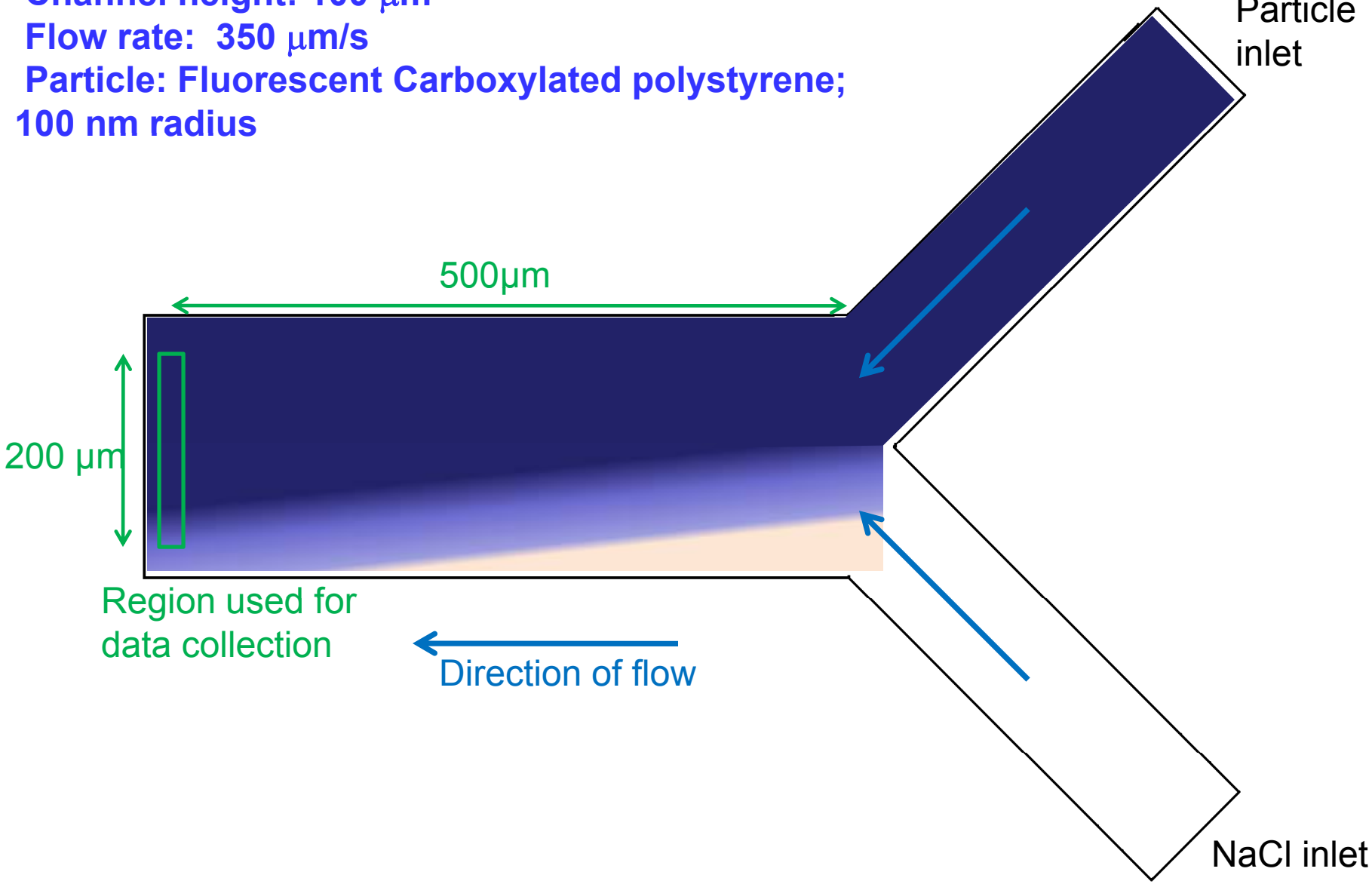

Chemotaxis of Carboxylated Polystyrene Nanospheres

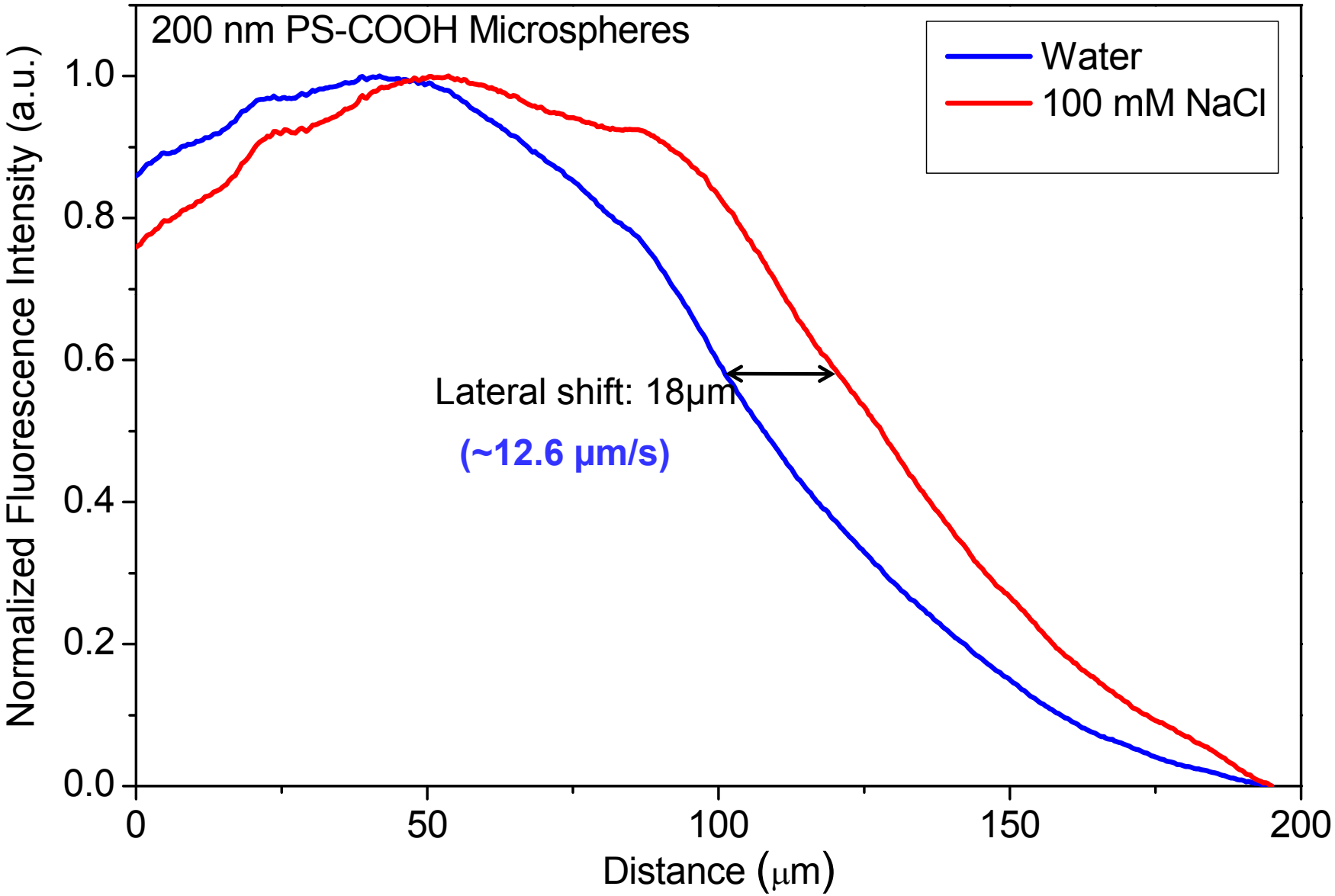

Comparison of Movement in an Applied Electric Field to Diffusiophoretic Migration

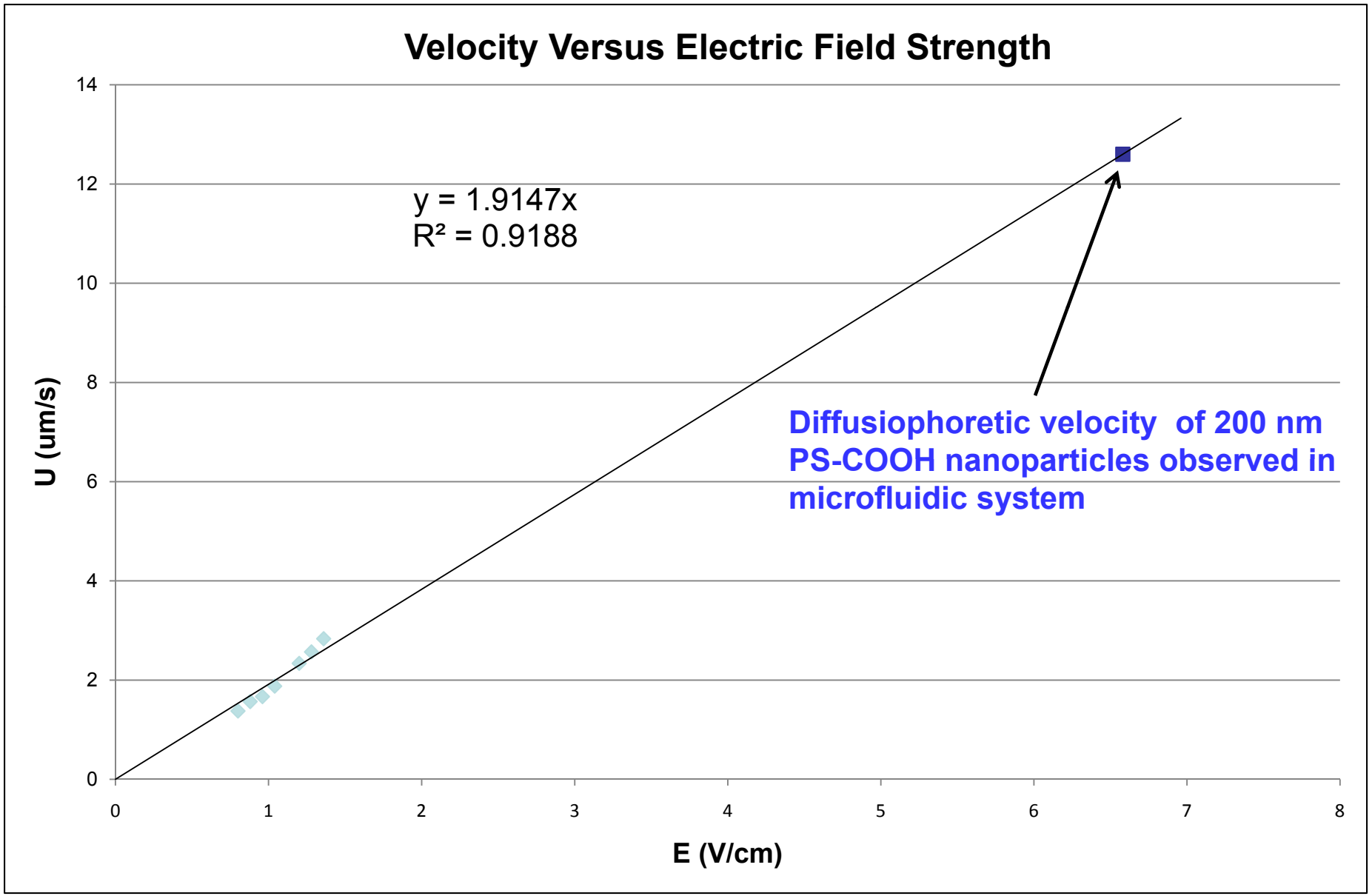

Theoretical Determination of Electric Field Strength Required to Match Observed Diffusiophoretic Velocity

Smoluchowski Equation:

$$E = \frac{U\eta}{\varepsilon\zeta}$$

U: velocity
η: viscosity
ε: permittivity
ζ: zeta potential of particles

Result: Assuming ζ = -60 mV,
diffusiophoretic velocity of 12.6 μm/s requires an electric field of 4.12 V/cm

Under low Reynolds number conditions,
diffusiophoretic velocity independent of radius of the particle

Microfluidics Modeling

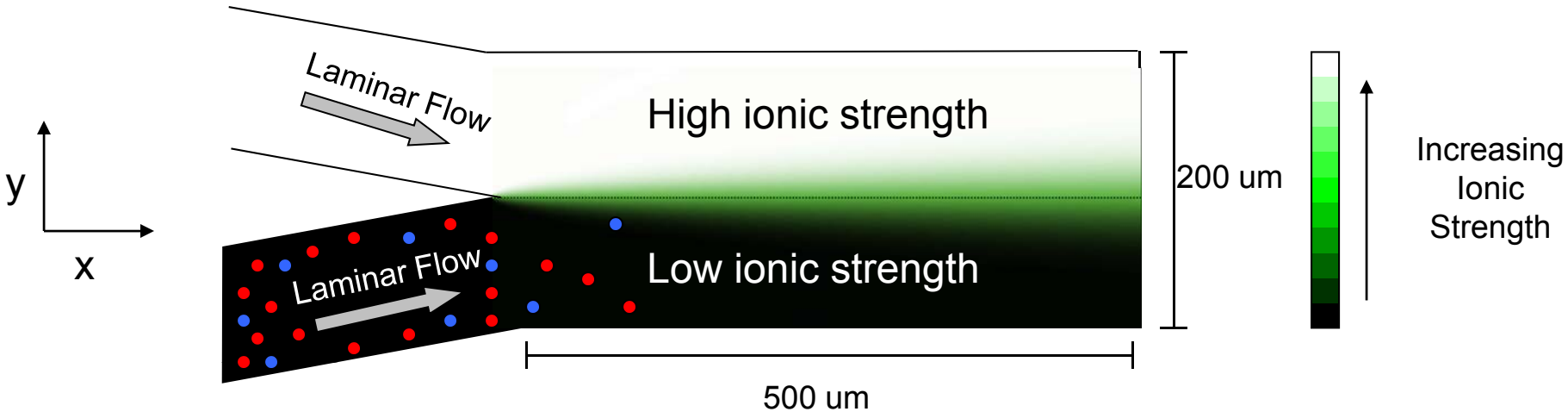

- Simple channel, purely unidirectional laminar flow assumed
- Wall effects ignored (floor effects not ignored)
- Chemicals and particles diffuse in across the channel (y-direction) according to Fick's laws (1D-diffusion)
- Chemical and particles flow down the channel (x-direction) at a given constant rate
- Particles react to their chemical environments and move accordingly across the channel (y-direction, 1D)

Modeling Diffusiophoresis

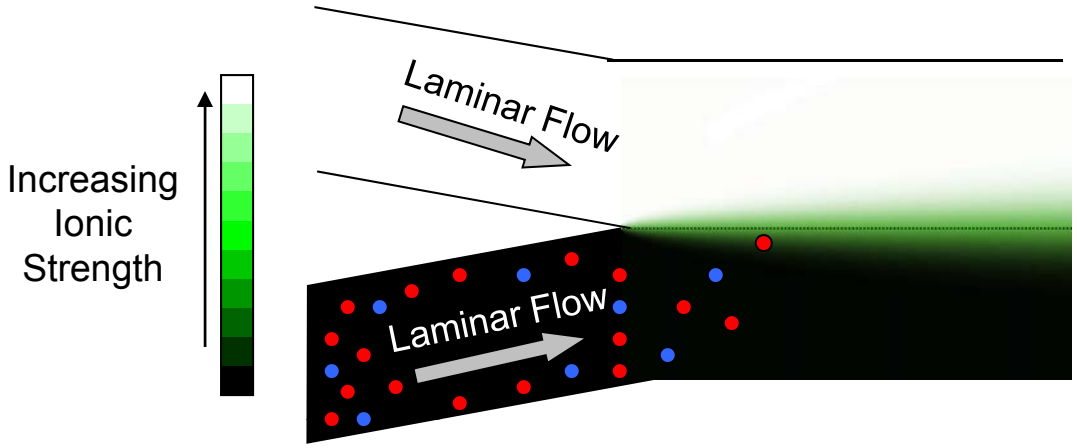

User Defined Parameters

- Incoming particle number density
- Incoming chemical concentration (Molar)
- Flow rate
- Particle diffusion constants: $D = \frac{k_B T}{6\pi\eta a}$
  - Temperature (T)
  - Viscosity (η)
  - Particle Size (a_{active} , $a_{inactive}$)
- Monovalent ion diffusion constants
  - Salt as a whole diffuses with a diffusion constant equal to the harmonic average of these.
- Zeta potentials of particles and underlying substrate (z-direction)
  - Potentials of walls at max and min y direction are ignored.

Modeling Salt Gradients in a Microfluidic Flow

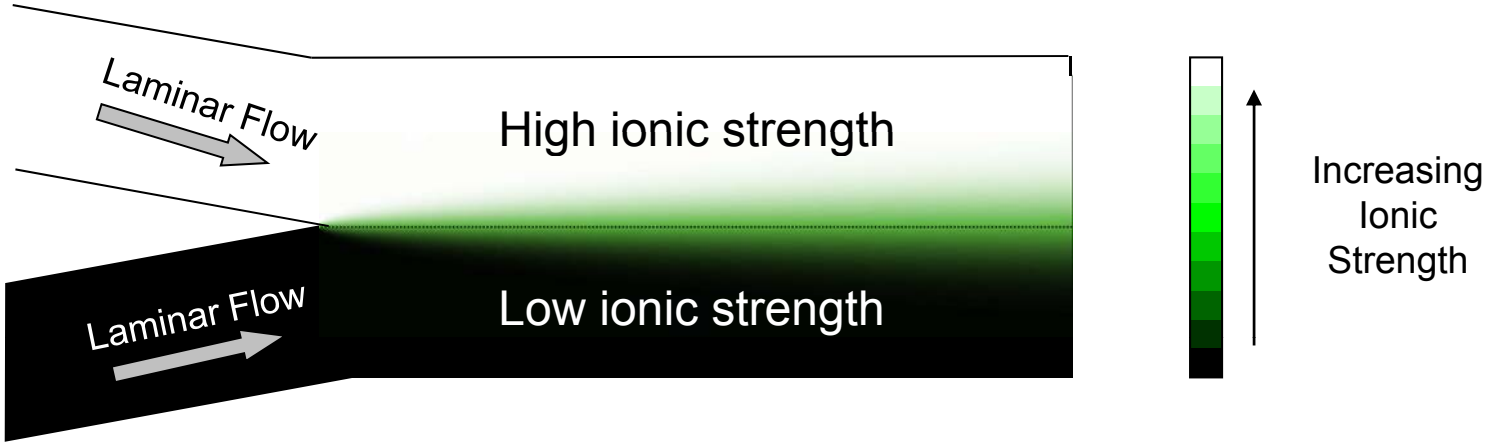

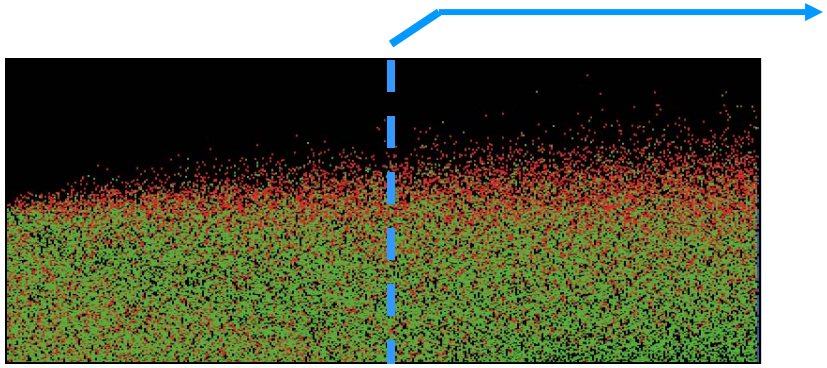

- Ion sensitive colloidal particles
- *Non*-ion sensitive particles

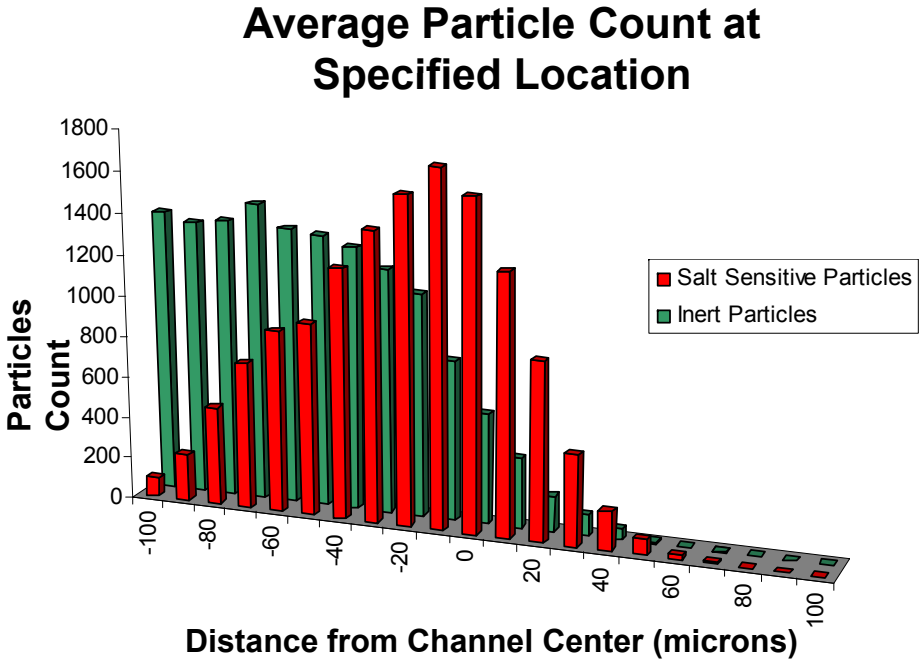

Migration as a Function of Diffusion Constants

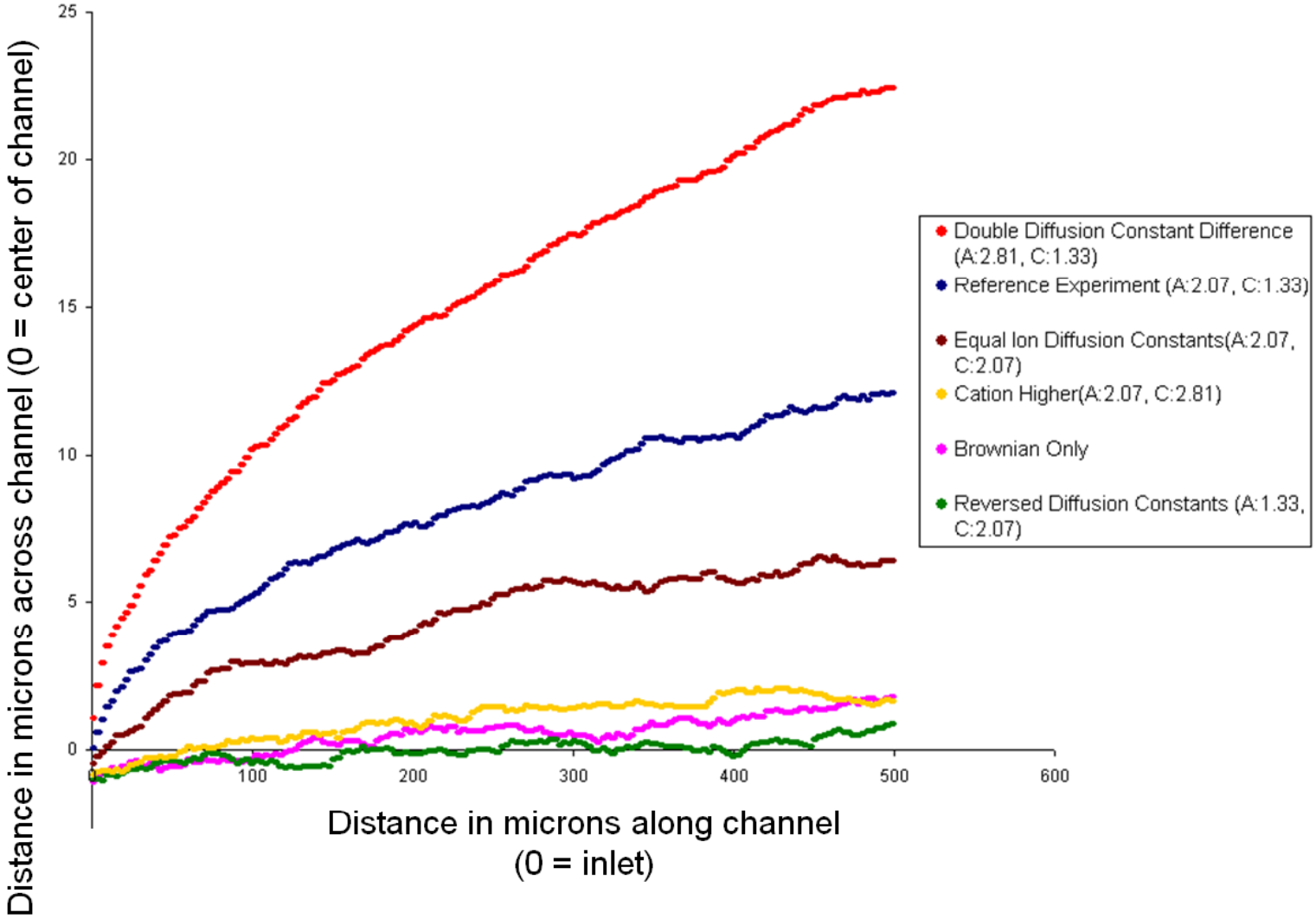

Good Agreement Between Modeling and Experimental Microfluidics Data

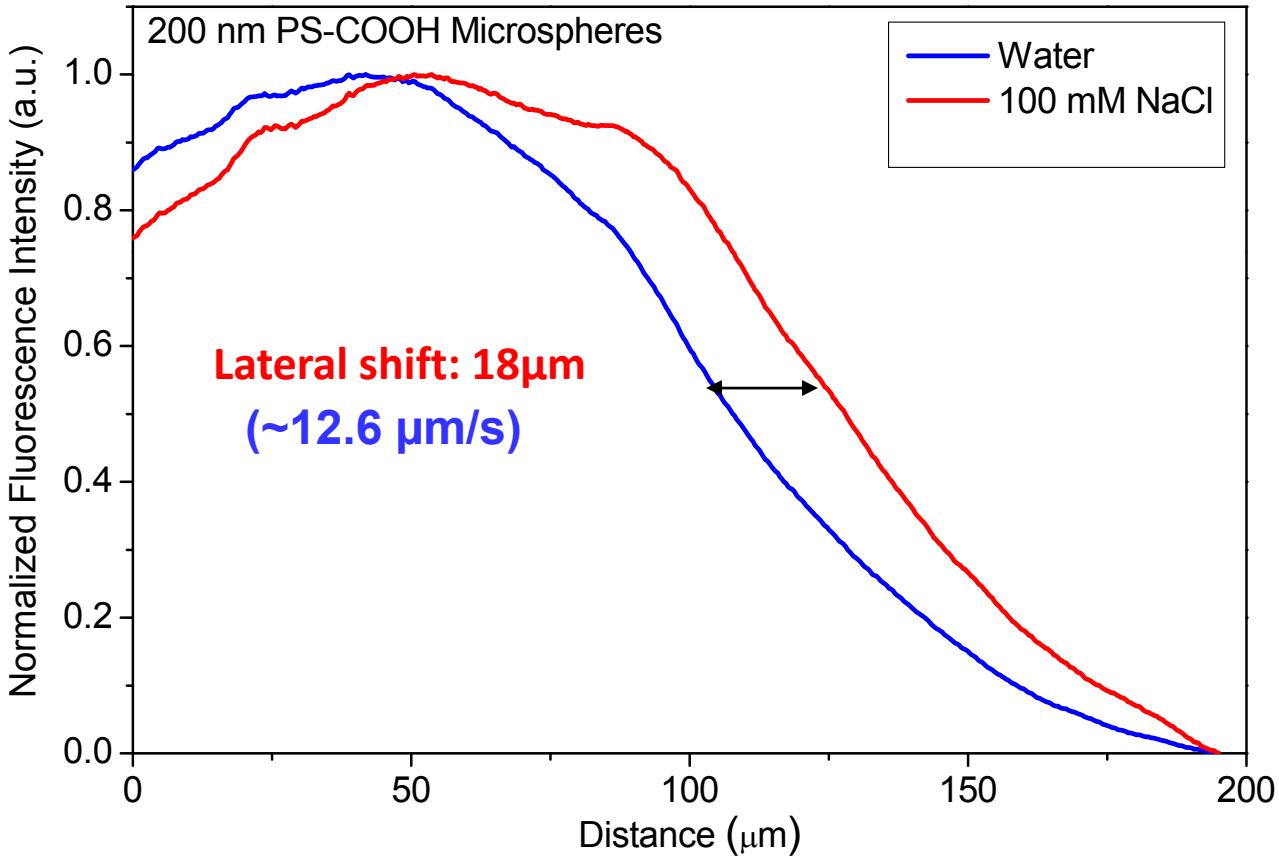

Channel width: 200 µm

Flow rate = 350 µm/s

Imaged at 500 µm

Experiment time: ~1.42 s

$D_A = 2.07 \times 10^{-5}$ cm^2/s (Cl^-)

$D_C = 1.33 \times 10^{-5}$ cm^2/s (Na^+)

Particle sizes: 0.2 µm

Viscosity: 0.001 Pa

Temperature: 25 °C

Effect of Particle Zeta Potential on Particle Movement in Microfluidic Channel

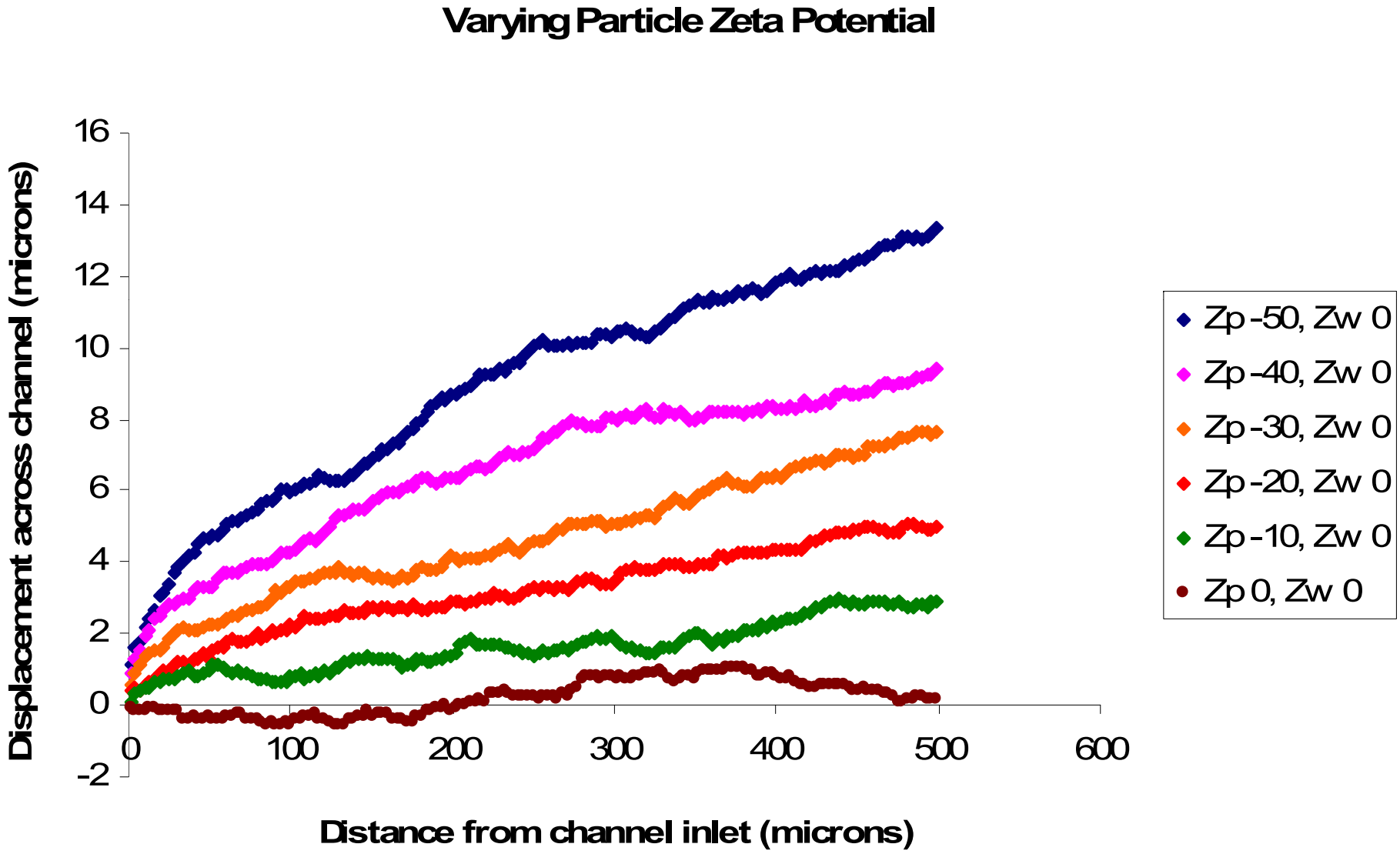

Calculating Theoretical Diffusion Profile

Fick's Second Law

$$\frac{\partial \phi}{\partial t} = D\frac{\partial^2 \phi}{\partial x^2}$$

The rate of change in the concentration at any point depends on the difference between the fluxes entering and exiting that point.

$$C(x,t) = C_S\left[1 - \frac{2}{\sqrt{\pi}}\int_{\frac{x}{2\sqrt{Dt}}}^{\infty} e^{-n^2}\,dn\right]$$

Assuming a perfect source of electrolyte with a concentration of C_S diffusing into an infinite water bath. Assume the water bath starts out without any electrolyte

Diffusiophoresis Equation

$$U = \underbrace{\left(\frac{dLn(C)}{dx}\right)\left(\frac{D_C - D_A}{D_C + D_A}\right)\left(\frac{k_B T}{e}\right)}_{\text{Electric Field}}\frac{\varepsilon\left(\zeta_p - \zeta_w\right)}{\eta} + \underbrace{\left(\frac{dLn(C)}{dx}\right)\left(\frac{2\varepsilon k_B^2 T^2}{\eta e^2}\right)Ln\left[1 - \tanh^2\left(\frac{e\left(|\zeta_P| - |\zeta_W|\right)}{4k_B T}\right)\right]}_{\text{Chemophoretic Term}}$$

Using the electrolyte profile calculated above, we can calculate the speed if we know the temperature, diffusion constants, and zeta potentals

Concentration vs Time at 3 Distances from Source

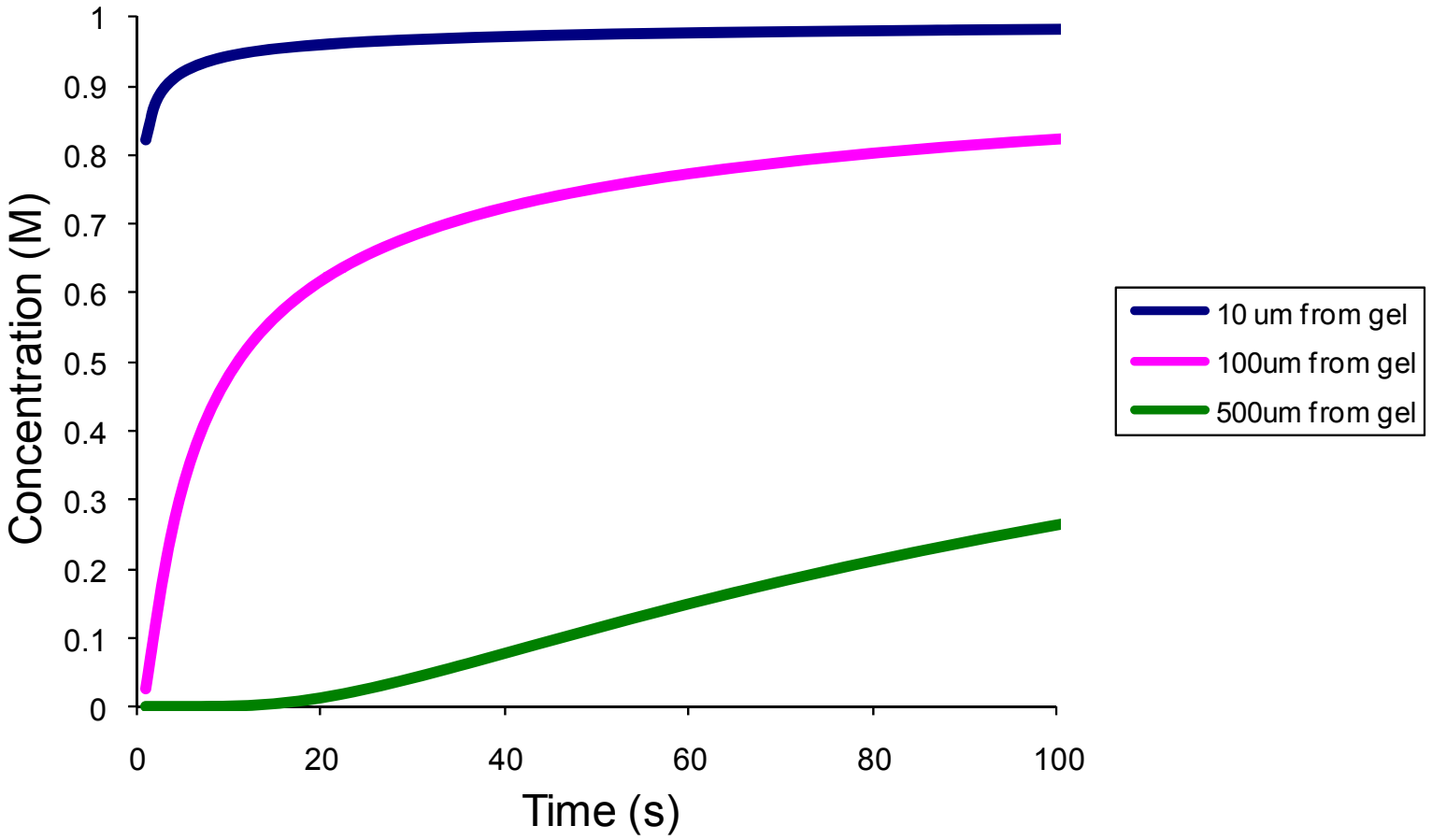

Assuming Average D = 1×10^{-9} m^2/s
Source Concentration = 1 M

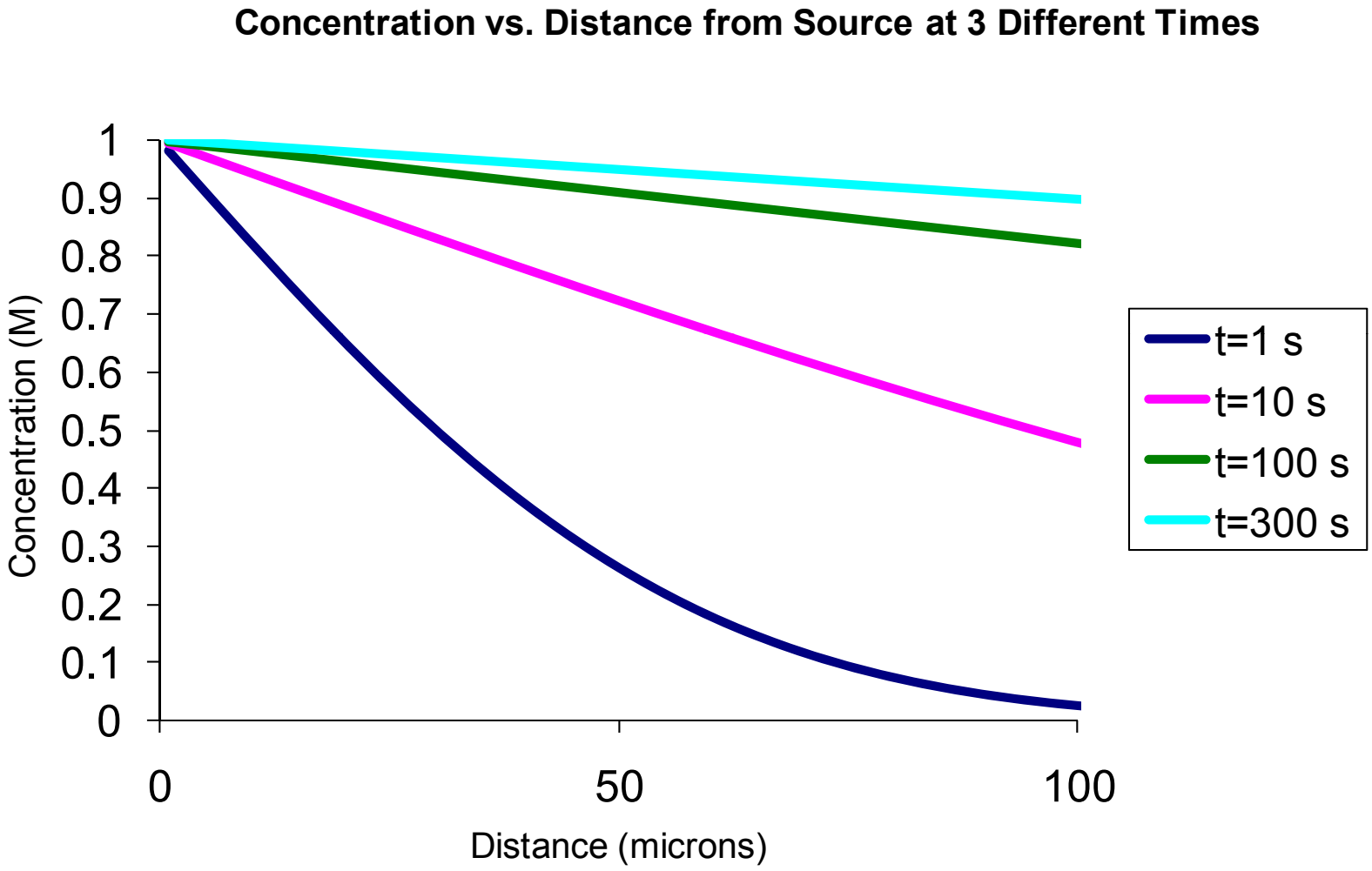

Assuming Average D = 1×10^{-9} m^2/s
Source Concentration = 1 M

Possible Relevance to Oil Recovery

Flush the well with fresh water

Some pockets of salt water remain in crevices

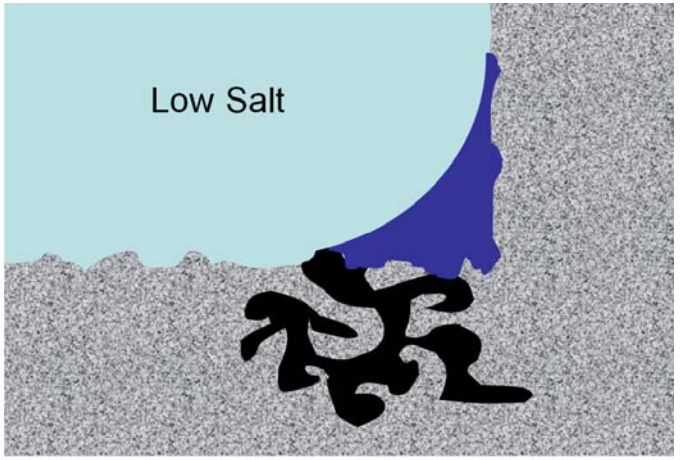

Those pockets of high salt will diffuse out, creating an electric field that acts on all charged surfaces, including exposed oil-water interfaces

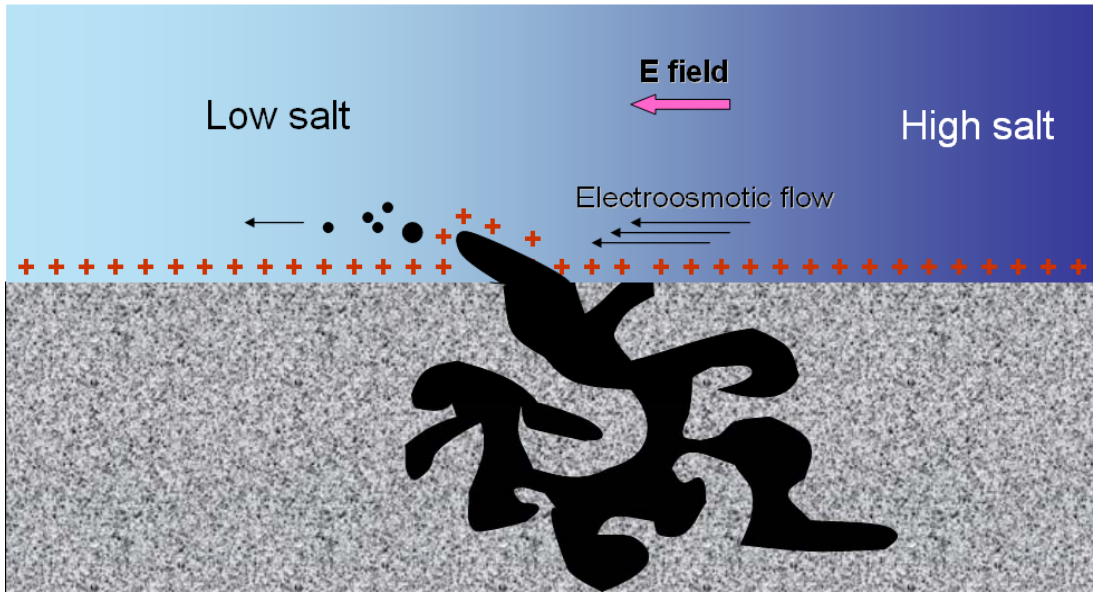

LoSal Enhanced Oil Recovery (BP)

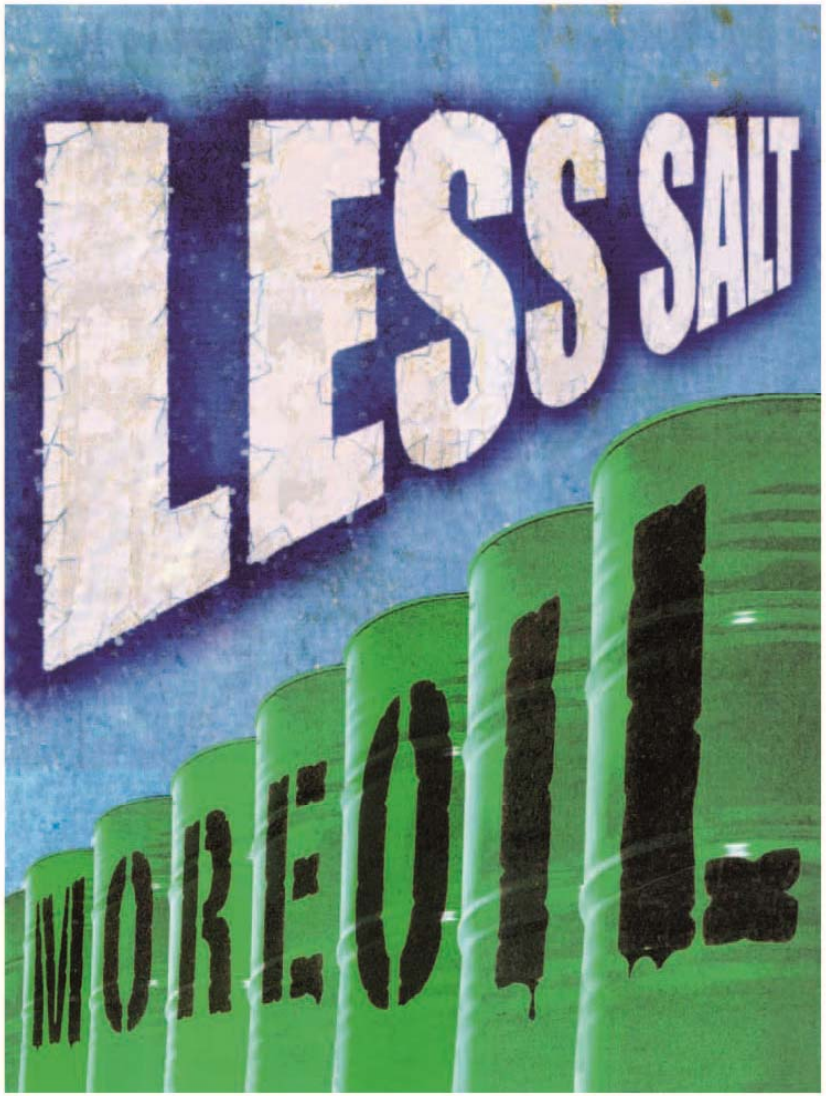

6 | Frontiers | August 2009

BP, *Frontiers*, August, 2009

Movement Through Polymerization

Actin Polymerization

***From: Int. J. Biol. Sci.* 2007, 3:303-317**

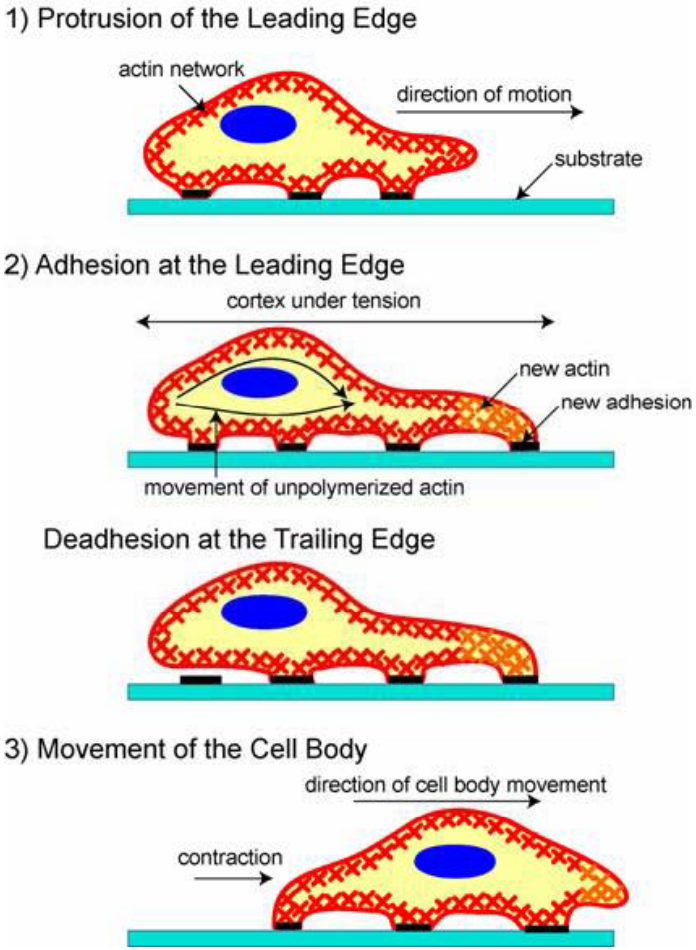

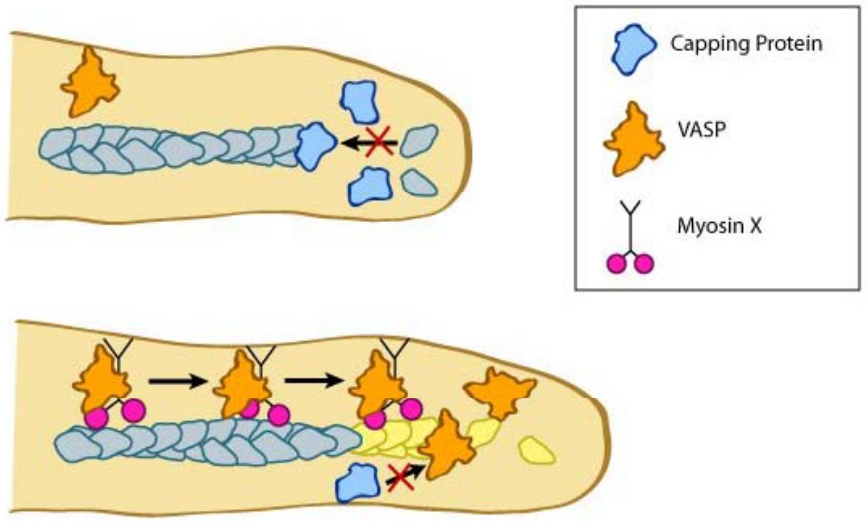

***From: Biochem. Biophys. Res. Commun.* 2004, 319:214-220**

Enzyme polymerizes actin monomer which aids in cell motion

Angew. Chem., 2011

Polymerization-Powered Micromotors

These Motors Utilize Asymmetrically Bound Grubbs-type Catalyst On Au/Silica Janus Microspheres To Convert Monomer Into Polymer

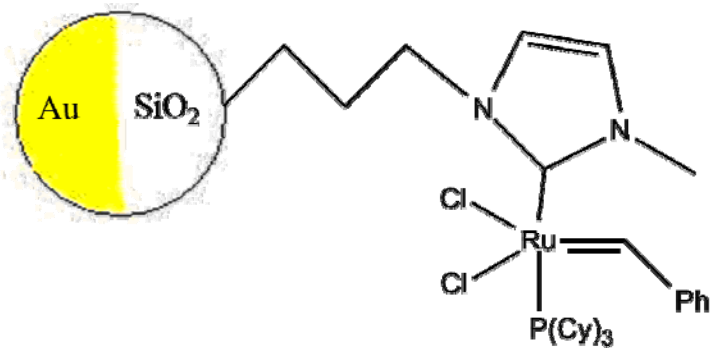

Motor

Monomer **Polymer**

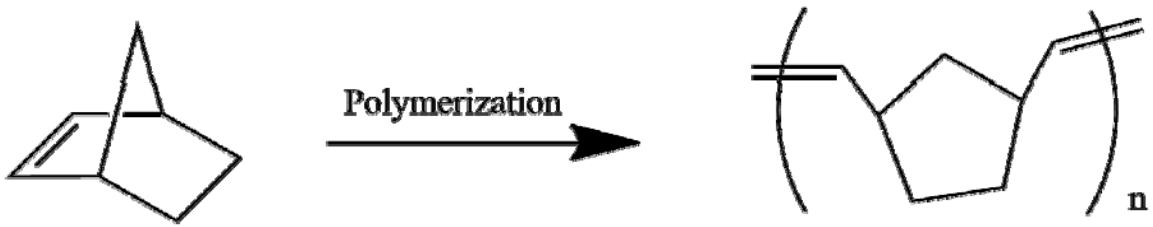

Particle Comparison

Before Polymerization

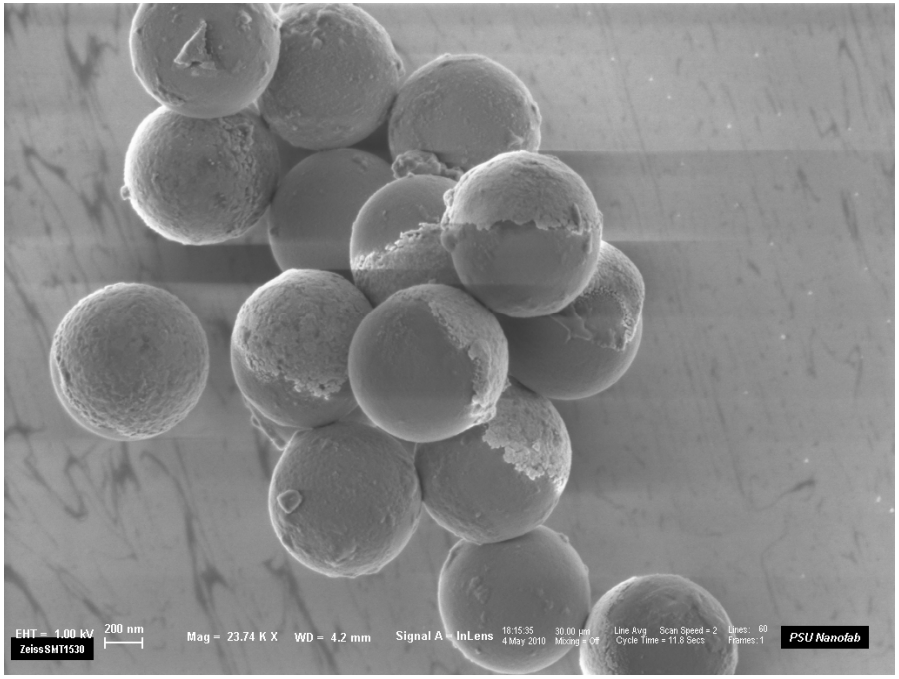

After Polymerization

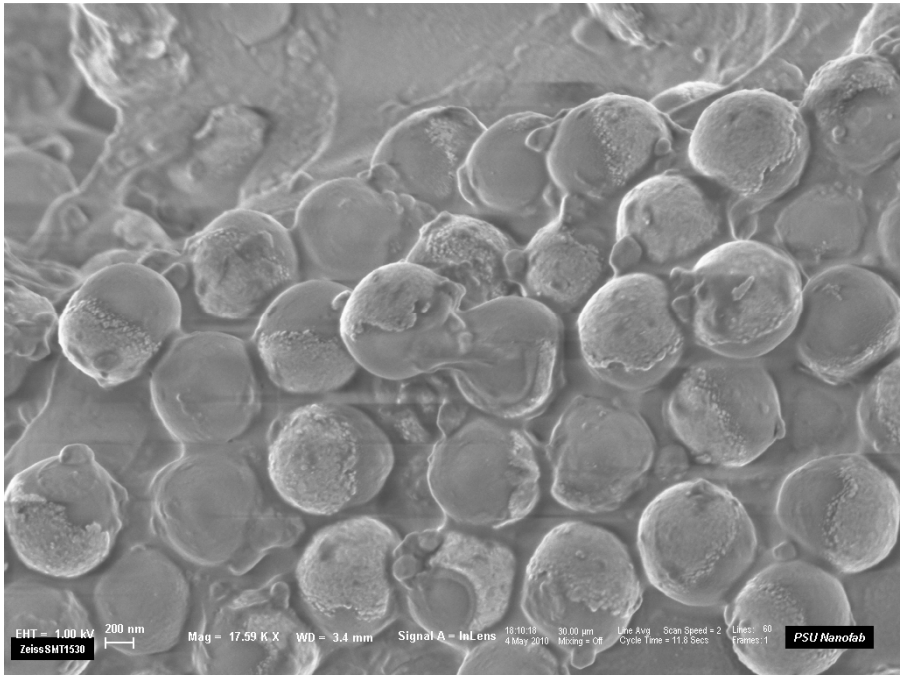

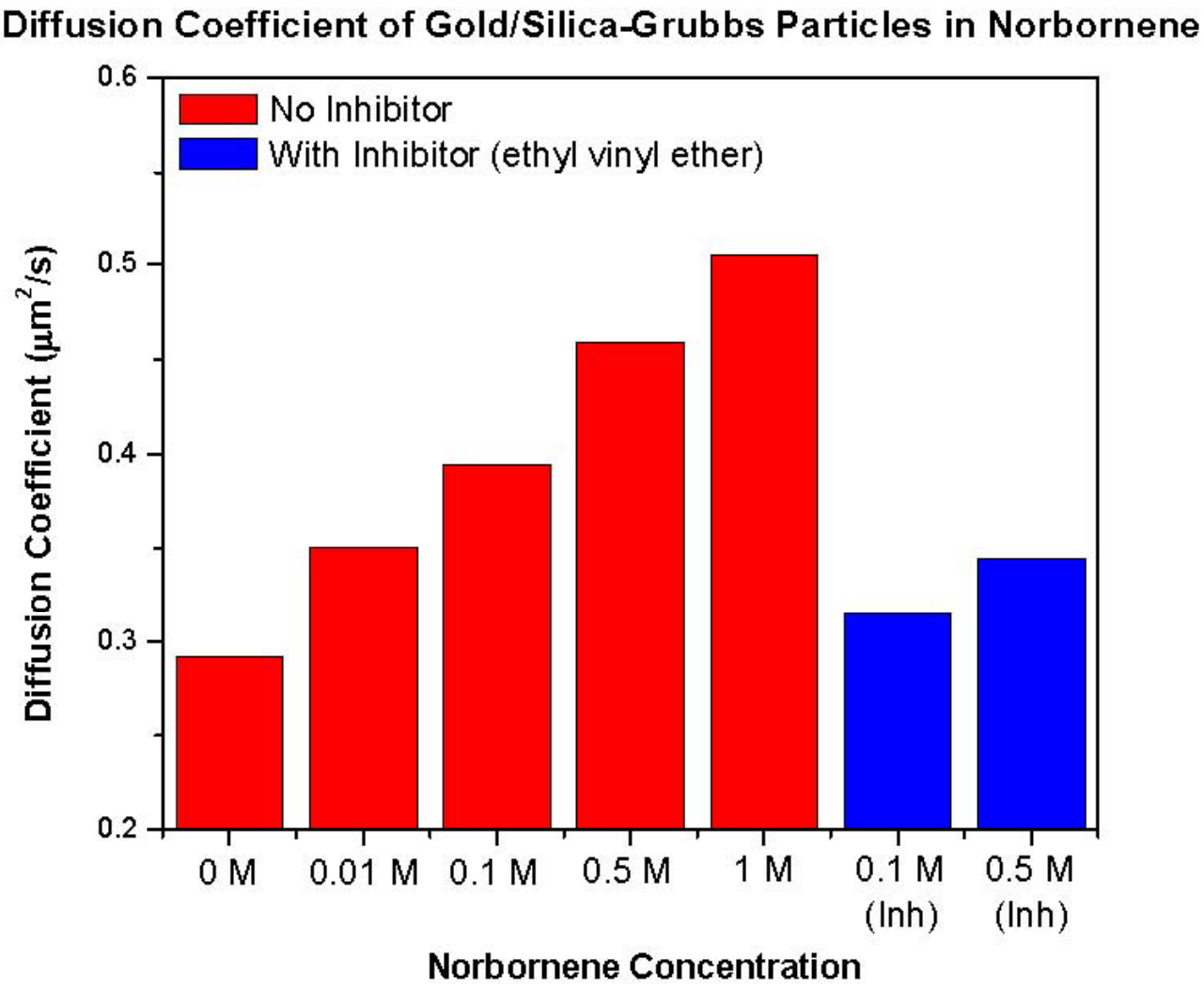

Note: Polymer Formed Dissolves in Solvent, Does *Not* Precipitate Out

Osmophoretic Mechanism
(*Anderson, Golestanian, Kapral, Brady, Showalter, ..*)

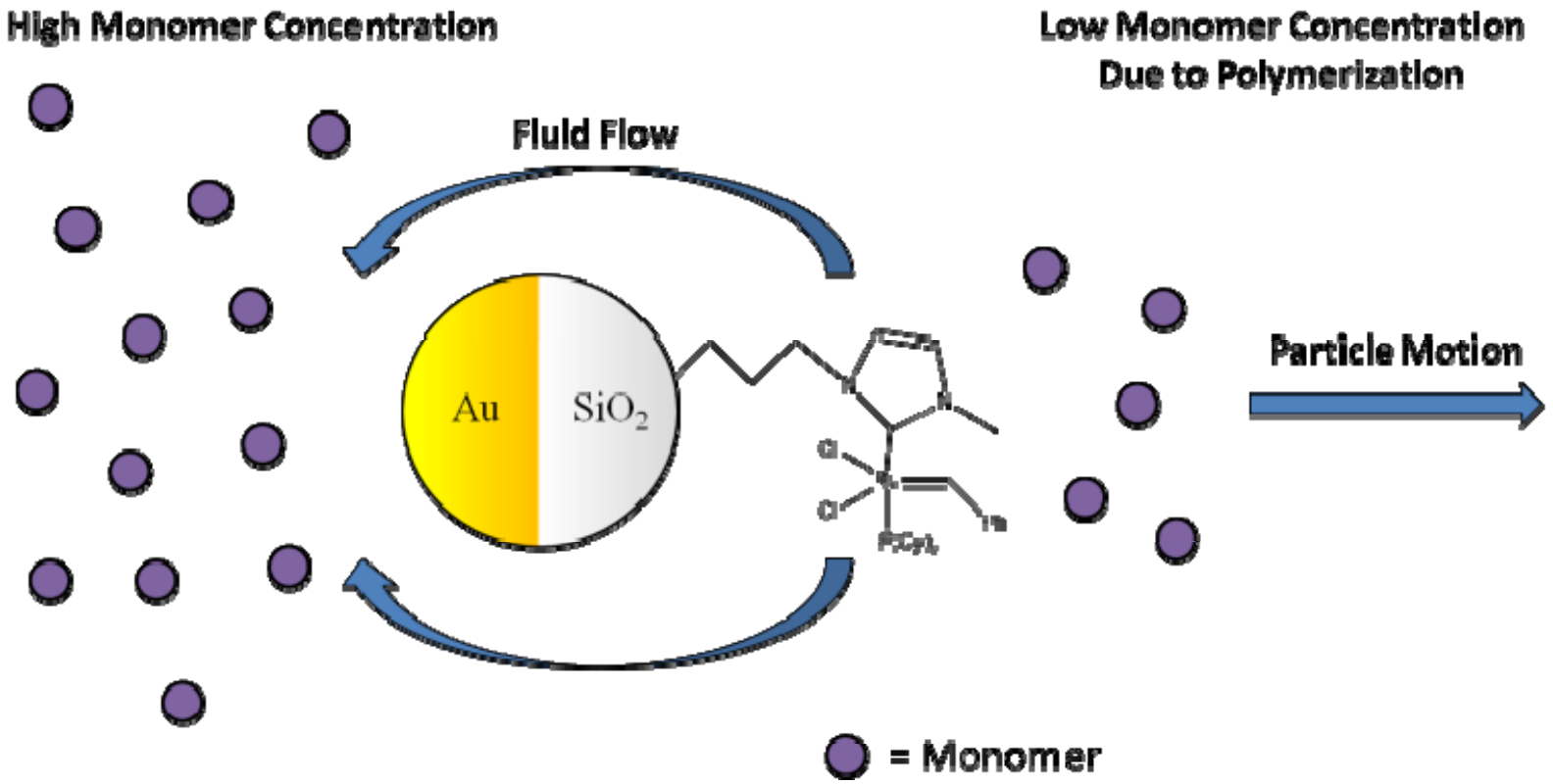

The motor consumes monomers at the silica face creating an area of low monomer concentration

Fluid in the low concentration region flows *towards* the higher concentration region at the gold face.

Consequently, the motor moves in the *opposite* direction

Does Enhanced Diffusion with Increasing Substrate Concentration Translate into Directed Motion: *Chemotaxis*?

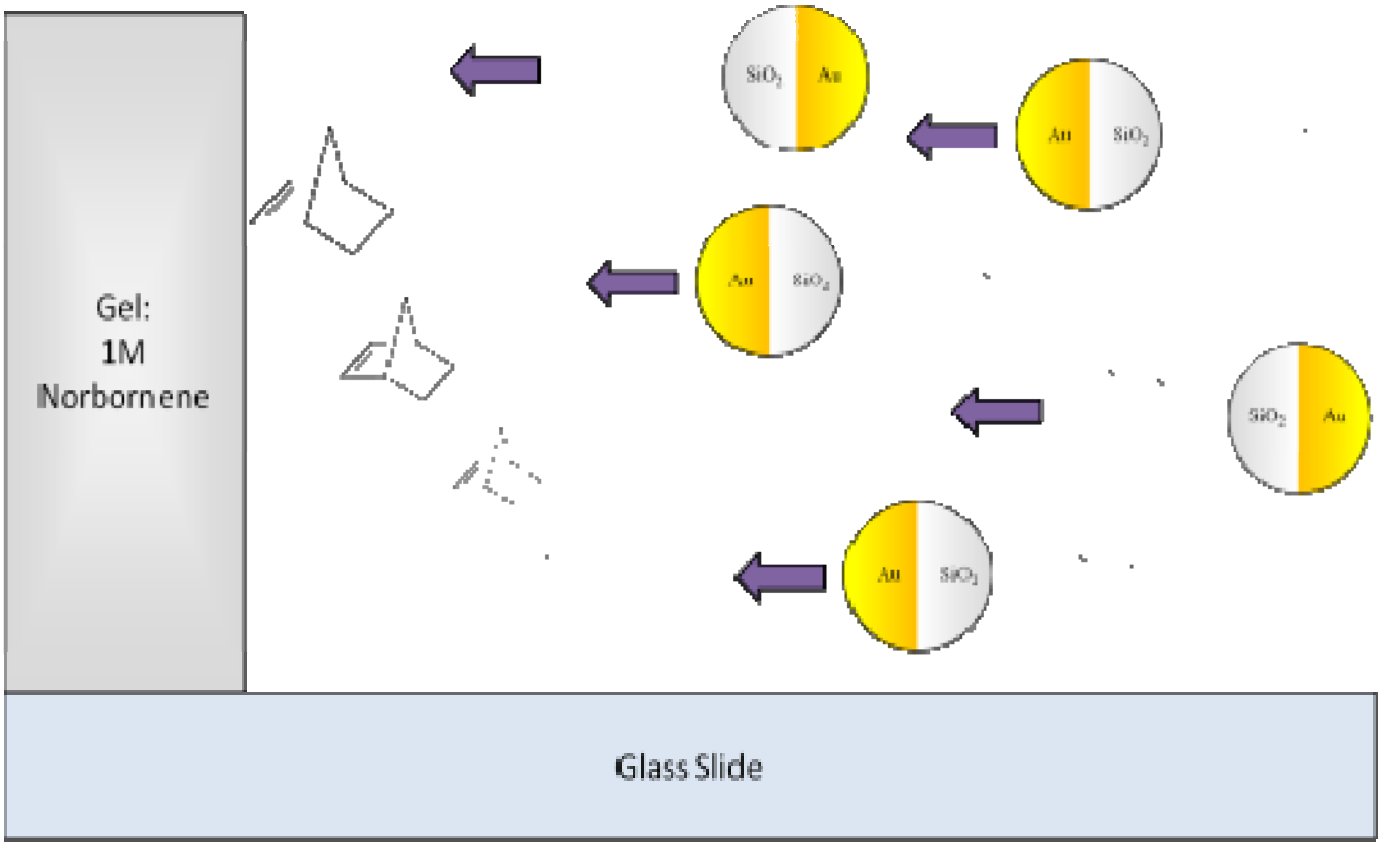

Chemotaxis of Polymerization-Powered Motors

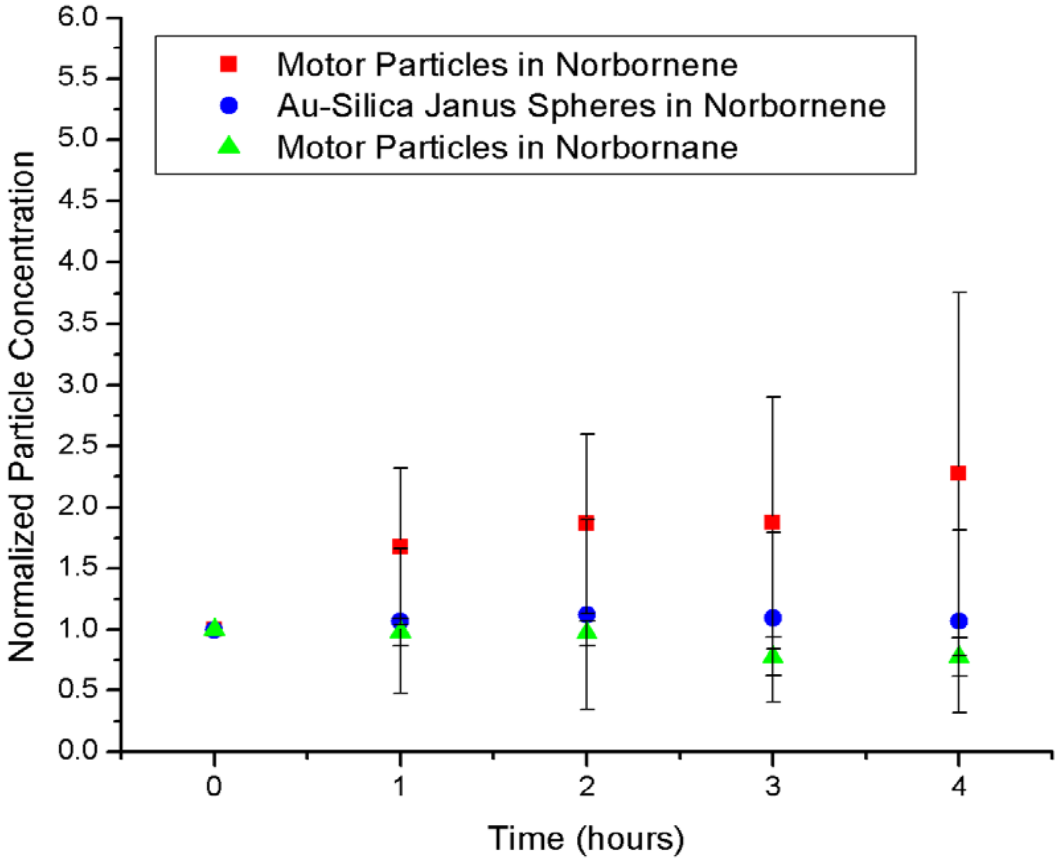

Normalized particle population at the gel edge as a function of time:
The motor particles in a norbornene gradient (red)
Unfunctionalized Au-Silica Janus spheres in norbornene gradient (blue)
Motor particles in a norbornane gradient (green)

***Angew. Chem.*, 2011**

Substrate Catalysis Enhances Single Enzyme Diffusion

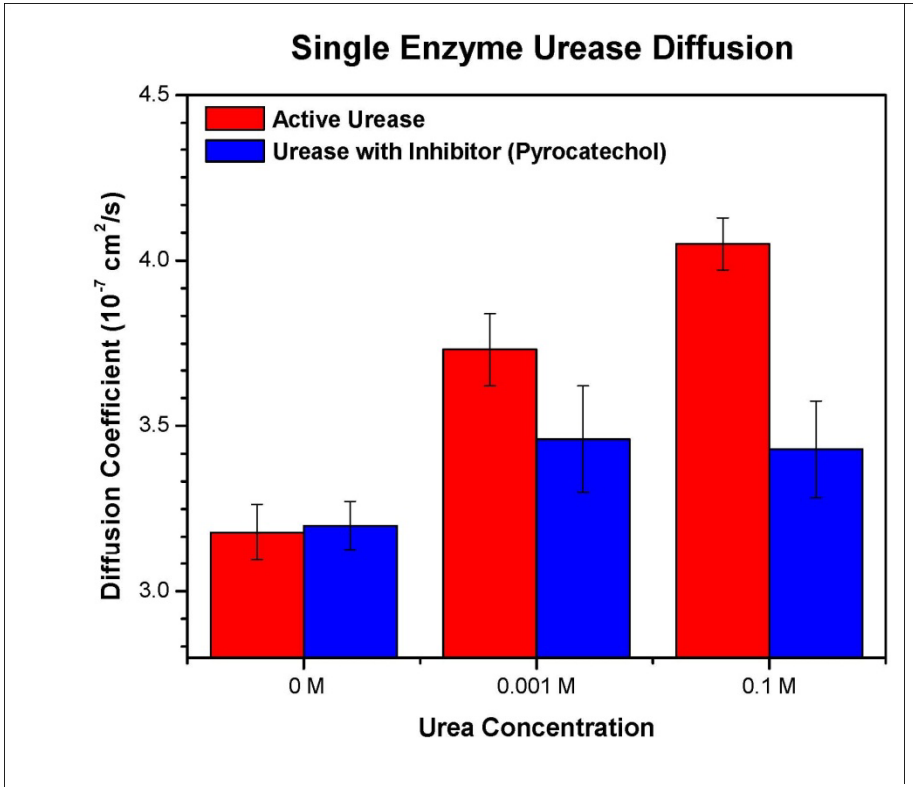

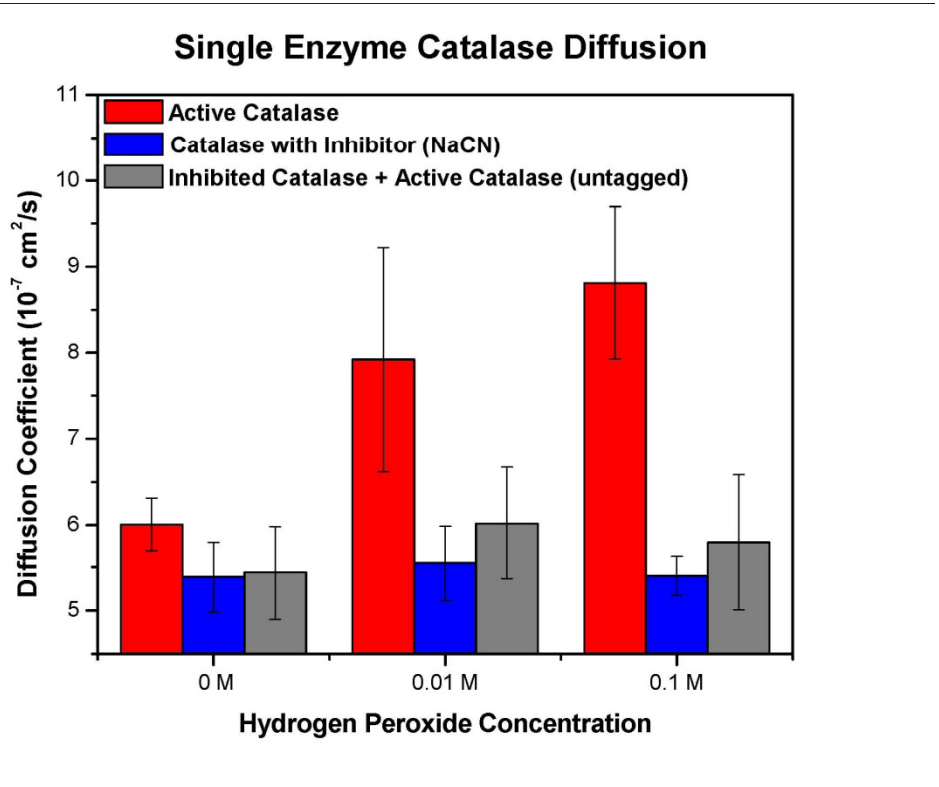

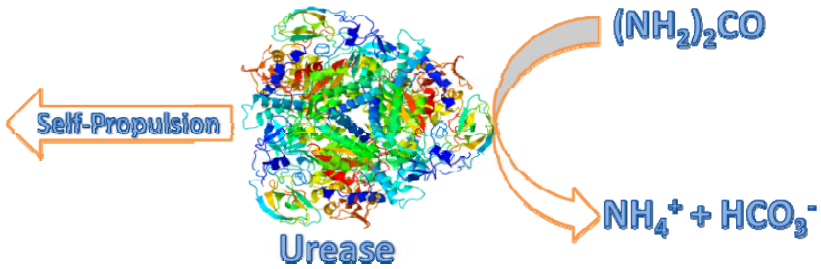

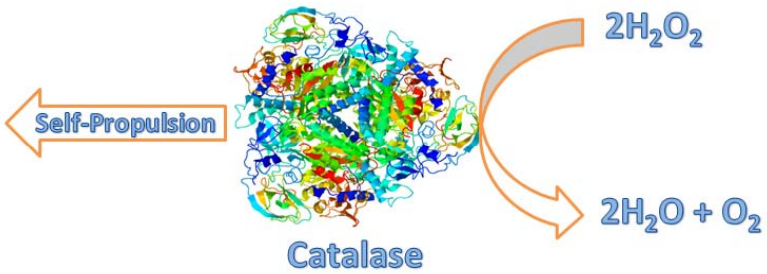

J. Am. Chem. Soc., 2010

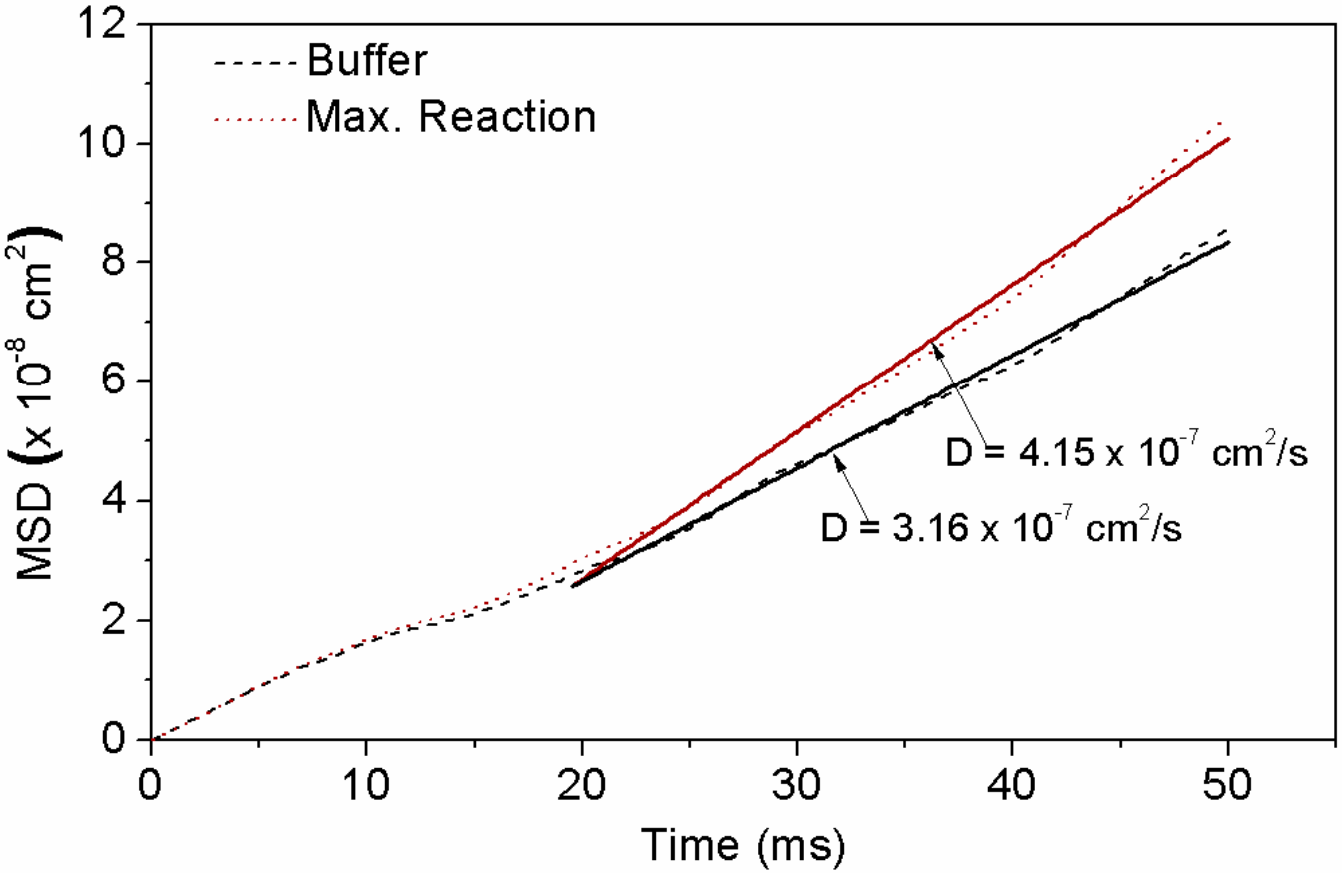

Mean square displacement (MSD) of urease obtained from Brownian dynamics simulations,

assuming 10 nanosecond impulse time per reaction:

No reaction (*black*)

Maximum reaction rate assuming a force of 12 pN/turnover (*red*)

Solid lines are linear fits at longer time scales.

J. Am. Chem. Soc., 2010

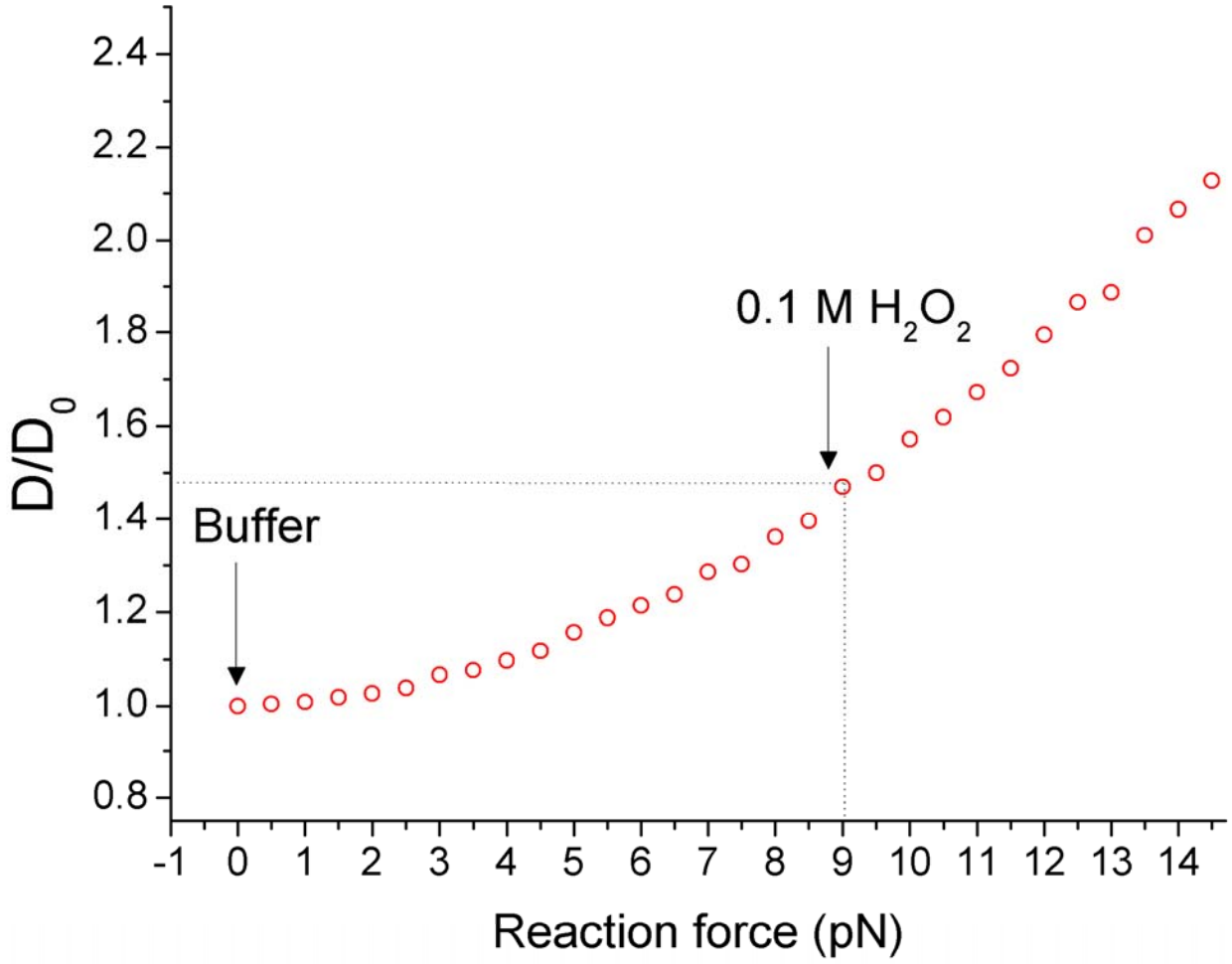

Relative diffusion coefficient of catalase obtained from Brownian dynamics simulations, *assuming 10 nanosecond impulse time per reaction* :

Maximum reaction rate assuming a force of 9 pN/turnover (red)

Catalase Trajectory

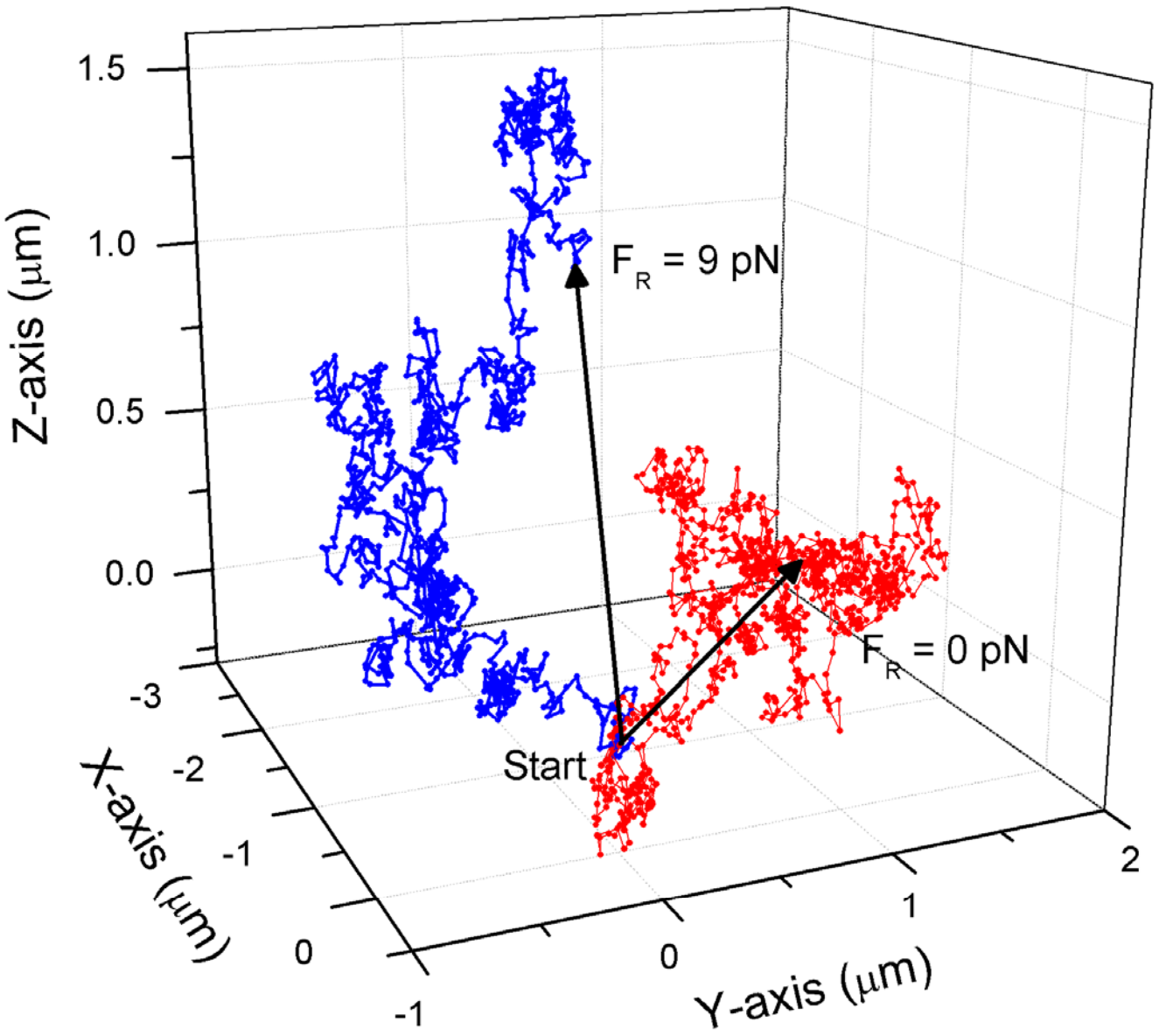

Single Enzyme Chemotaxis

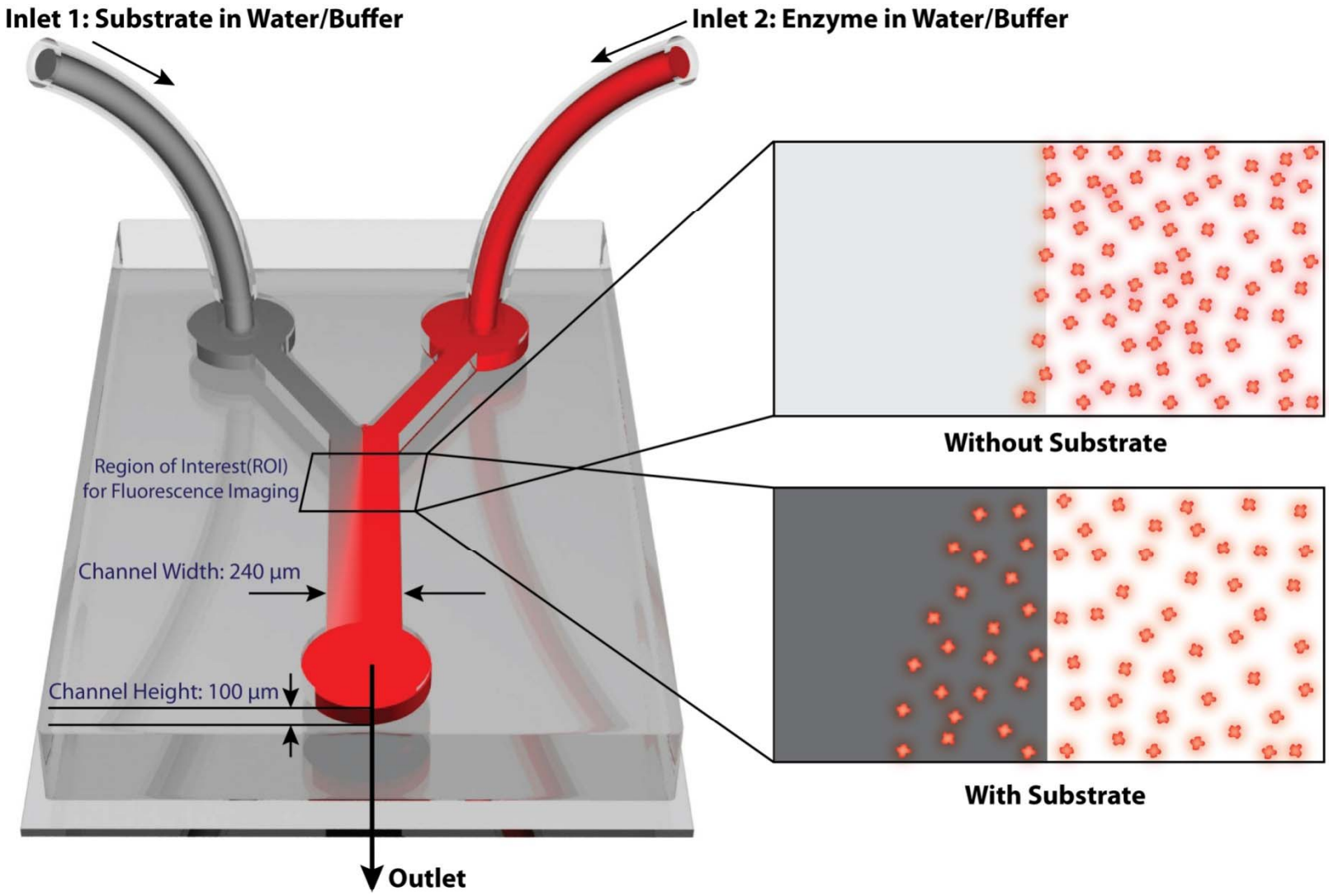

Y-shaped microfluidic channel used for single-molecule enzyme chemotaxis studies

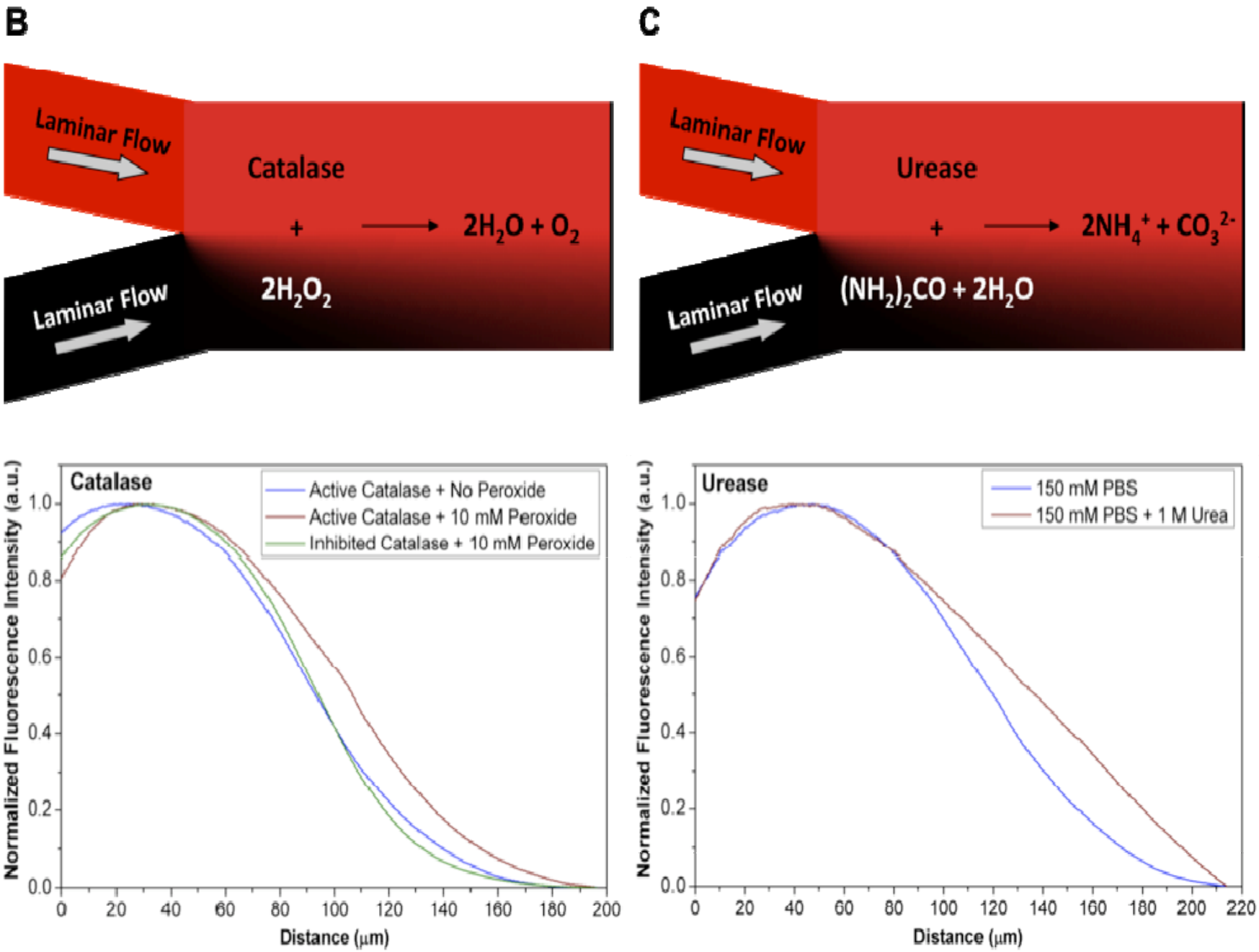
B
Laminar Flow
Catalase
+
$2H_2O + O_2$
Laminar Flow
$2H_2O_2$
C
Laminar Flow
Urease
+
$2NH_4^+ + CO_3^{2-}$
Laminar Flow
$(NH_2)_2CO + 2H_2O$
Catalase
Active Catalase + No Peroxide
Active Catalase + 10 mM Peroxide
Inhibited Catalase + 10 mM Peroxide
Normalized Fluorescence Intensity (a.u.)
Distance (μm)
Urease
150 mM PBS
150 mM PBS + 1 M Urea
Normalized Fluorescence Intensity (a.u.)
Distance (μm)

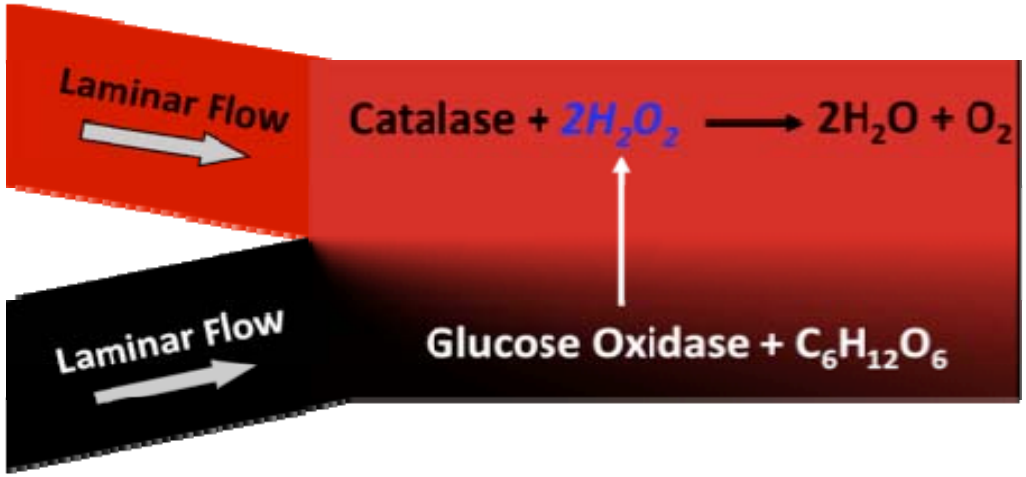

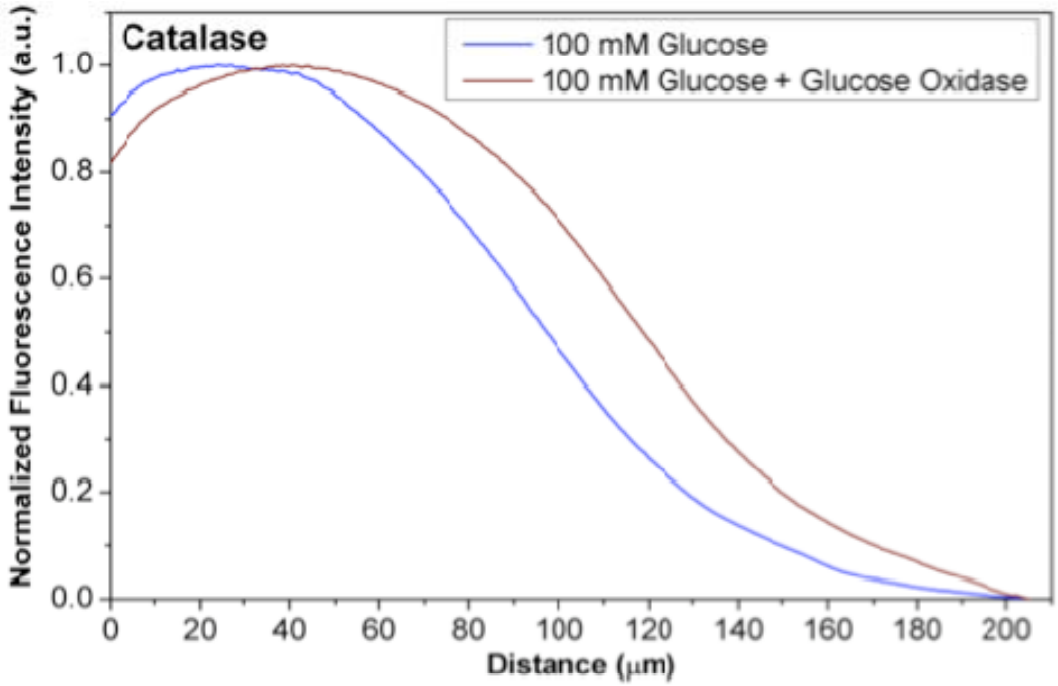

Shift for catalase towards 100 mM glucose and glucose oxidase

Behavior of Free Dye Molecules towards Different Substrate Concentration Gradients

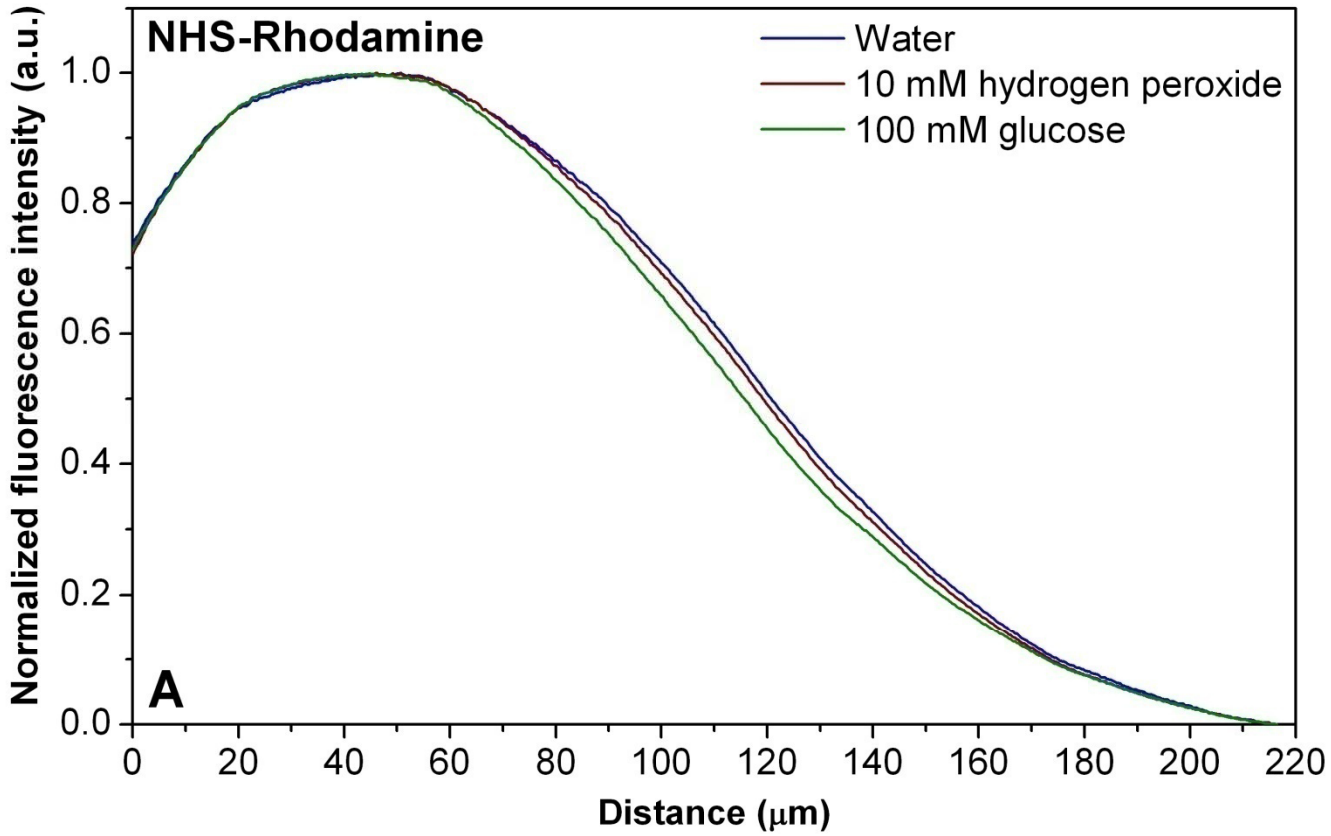

Applicability of the Scallop Theorem

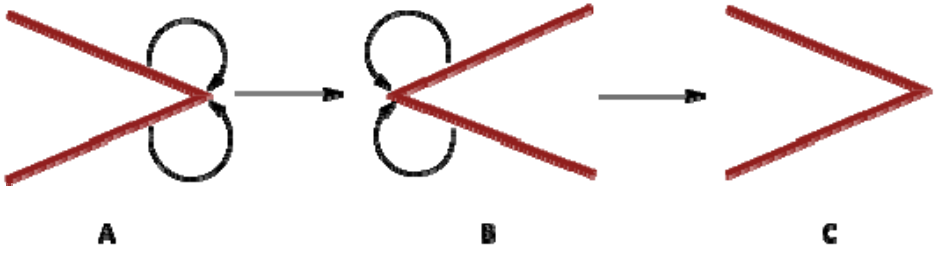

At low Reynold's number propulsion by time-reversible reciprocal motion not possible?? (Scallop Theorem)

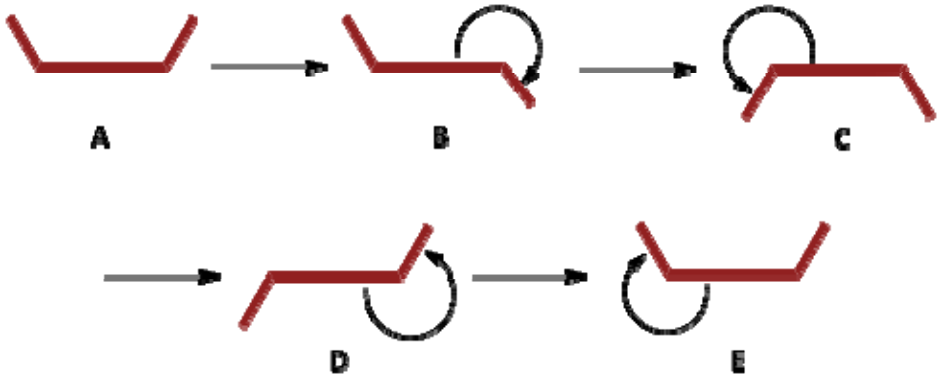

At low Reynold's number propulsion by non-reciprocal motion can be achieved

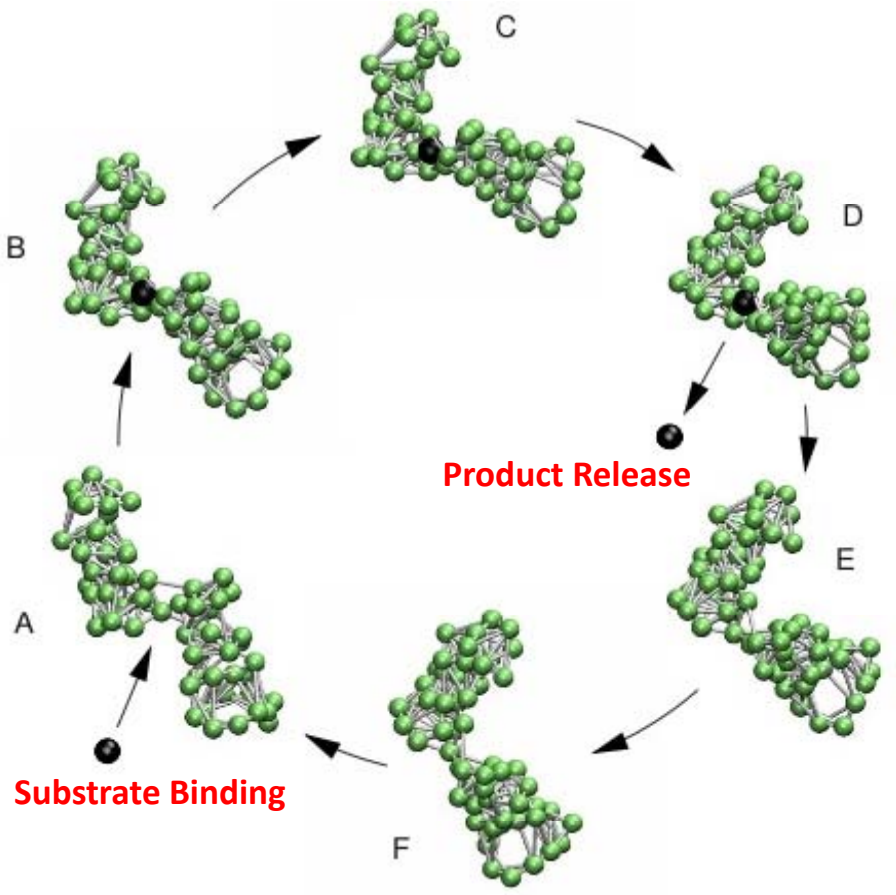

Non-reciprocal conformational changes in a model enzyme

1. Sakaue, T.; Kapral, R.; Mikhailov, A. S. *Eur. Phys. J. B* 2010, *75*, 381–387
2. Golestanian, R. *Phys. Rev. Lett.* 2010, *105*, 018103(1)-018103(4)

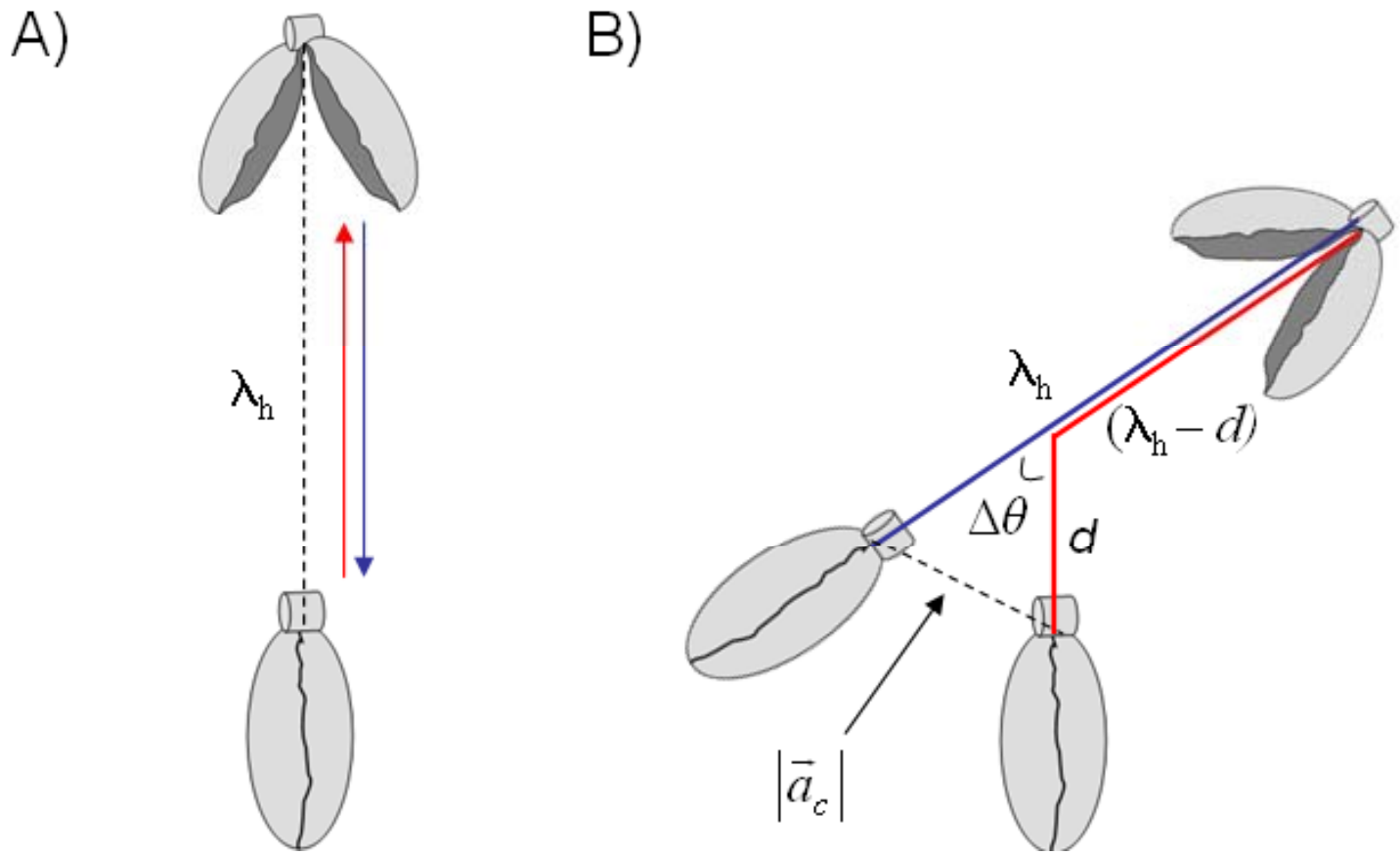

A) The reciprocal swim cycle of an unperturbed scallop opening and closing its shell.

B) The motion path of a similar swimmer which undergoes a single rotation *after* it has traveled a distance (*d*) into its cycle.

The *forward* paths are shown in red, the *return* paths are shown in blue.

Also, Lauga, *PRL*, 2011

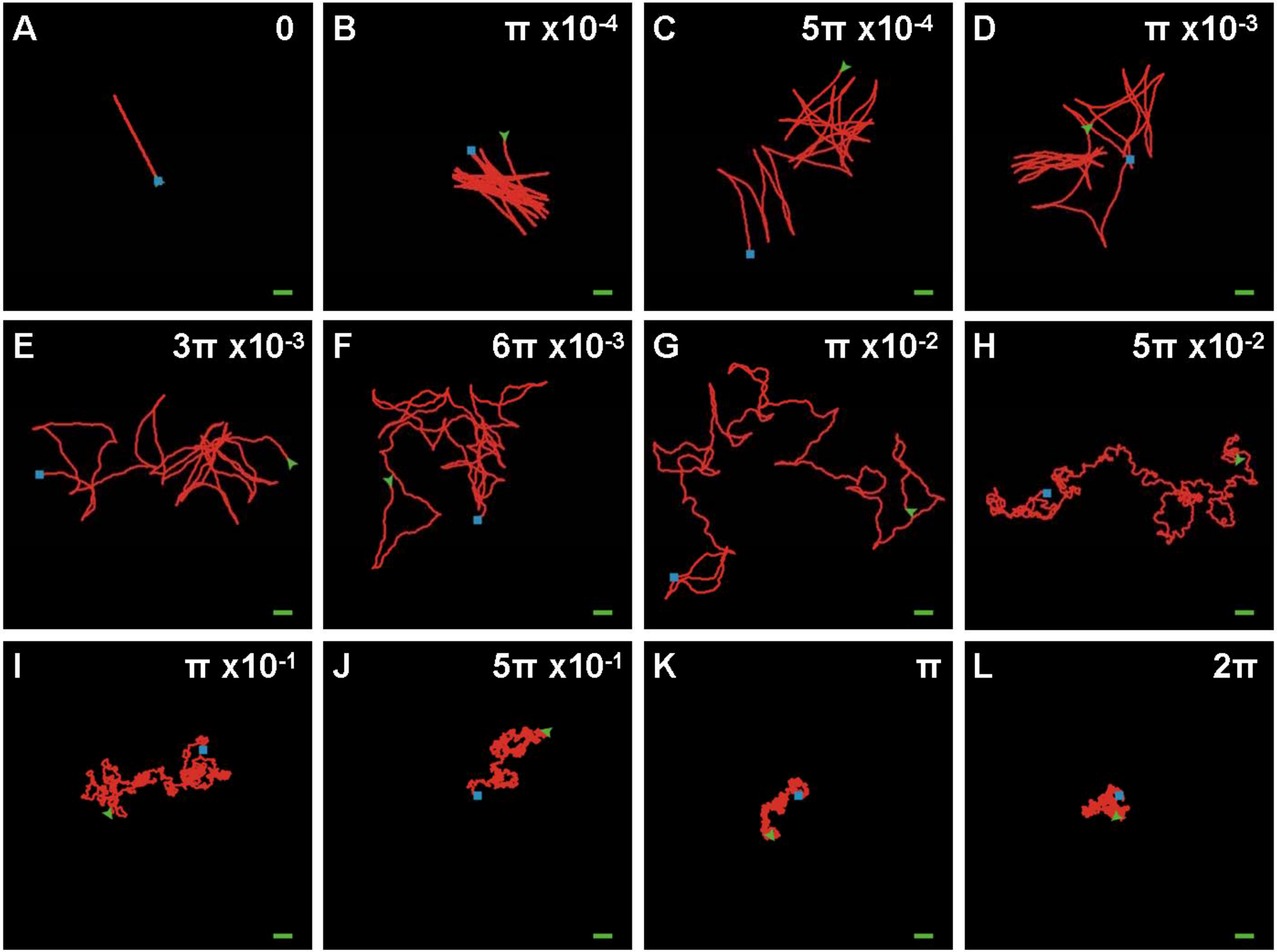
A
0
B
π x10-4
C
5π x10-4
D
π x10-3
E
3π x10-3
F
6π x10-3
G
π x10-2
H
5π x10-2
I
π x10-1
J
5π x10-1
K
π
L
2π

Designing Intelligent Nano/Microbots: Synthetic Active Matter

1. Introduction to Synthetic Active Matter
2. Powering Active Particle and Fluid Motion
3. Collective Behavior of Autonomous Nano/Microbots

AYUSMAN SEN

Department of Chemistry, Penn State University
E-mail: asen@psu.edu

Intelligent Catalytic Motors

Intelligence requires (a) information and (b) ability to process (act on) information – information processor

Information: Gradient – Chemical, Light

Information processor: Self-powered object

Result of Information + Information Processing:
Collective/Emergent behavior
e.g., Spatial and/or Temporal Assemblies

***Both* information and information processor require continuous input of energy**

Information Processor can *change* the Information
e.g., Assume an initial fuel gradient:
Higher the motor density → Faster fuel consumption →
Steeper fuel gradient → More directional (& faster) chemotaxis

Artists drawing of a nanoscale submarine moving through a human capillary.

- taken from Audi Magazine, 10/03